

Novel dynamic critical phenomena induced by superfluidity and the chiral magnetic effect in Quantum Chromodynamics

Noriyuki Sogabe

June 26, 2020

A Thesis for the Degree of Ph.D. in Science

Novel dynamic critical phenomena induced by
superfluidity and the chiral magnetic effect in Quantum
Chromodynamics

February 2020

Graduate School of Science and Technology
Keio University

Noriyuki Sogabe

Acknowledgements

First and foremost, I would like to express the most profound appreciation to my supervisor Prof. Naoki Yamamoto. He has taught me the joy of physics and led my life in an exciting direction. His broad knowledge and intuition have strongly influenced my understanding of physics. I am fortunate to have Naoki as my adviser and should thank him for his patience. It has been an honor to be his first Ph.D. student.

I am deeply grateful to my collaborator, Masaru Hongo, for my works on the interplay between the CME and the dynamic critical phenomena. I would also like to thank many people in the community, whom I met at conferences, workshops, seminars, and summer schools. I am particularly grateful to Profs. Kenji Fukushima and Yoshimasa Hidaka. I would also like to express my gratitude to the referees of my Ph.D. defense, Profs. Youhei Fujitani, Yasuhiro Nishimura, and Kohei Soga.

I want to thank Aron Beekman, Gergely Fejős, Tomoyuki Ishikawa, Kentaro Nishimura, Di-Lun Yang, who I was sharing the office with for numerous discussions and relaxing chat. I am also very thankful to the other (including previous) members of the theoretical physics group at Keio University, particularly Daichi Kagamihara and Hiroaki Wakamura, for their friendship and encouragement.

I appreciate the financial support of research from the Japan Society for the Promotion of Science. When I started writing this thesis during a journey to visit Germany, I was stuck at the Frankfurt airport affected by the typhoon Hagibis. I want to thank my friend, Alexander Max Eller, and his mother, Galvi, to allow me to stay at their house.

Last but not least, I would like to thank my family for all their love, support, encouragement, and patience. Without them, I could not have completed my Ph.D. thesis.

Noriyuki Sogabe

Summary

Understanding the phase structure of Quantum Chromodynamics (QCD) at finite temperature and finite baryon chemical potential is a long-standing problem in the standard model of particle physics. So far, in addition to the nuclear liquid-gas critical point, the possible existence of two critical points is theoretically suggested in the QCD phase diagram: one is the high-temperature critical point between the hadron phase and the quark-gluon plasma phase and the other is the high-density critical point between the nuclear and quark superfluid phases. Since these critical points can be potentially tested in relativistic heavy-ion collision experiments, theoretical predictions for critical phenomena near these critical points are important. On the other hand, heavy-ion collision experiments have another goal to search for the chiral transport phenomena related to the quantum anomaly. One typical example is the chiral magnetic effect, which is the electric current along the magnetic field. In particular, it is known that the chiral magnetic effect leads to the generation of a novel density wave called the chiral magnetic wave.

In this thesis, we first construct the low-energy effective field theory near the high-density QCD critical point and study its static and dynamic critical phenomena. We find that the critical slowing down of the speed of the superfluid phonon near the critical point. Furthermore, we show that the dynamic universality class of the high-density critical point is not only different from that of the high-temperature critical point, but also a new dynamic universality class beyond the conventional classification by Hohenberg and Halperin. Since this new universality class stems from the interplay specific to QCD between the chiral order parameter and the superfluid photon, the observation of the dynamic critical phenomena in the vicinity of the high-density critical point would provide an indirect evidence of the superfluidity in high-density QCD matter.

We next consider the second-order chiral phase transition in massless QCD under an external magnetic field and study the interplay between the dynamic critical phenomena and the chiral magnetic effect. For this purpose, we construct the nonlinear Langevin equations including the effects of the quantum anomaly and perform the dynamic renormalization group analysis. As a result, we show that the presence of the chiral magnetic effect and the resulting chiral magnetic wave change the dynamic universality class of the system from the so-called model E into the model A within the conventional classification. We also find that the speed of the chiral magnetic wave tends to vanish when the phase transition is approached. This phenomenon is characterized by the same critical exponents as those for the critical attenuation of the sound wave near the critical points in liquid-gas phase transitions.

Contents

Acknowledgements	3
Summary	5
1 Introduction	11
2 Overview of QCD	15
2.1 Quantum Chromodynamics	15
2.1.1 Lagrangian	15
2.1.2 Asymptotic freedom	16
2.1.3 Symmetries	17
2.2 Phase structure	20
2.2.1 Order parameters	20
2.2.2 Formation of diquark condensate in high-density QCD	22
2.2.3 Symmetry breaking patterns	23
2.3 Chiral magnetic effect	24
2.3.1 Symmetry argument	25
2.3.2 Derivation	26
2.3.3 Chiral magnetic wave	30
3 Theory of dynamic critical phenomena	33
3.1 Dynamic universality class	33
3.2 Formulation	35
3.2.1 Ginzburg-Landau theory	35
3.2.2 Langevin theory	37
3.2.3 Dynamic perturbation theory	39
3.3 Renormalization group analysis	40
3.3.1 Statics	41

3.3.2	Dynamics	45
4	Dynamic critical phenomena of the high-density QCD critical point	47
4.1	Hydrodynamic variables	47
4.2	Static critical phenomena	48
4.3	Dynamic critical phenomena	50
4.3.1	Langevin theory	50
4.3.2	Hydrodynamic modes	52
4.3.3	Dynamic critical exponent	53
4.4	Conclusion and discussion	54
5	Dynamic critical phenomena induced by the chiral magnetic effect in QCD	57
5.1	Setup	57
5.1.1	Symmetries	57
5.1.2	Hydrodynamic variables	59
5.2	Formulation	60
5.2.1	Langevin theory	60
5.2.2	Dynamic perturbation theory	61
5.3	Renormalization-group analysis	66
5.3.1	Statics	67
5.3.2	Dynamics	69
5.3.3	Physical consequences	78
5.4	Conclusion and discussion	79
6	Summary and outlook	81
A	Static RG of the scalar field theory	83
A.1	Perturbative RG equation	83
A.2	Wilson-Fisher fixed point	88
A.3	Useful integrals	89
B	Coupling to energy-momentum densities	91
B.1	Statics	91
B.2	Dynamics	93
B.2.1	Full Langevin equations	93
B.2.2	Decomposition of momentum density	95

<i>CONTENTS</i>	9
B.2.3 Hydrodynamic modes	96
B.2.4 Dynamic critical exponent	98
C Calculation of the self-energies and the vertex function	101
C.1 Self-energy Π	101
C.2 Self-energy Σ	103
C.3 Vertex function \mathcal{V}	107
D Linear-stability analysis on the fixed points (iii) and (iv)	111

Chapter 1

Introduction

Quantum Chromodynamics (QCD) is the fundamental theory of the strong interaction between quarks and gluons. One of the remarkable features of QCD is the asymptotic freedom: the coupling constant of the strong interaction becomes small when the typical energy scale of the system is getting large. When the energy scale is lower than the intrinsic scale of QCD, $\Lambda_{\text{QCD}} \sim 200$ MeV, the coupling constant becomes large, and the perturbation theory breaks down. In this low-energy regime, quarks and gluons are confined in color-neutral hadrons, such as baryons made of three quarks and mesons consisting of a quark and an antiquark. Another property of low-energy QCD is the spontaneous breaking of chiral symmetry. The chiral symmetry of QCD in the massless quark limit is broken in the vacuum. In the real world with finite quark masses, the chiral symmetry is an approximate symmetry for the light quarks, especially up and down quarks whose masses are sufficiently smaller than Λ_{QCD} .

What happens to matter when it is heated and/or squeezed up to the orders of Λ_{QCD} ? Such matter under extreme conditions at high temperature $T \sim 10^{12}$ kelvin and/or baryon chemical potential μ_{B} (corresponding to mass density $\sim 10^{12}$ kg/cm³), can also be described by QCD. However, it has been a long-standing problem to understand the phase structure of QCD at finite T and μ_{B} [1]. Figure 1.1 shows a conjectured phase digram. At low T and low μ_{B} , the chiral symmetry is spontaneously broken in the hadron phase, whereas it is restored at sufficiently high T , and the quark-gluon plasma is realized. On the other hand, at high μ_{B} , quarks form Cooper pairs induced by the attractive one-gluon exchange interaction. It follows that the gluons acquire finite masses in an analogy of the gapped photons in

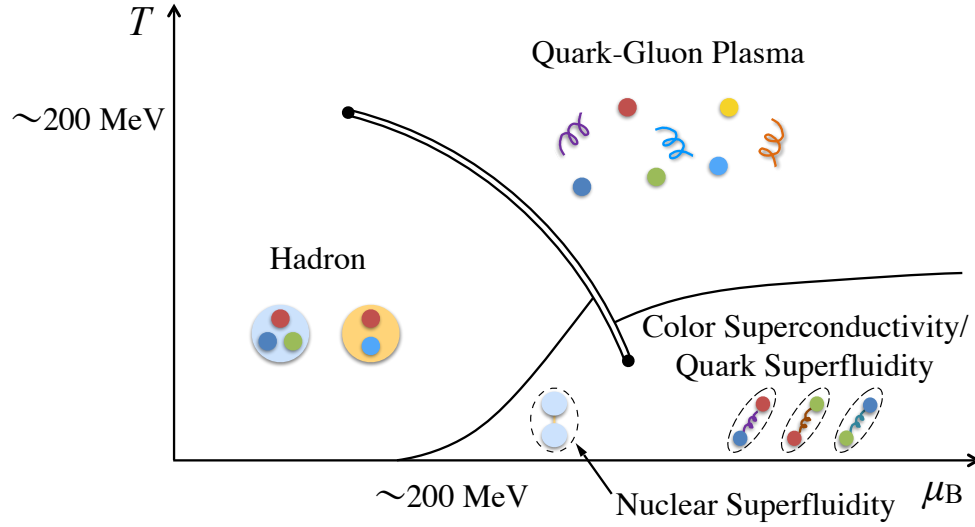


Figure 1.1: Schematic phase diagram of QCD

ordinary superconductors. This state is called the “color superconductivity.” Besides, quark matter and nuclear matter can exhibit the superfluidity as a consequence of the spontaneous breaking of the symmetry associated with the baryon number conservation.

As is also illustrated in Fig. 1.1, there are two possible QCD critical points where the first-order chiral phase transition line (the doubled line in Fig. 1.1) terminates. One is the high-temperature critical point between the hadron phase and the quark-gluon plasma phase [2]; the other is the high-density critical point between the nuclear and quark superfluid phases [3, 4, 5]. An important task is to understand the dynamic critical phenomena in QCD. In general, dynamic critical phenomena can be classified based on the symmetries and the low-energy gapless modes of systems near a second-order phase transition or a critical point. Such a classification of dynamic critical phenomena is called the dynamic universality class [6]. In QCD, the high-temperature critical point belongs to the same dynamic universality class as that of the nuclear liquid-gas critical point [7, 8, 9, 10], the so-called model H within the conventional classification by Hohenberg and Halperin [6]. On the other hand, the second-order chiral phase transition in massless two-flavor QCD at finite T and zero μ_B belongs to the same class as that of $O(4)$ antiferromagnets [11].

Relativistic heavy-ion collision experiments can potentially test these

QCD critical points [12]. In particular, one of the big goals of the Beam Energy Scan (BES) program at the Relativistic Heavy Ion Collider (RHIC) is to search for the high-temperature QCD critical point [13]. Moreover, theoretical predictions specific to dense QCD matter would be crucial for the future low-energy heavy-ion collisions at Facility of Antiproton and Ion Research (FAIR), Nuclotron-based Ion Collider Facility (NICA), Japan Proton Accelerator Research Complex (J-PARC), and Heavy Ion Research Facility (HIRF).

On the other hand, the BES program at RHIC has another goal [13] to search for the anomalous chiral transport phenomena related to the quantum anomaly [14, 15]. One typical example is the chiral magnetic effect (CME), which is the generation of the electric current along the magnetic field [16, 17, 18, 19]. In particular, a remarkable consequence of the CME is the creation of the density-wave called the chiral magnetic wave (CMW) [20, 21]. Although possible signals consistent with the presence of the CME may have been observed in RHIC [22, 23] and also in Large Hadron Collider (LHC) [24], it is pointed out that there are ambiguities in this interpretation due to possible background effects not related to the CME [25]. ¹These ambiguities are currently tested by comparing collisions of the isobaric nuclei such as $^{96}_{44}\text{Ru}$ and $^{96}_{40}\text{Zr}$, with the same background contributions but different CME signals due to the nuclear-charge difference [26].

In this thesis, we study the novel dynamic critical phenomena induced by the superfluidity and the CME in QCD, *respectively*. In each case, we use the low-energy effective theory based on the symmetries and the hydrodynamic variables of QCD.

For the first subject, we construct the low-energy effective theory of the system near the high-density QCD critical point and study its static and dynamic critical phenomena [28]. In particular, we find the critical slowing down of the speed of the superfluid phonon. Moreover, we find that the dynamic universality class of the high-density critical point is not only different from that of the high-temperature critical but also is a *new class beyond the Hohenberg and Halperin's conventional classification* [6]. This new universality class stems from the interplay specific to QCD between the chiral order parameter and the superfluid photon. Therefore, observation of the dynamic

¹ On the other hand, the CME has already been observed in the table-top experiments of the Weyl/Dirac semimetals (see, e.g., Ref. [27]). In these systems, relativistic fermions appear as quasiparticles close to the band touching points.

critical phenomenon in the vicinity of the high-density critical point would provide indirect evidence of superfluidity in the dense-QCD matter.

For the second subject, we study the dynamic critical phenomena of the second-order chiral phase transition in massless QCD under an external magnetic field [29], and clarify the interplay between the dynamic critical phenomena and the CME in QCD. For this purpose, we first construct the nonlinear Langevin equations incorporating the quantum-anomaly effects [30, 31], and study it by using the dynamic renormalization group [32, 33, 34]. As a result, we show that the inclusion of the CME changes the dynamic universality class from the model E into model A within the conventional classification. We also find that the speed of the CMW tends to zero near the phase transition. We here observe the same critical exponents as those of the critical attenuation of the sound wave known in the system near the liquid-gas critical point [35].

This thesis is organized as follows. In Chap. 2, we give a brief overview of QCD. In Chap. 3, we review the theory of dynamic critical phenomena. Based on the reviews above, in Chap. 4, we study the static and dynamic critical phenomena of the high-density QCD critical point. In Chap. 5, we clarify the interplay between the dynamic critical phenomena and the CME in QCD. Finally, we conclude with Chap. 6. Among others, Chaps. 4 and 5 are based on our original papers [28] and [29], respectively. The work [28] is a collaboration with N. Yamamoto, and the work [29] is a collaboration with M. Hongo and N. Yamamoto.

In this thesis, we will work in natural units, where the speed of light, the reduced Plank constant, the elementary charge, and the Boltzmann constant are set equal to unity, $c = \hbar = e = k_B = 1$.

Chapter 2

Overview of QCD

We here give an overview of QCD. We start with its basic properties in Sec. 2.1. Next, in Sec. 2.2, we review the phase structure of QCD. In Sec. 2.3, we provide a brief explanation of the CME.

2.1 Quantum Chromodynamics

In Sec. 2.1.1, we first introduce the Lagrangian of QCD. In section 2.1.2, we next explain the asymptotic freedom. Then, in Sec. 2.1.3, we summarize the internal symmetries of QCD.

2.1.1 Lagrangian

The Lagrangian (density) of QCD is given by

$$\mathcal{L}_{\text{QCD}} = \mathcal{L}_{\text{quark}} + \mathcal{L}_{\text{gluon}}, \quad (2.1)$$

where

$$\mathcal{L}_{\text{quark}} = \bar{q}_i (i\gamma^\mu D_\mu - m_i) q_i, \quad (2.2)$$

$$\mathcal{L}_{\text{gluon}} = -\frac{1}{2} \text{Tr} G_{\mu\nu} G^{\mu\nu}. \quad (2.3)$$

Here, $\mathcal{L}_{\text{quark}}$ is the kinetic term for the quark field q . The quark field $q(x)$ has the internal degrees of freedom in addition to the coordinates $x^\mu = (t, \mathbf{x})$: the first one is the flavor labeled by $i = 1, \dots, N_f$. There are six flavors of quarks in QCD: up (u), down (d), charm (c), strange (s), top (t), bottom

(b). Quarks of different flavors have different masses m_i . U, c, and t quarks have the electric charge $+2/3$, while d, s, and b quarks have the electric charge $-1/3$, in a unit of the elementary charge. The second one is the spinor component running $1, \dots, 4$ with γ^μ being a 4×4 matrix in the Dirac space. The antiquark field is defined by $\bar{q}_i \equiv q_i^\dagger \gamma^0$. The last one is the color labeled by $1, \dots, N_c$. The quark field is coupled to the gluon field A_μ^a ($a = 1, \dots, N_c^2 - 1$) through the covariant derivative,

$$D_\mu \equiv \partial_\mu - igA^\mu, \quad (2.4)$$

where g is the interaction strength; t^a is the generators of the color $SU(N_c)$ space with

$$[t^a, t^b] = if_{abc}t^c, \quad \text{Tr}(t^a t^b) = \frac{\delta^{ab}}{2}. \quad (2.5)$$

Here, f_{abc} is called the structure constants.

Let us see that $\mathcal{L}_{\text{gluon}}$ includes the kinetic term for the gluon fields and their self-interactions. In Eq. (2.3), $G_{\mu\nu}^a$ is the field strength defined in the following form:

$$G_{\mu\nu} \equiv \frac{i}{g}[D_\mu, D_\nu]. \quad (2.6)$$

By using Eq. (2.4), one can write Eq. (2.6) into

$$G_{\mu\nu} = (\partial_\mu A_\nu^a - \partial_\nu A_\mu^a + gf_{abc}A_\mu^b A_\nu^c) t^a. \quad (2.7)$$

From this expression, one can also rewrite $\mathcal{L}_{\text{gluon}}$ into

$$\mathcal{L}_{\text{gluon}} = -\frac{1}{4} (\partial_\mu A_\nu^a - \partial_\nu A_\mu^a)^2 - gf_{abc}(\partial^\mu A_\nu^a) A_\mu^b A_\nu^c - \frac{g^2}{4} f_{abc} f_{ade} A_\mu^b A_\nu^c A_d^\mu A_e^\nu. \quad (2.8)$$

Here, the first term is the kinetic term for the gluon fields; the second and the third terms are 3- and 4-points interaction terms among the gluons.

2.1.2 Asymptotic freedom

One of the remarkable features of QCD is the asymptotic freedom [36, 37]: the coupling constant g becomes smaller when the typical energy scale is

getting large. Generally, in field theories, when one takes into account perturbative loop-corrections, there are some divergences in the calculations. To remove those divergences and obtain some physically meaningful results, the parameters in the Lagrangian should be no more constants but depend on the typical energy scale at which such divergences are removed by renormalizing the parameters. This is also the case for the interaction parameter g introduced in Eq. (2.4) in QCD. It is known that the interaction strength g satisfies the following renormalization group equation to its leading order:

$$\mu \frac{\partial g}{\partial \mu} = -\frac{b_0}{(4\pi)^2} g^3 + \mathcal{O}(g^5), \quad (2.9)$$

with μ being the renormalization scale and $b_0 \equiv \frac{11}{3}N_c - \frac{2}{3}N_f$. Since Eq. (2.9) can be solved by the separation of variables method at this order, by defining $\alpha_s \equiv g^2/(4\pi)$, one finds the solution as

$$\alpha_s(\mu) = \frac{2\pi}{b_0 \log(\mu/\Lambda_{\text{QCD}})}, \quad (2.10)$$

where $\Lambda_{\text{QCD}} \approx 200$ MeV is the typical energy scale of QCD, and several experiments determines its value [38]. This solution shows that the interaction strength $\alpha_s(\mu)$ runs towards a smaller value as $\propto 1/\log(\mu)$ when the typical energy scale of the system μ increases.

2.1.3 Symmetries

The internal symmetries of QCD can be summarized as

$$\mathcal{G} = \text{SU}(N_c)_C \times \text{SU}(N_f)_L \times \text{SU}(N_f)_R \times \text{U}(1)_B, \quad (2.11)$$

where each symmetry group is defined as follows. Note here that the U(1) axial symmetry is not included in \mathcal{G} from the reason given at the end of this subsection.

Color gauge symmetry

The color gauge symmetry $\text{SU}(N_c)_C$ is the invariance under the following gauge transformation in color $\text{SU}(N_c)$ space:

$$q \rightarrow V_C q, \quad A_\mu \rightarrow V_C A_\mu V_C^\dagger + \frac{i}{g} (\partial_\mu V_C) V_C^\dagger, \quad V_C \equiv e^{-i\theta^a(x)t^a}. \quad (2.12)$$

Here $\theta^a(x)$ is a local transformation parameter that depends on the coordinates (for the definition of t^a , see Eq. (2.5)).

To see the invariance of QCD Lagrangian under Eq. (2.12), we first calculate the transformation laws for $D_\mu q$ and the field strength $G_{\mu\nu}$,

$$D_\mu q \rightarrow V_C(D_\mu q), \quad (2.13)$$

$$G_{\mu\nu} \rightarrow V_C G_{\mu\nu} V_C^\dagger. \quad (2.14)$$

Here, one can derive the second transformation by using the first one. (See Eqs. (2.4) and (2.6) for the definitions of the covariant derivative D_μ and $G_{\mu\nu}$, respectively.) From Eqs. (2.13) and (2.14), one can confirm that \mathcal{L}_{QCD} is invariant under the color gauge transformation (2.12).

Chiral symmetry

The chiral symmetry $\text{SU}(N_f)_L \times \text{SU}(N_f)_R$ is the invariance under the independent rotation of right-handed and left-handed components of the quark field in the flavor space. Here, the right-handed quark q_R and the left-handed quark q_L are defined by

$$q_L \equiv \frac{1 - \gamma_5}{2} q, \quad q_R \equiv \frac{1 + \gamma_5}{2} q. \quad (2.15)$$

These transformations under the chiral transformation are

$$q_L \rightarrow V_L q_L, \quad q_R \rightarrow V_R q_R, \quad V_{L,R} \equiv e^{-i\theta_{L,R}^a \lambda^a}. \quad (2.16)$$

Here, λ^a being the generator of $\text{SU}(N_f)_{L,R}$. Note that the transformation parameters $\theta_{L,R}^a$ do not depend on x^μ (generally such a transformation is called a global symmetry), unlike $\theta^a(x)$ introduced in Eq. (2.12) for the color gauge symmetry.

Let us see the chiral transformation (2.16) of the QCD Lagrangian (2.1). We first decompose the quark fields into

$$q = q_R + q_L, \quad (2.17)$$

and rewrite the quark sector of the QCD Lagrangian (2.2) into

$$\mathcal{L}_{\text{quark}} = \bar{q}_L i \gamma^\mu D_\mu q_L + \bar{q}_R i \gamma^\mu D_\mu q_R - \bar{q}_L \hat{m} q_R - \bar{q}_R \hat{m} q_L. \quad (2.18)$$

Here, \hat{m} denotes the matrix in the flavor space, and its components are given by m_i . In Eq. (2.18), the first two terms are invariant under the chiral transformation, whereas the last two mass terms are not invariant except for the particular *vector*-like choice of the transformation parameters $\lambda_L^a = \lambda_R^a$.¹ Therefore, the chiral symmetry is exact only when one sets the quark masses m_i to zero (this massless limit is called the chiral limit). Practically, the mass of u quark, $m_u \approx 3$ MeV and that of d quark, $m_d \approx 5$ MeV are small compared to Λ_{QCD} introduced in Sec. 2.1.2. In general, the chiral symmetry is an approximate symmetry of QCD, when m_i is small compared to any typical energy scales of the system.

Baryon number symmetry

The baryon number symmetry $U(1)_B$ is the invariance under

$$q \rightarrow e^{-i\alpha_B} q, \quad (2.19)$$

where α_B is the global transformation parameter. The QCD Lagrangian is invariant under this transformation.

U(1) axial symmetry and its quantum anomaly

In addition to the symmetry group \mathcal{G} , the *classical Lagrangian* of QCD has the approximate axial symmetry $U(1)_A$, which is the invariance under

$$q \rightarrow e^{-i\alpha_A \gamma_5} q, \quad (2.20)$$

where α_A is the transformation parameter. This transformation is equivalent to

$$q_L \rightarrow e^{i\alpha_A} q_L, \quad q_R \rightarrow e^{-i\alpha_A} q_R. \quad (2.21)$$

Similarly to the chiral symmetry, $U(1)_A$ can be regarded as an approximate symmetry of QCD at the *classical Lagrangian level* in the presence of small quark masses m_i . However, it is known that the quantum effects break the $U(1)$ axial symmetry [39, 40],

$$U(1)_A \xrightarrow{\text{anomaly}} \mathbb{Z}(2N_f)_A. \quad (2.22)$$

¹ *Vector* transformations are in-phase between left- and right-handed quarks. Meanwhile, *Axial* transformations are opposite-phase rotation with different chirality.

Here, $\mathbb{Z}(2N_f)_A$ corresponds to the symmetry under the parameter choices of the parameter $\alpha_A = n\pi/N_f$ ($n = 1, \dots, 2N_f$).² Because of the presence of this quantum anomaly effect, we distinguish $U(1)_A$ from the symmetry group \mathcal{G} . We will discuss the residual part $\mathbb{Z}(2N_f)_A$ in the context of the continuity between the nuclear/quark superfluid phases at the end of Sec. 2.2.3.

2.2 Phase structure

We introduce the order parameters of QCD and discuss those symmetry breaking patterns in Sec. 2.2.1. Section 2.2.2 is devoted to explaining why the diquark condensation is favored at high-density QCD. In Sec. 2.2.3, we classify the phases of Fig. 1.1 by using the order parameters.

2.2.1 Order parameters

The symmetry group of QCD, \mathcal{G} given in Eq. (2.11) can be spontaneously broken in the ground states. This spontaneous symmetry breaking can be characterized by the two representative order parameters in QCD defined as follows.

Note that in this subsection, we explicitly write the flavor and the color indices:

$$i, j, k, \dots = \text{u, d, s, } \dots \quad (\text{flavor}); \quad (2.23)$$

$$A, B, C, \dots = \text{r, g, b, } \dots \quad (\text{color}), \quad (2.24)$$

where color indices range over red, green, and blue, ... (r,g,b,...) in general. The general transformation laws under all of the symmetries introduced in Sec. 2.1.3, $\mathcal{G} \times U(1)_A$ can be written as follows:

$$(q_L)_A^i \rightarrow e^{i\alpha_A} e^{-i\alpha_B} (V_L)_{ij} (V_C)_{AB} (q_L)_B^j, \quad (2.25)$$

$$(q_R)_A^i \rightarrow e^{-i\alpha_A} e^{-i\alpha_B} (V_R)_{ij} (V_C)_{AB} (q_R)_B^j. \quad (2.26)$$

²Unlike the chiral anomaly in the background electromagnetic field in Eq. (2.66), the divergence of the $U(1)_A$ current in the presence of the gluons, discussed here, is related to the topological charge called the instanton number of the non-Abelian gauge field. This *topological nature* leads to the invariance for some particular *discrete* choices of the parameters for $U(1)_A$ transformation, $\mathbb{Z}(2N_f)_A$. See, e.g., Refs. [39, 41] for the details.

Chiral order parameter

One of the important order parameters in QCD is the chiral order parameter defined by

$$\Phi_{ij} \equiv \langle (\bar{q}_R)_A^j (q_L)_A^i \rangle, \quad (2.27)$$

which is the matrix in the flavor space. By using Eqs. (2.25) and (2.26), one finds that this order parameter is transformed under $\mathcal{G} \times U(1)_A$ as

$$\Phi_{ij} \rightarrow e^{-2i\alpha_A} (V_L)_{ik} \Phi_{kl} (V_R^\dagger)_{lj}. \quad (2.28)$$

We note that the determinant of Φ characterizes the quantum anomaly [40]. The transformation law under (2.28):

$$\det \Phi \rightarrow e^{-2i\alpha_A} \det \Phi, \quad (2.29)$$

follows that $\det \Phi$ preserves the chiral symmetry $SU(N_f)_L \times SU(N_f)_R$ but breaks $U(1)_A$. Here, we use Eq. (2.28) and $\det V_L = \det V_R = 1$ to derive Eq. (2.29).

The chiral order parameter breaks the chiral symmetry into the subgroup:

$$SU(N_f)_L \times SU(N_f)_R \rightarrow SU(3)_{L+R}, \quad (2.30)$$

where $SU(N_f)_{L+R}$ is the invariance under the *vector*-like choice of the parameters, $V_L = V_R$. Therefore, the chiral order parameter is an order parameter characterizing the spontaneous breaking of the chiral symmetry. Note here that $U(1)_A$ is not spontaneously broken, because the quantum effects have already broken this symmetry as we explained in Sec. 2.1.3.

Diquark condensate

The second order parameter in QCD is the diquark condensate. Each of the right-hand and left-handed quark fields is defined by

$$(d_L^\dagger)_{Ai} \equiv \varepsilon_{ABC} \varepsilon_{ijk} \langle (q_L)_B^j \mathcal{O}_C (q_L)_C^k \rangle, \quad (2.31)$$

$$(d_R^\dagger)_{Ai} \equiv \varepsilon_{ABC} \varepsilon_{ijk} \langle (q_R)_B^j \mathcal{O}_C (q_R)_C^k \rangle. \quad (2.32)$$

Here, two of the quark fields in each of $d_{R,L}^\dagger$ are chosen to be antisymmetric under the exchanges of the color and flavor, respectively (and also the spin

which is not explicit in these expressions). The labels of quarks in the right-hand sides will be confirmed in Sec. 2.2.2. Besides, \mathcal{O}_C denotes the charge conjugation operator

$$\mathcal{O}_C \equiv i\gamma^2\gamma^0, \quad (2.33)$$

which is also necessary for the diquark condensate being a Lorentz scalar. By using Eqs. (2.25) and (2.26), the diquark condensates are transformed by $\mathcal{G} \times U(1)_A$ as follows:

$$(d_L)_{Ai} \rightarrow e^{2i\alpha_A} e^{-2i\alpha_B} (V_L)_{ij} (V_C)_{AB} (d_L)_{Bj}, \quad (2.34)$$

$$(d_R)_{Ai} \rightarrow e^{-2i\alpha_A} e^{-2i\alpha_B} (V_R)_{ij} (V_C)_{AB} (d_L)_{Bj}. \quad (2.35)$$

Let us consider the realistic colors and focus our attention on the light quarks, and set $N_C = N_f = 3$. The diquark condensate breaks the color gauge symmetry and the chiral symmetry into their *mixed* subgroup:

$$SU(3)_C \times SU(3)_L \times SU(3)_R \rightarrow SU(3)_{C+L+R}. \quad (2.36)$$

Here, $SU(3)_{C+L+R}$ symmetry is the invariance under the particular combination of the gauge transformation and the chiral transformation, $V_C^\dagger = V_L = V_R$. One can confirm this invariance by using the transformation law of the diquark condensate (2.34). The resulting phase is invariant under *simultaneous* color and flavor transformations. For this reason, it is called the color flavor locked phase [42]. From Eq. (2.36), the diquark condensate is an order parameter characterizing the color superconductivity, which is the ‘‘spontaneous breaking’’ of the color gauge symmetry. In addition to this color gauge symmetry breaking, the diquark condensate also breaks the baryon symmetry,

$$U(1)_B \rightarrow \mathbb{Z}(2)_B, \quad (2.37)$$

where $\mathbb{Z}(2)_B$ is the discrete symmetry, which corresponds to the choices of the parameter, $\alpha_B = 0, \pi$ in Eq. (2.19). Therefore, the diquark condensate is also an order parameter for the superfluidity characterized by the spontaneously breaking of the $U(1)_B$ symmetry.

2.2.2 Formation of diquark condensate in high-density QCD

In the high-density QCD ($\mu_B \gg \Lambda_{\text{QCD}}, T$), quarks form a diquark condensate. In this regime, the degenerate quarks near the Fermi surface can be described

by the weakly coupled QCD due to the asymptotic freedom. The interaction between two quarks is dominated by the one-gluon exchange which is proportional to a product of the SU(3) interaction vertices,

$$(t^a)_{AB}(t^a)_{CD} = \frac{1}{6}(\delta_{AB}\delta_{CD} + \delta_{AC}\delta_{BD}) - \frac{1}{3}(\delta_{AB}\delta_{CD} - \delta_{AC}\delta_{BD}). \quad (2.38)$$

Here, the first/last two terms represent the repulsive/attractive interaction between the quarks whose color labels are symmetric/antisymmetric under the exchange of A and C or B and D , respectively. Degenerate fermionic systems with a 2-body (4-point) attractive interaction have the instabilities towards the formation of the Cooper pairs [43, 44]. According to this BCS mechanism, quarks form Cooper pairs in the attractive channels, and the finite diquark condensate is realized as the ground state of high-density QCD [45, 46, 47, 48].

The color, flavor, and spin structure of the diquark condensate are determined as follows. The color indices should be antisymmetric to have an attractive interaction. The spin indices should also be antisymmetric so that the total spin of the diquark condensate is zero. This isotropic combination is energetically favorable in general because it allows efficient use of the Fermi surface. Finally, from the Pauli principle, the flavor indices should also be antisymmetric.

2.2.3 Symmetry breaking patterns

Here, we will look at the phases classified by the chiral order parameter Φ_{ij} and the diquark condensate $d_{R,L}$ [3, 4]. Let us consider $N_C = N_f = 3$ and the most symmetric ground state:

$$\Phi_{ij} = \sigma\delta_{ij}, \quad (2.39)$$

$$(d_L)_{Ai} = -(d_R)_{Ai} = \delta_{Ai}\phi. \quad (2.40)$$

Here, σ is called the chiral condensate.

In principle, there are four possible phases characterized by σ and ϕ , as summarized in Table 2.1. Here, the symmetry breaking patterns of the individual phases are also listed (\mathcal{H} denotes the unbroken symmetry of \mathcal{G}). The chiral condensate σ classifies the quark-gluon plasma phase and the hadron phase. It is approximately zero (of an order of the quark mass) in the quark-gluon plasma phase and is finite in the hadron phase. On the other

Phase	Unbroken Symmetries \mathcal{H}	Order Parameters	
Quark-Gluon Plasma	\mathcal{G}	$\sigma \sim 0$	$\phi = 0$
Hadron	$SU(3)_C \times SU(3)_{L+R} \times U(1)_B$	$\sigma \neq 0$	$\phi = 0$
Color Superconductivity/ Quark Superfluidity	$SU(3)_{C+L+R} \times \mathbb{Z}(2)_B$	$\sigma \sim 0$	$\phi \neq 0$
Nuclear Superfluidity	$SU(3)_{C+L+R} \times \mathbb{Z}(2)_B$	$\sigma \neq 0$	$\phi \neq 0$

Table 2.1: Symmetry breaking patterns of QCD phase diagram [3]

hand, any symmetries cannot distinguish the two superfluid phases, so that these two phases can be continuously connected. This conjecture is called the hadron-quark continuity [49].

Let us see the crossover of the superfluid phases on the aspects of the chiral symmetry and the $U(1)_A$ symmetry following the argument in Ref. [3]. We consider the order parameter, $(d_L)_{Ai}(d_R^\dagger)_{Aj} = -\phi^2\delta_{ij}$, which breaks these symmetries,

$$(d_L)_{Ai}(d_R^\dagger)_{Aj} \rightarrow e^{4i\alpha_A}(V_L)_{ik}(d_L)_{Ak}(d_R^\dagger)_{Al}(V_R)_{lj}. \quad (2.41)$$

The quark superfluid phase with finite $\phi^2 \neq 0$ breaks the chiral symmetry but preserves $\mathbb{Z}(4)_A$ ($\alpha_A = 0, \pi/2, \pi, 3\pi/2$) of $U(1)_A$ as a subgroup. On the other hand, in the nuclear superfluid phase, $\sigma \neq 0$ and $\phi^2 \neq 0$ break the chiral symmetry but preserves $\mathbb{Z}(2)_A$ ($\alpha_A = 0, \pi$). At a glance, the residual discrete $U(1)_A$ symmetries look different. However, the quantum anomaly has already broken $U(1)_A$ into $\mathbb{Z}(6)_A$, which includes $\mathbb{Z}(2)_A$ but not $\mathbb{Z}(4)_A$. The residual $U(1)_A$ symmetry is the same $\mathbb{Z}(2)_A$ in both phases, in the presence of the quantum anomaly. Not only the chiral symmetry but also $U(1)_A$ symmetry cannot classify the nuclear/quark superfluid phases.

2.3 Chiral magnetic effect

So far, we have discussed the static properties of QCD. In this section, we discuss its dynamics. Chiral transport phenomena are the novel macroscopic transport phenomena induced by the chirality of quarks in QCD. As an example, we here discuss the so-called chiral magnetic effect (CME). In Sec. 2.3.1,

we first demonstrate that the CME is a phenomenon specific to the presence of the chirality imbalance from the symmetry arguments. Next in Sec. 2.3.2, we derive the CME for noninteracting quarks under an external magnetic field. Finally, in Sec. 2.3.3, we discuss the relevance of the CME to the low-energy hydrodynamic modes. In this section, we consider the chiral limit and set $m_i = 0$.

2.3.1 Symmetry argument

We here discuss the symmetry aspects of the CME. Let us write the electric current \mathbf{j} by using the electric field \mathbf{E} and the magnetic field \mathbf{B} . From the rotational symmetry of the system, we obtain

$$\mathbf{j} = \sigma_E \mathbf{E} + \sigma_B \mathbf{B}, \quad (2.42)$$

where σ_E and σ_B are some constants. The first term is nothing but the Ohmic law, which is allowed in the usual matter without chirality imbalance. On the other hand, the second term is allowed when σ_B is proportional to the chirality imbalance

$$\mu_5 = \frac{\mu_R - \mu_L}{2}. \quad (2.43)$$

The parity transformation leads to

$$\mathbf{j} \rightarrow -\mathbf{j}, \quad \mathbf{E} \rightarrow -\mathbf{E}, \quad \mathbf{B} \rightarrow \mathbf{B}, \quad (2.44)$$

and

$$\mu_5 \rightarrow -\mu_5. \quad (2.45)$$

One can understand the last transformation by using the fact that the parity transformation exchanges the chirality,

$$\mu_R \rightarrow \mu_L, \quad \mu_L \rightarrow \mu_R. \quad (2.46)$$

As we will see in Sec. 2.3.2 (in particular in Eq. (2.72)), the CME is the generation of such second term with [16, 17, 18, 19]

$$\sigma_B = \frac{\mu_5}{2\pi^2}. \quad (2.47)$$

2.3.2 Derivation

We here first derive the chiral anomaly in the presence of the background electromagnetic fields and the CME. In this subsection, we first neglect the gluons and discuss these effects later. The discussion here follows the original argument in Ref. [18] and also the recent lecture notes [50, 51].

Landau Level

Let us consider the Weyl equation for the left-handed quark q_L ,

$$i\bar{\sigma}^\mu D_\mu q_L = 0, \quad (2.48)$$

where $\bar{\sigma}^\mu = (1, -\sigma^i)$, $D_\mu = \partial_\mu - iA_\mu$, and A^μ is the $U(1)_{\text{em}}$ gauge field. The Weyl equation can be written as

$$i(\partial_t - \sigma^i D_i)q_L = 0. \quad (2.49)$$

We set the magnetic field in the z direction, $\mathbf{B} = (0, 0, B)$, and take the particular

$$(A_x, A_y, A_z) = (0, Bx, 0). \quad (2.50)$$

We write the 2-component field q_L as

$$q_L = e^{-i(\omega t - k_y y - k_z z)} \begin{pmatrix} q_- \\ q_+ \end{pmatrix}, \quad (2.51)$$

with ω and k_i ($i = y, z$) being the energy and the momentum of the quark, respectively. Then, by substituting Eq. (2.51) into Eq. (2.49), we find

$$\begin{pmatrix} \omega + k_z & -i(\partial_x - Bx + k_y) \\ -i(\partial_x + Bx - k_y) & \omega - k_z \end{pmatrix} \begin{pmatrix} q_- \\ q_+ \end{pmatrix} = 0. \quad (2.52)$$

We can readily obtain the following solution of this equation:

$$\omega = -k_z; \quad q_- \propto \exp\left[-\frac{(Bx - k_y)^2}{2B}\right], \quad q_+ = 0, \quad (2.53)$$

whereas a similar form,

$$\omega = k_z; \quad q_+ \propto \exp\left[\frac{(Bx - k_y)^2}{2B}\right], \quad q_- = 0, \quad (2.54)$$

is not a solution because we cannot normalize the eigenvector in a particular way at $x \rightarrow \infty$. On the other hand, the Weyl equation for the right-handed quark is

$$i\sigma^\mu D_\mu q_R = 0, \quad (2.55)$$

with $\sigma^\mu = (1, \sigma^i)$ yields the solution for $\omega = k_z$ with the normalized eigenvector. Therefore, we obtain the zero eigenenergies of the Dirac fermion q including both of the Weyl fermions q_L and q_R ,

$$\omega = \pm k_z, \quad (2.56)$$

where the signs correspond to different chirality of the quarks. These gapless eigenmodes are called the lowest Landau level.

In general, the dispersion relation for Eq. (2.52) can be calculated as

$$\omega^2 = k_z^2 + B(2n + 1 - s), \quad (2.57)$$

where $n = 0, 1, 2, \dots$ and $s = \pm 1$ is the eigenvalue of σ^z . The lowest Landau level corresponds to $(n, s) = (0, 1)$. Note that Eq. (2.57) does not depend on k_y , so that any eigenvalues are degenerated by all of the degrees of freedom that k_y can take in our gauge choice. This is called the Landau degeneracy, and it is given by $B/(2\pi)$ per unit area.³

Chiral anomaly

We here derive the chiral anomaly. Figure. 2.1(a) shows the spectrum in a static magnetic field, i.e., the dispersion relation (2.57). Here, the branches

³Let us calculate the Landau degeneracy. We consider the xy -plane bounded by $0 < x < L_x$, $0 < y < L_y$. The momentum in y direction can take $k_y = 2\pi n_y/L_y$, ($n_y \in \mathbb{Z}$). However, the center of the wave function $x_c \equiv B/k_y$ must be inside the range of x . This yields the upper limit of n_y such that

$$0 < \frac{B}{k_y} < L_x \Leftrightarrow 0 < n_y < \frac{L_x L_y B}{2\pi}. \quad (2.58)$$

All of the modes included in this inequality contribute to the degeneracy. The number of such modes per unit area is:

$$N_y = \frac{B}{2\pi}. \quad (2.59)$$

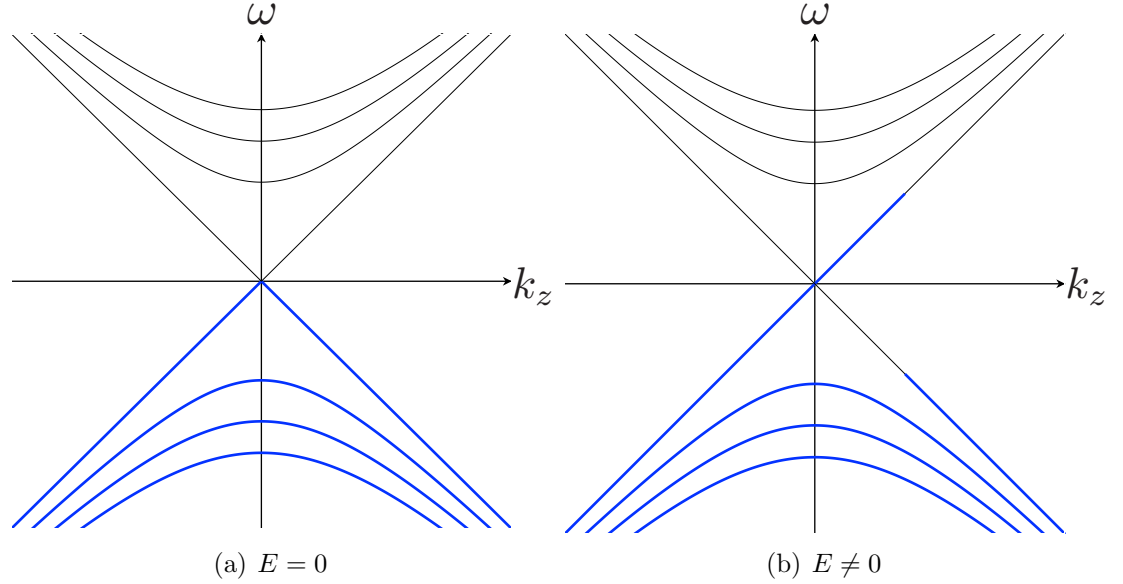


Figure 2.1: Occupied states of Dirac fermions in a static magnetic field in the presence/absence of the electric field E .

crossing the origin correspond to the lowest Landau level (2.56), and the other curves correspond to the higher Landau levels.

Next, we apply an electric field in the z -direction, $\mathbf{E} = (0, 0, E)$. Then, the electric field accelerates the particles,

$$\frac{\partial k_z}{\partial t} = E. \quad (2.60)$$

When we apply the electric field by time τ , the fermions acquire finite momentum,

$$\Delta k_z = E\tau. \quad (2.61)$$

We illustrate the occupied state after applying the electric field E as Fig. 2.1(b). We can interpret here that some of the minus-energy particles are excited to get positive energy. In this accelerating process, the charges for the right-

handed and left-handed fermions in volume V are varied by

$$\Delta Q_{\text{R}} = \frac{BV}{2\pi} \int_0^{\Delta k_z} \frac{dk_z}{2\pi} = \frac{\tau V E B}{4\pi^2}, \quad (2.62)$$

$$\Delta Q_{\text{L}} = -\frac{BV}{2\pi} \int_0^{\Delta k_z} \frac{dk_z}{2\pi} = -\frac{\tau V E B}{4\pi^2}. \quad (2.63)$$

Note that the factor $B/(2\pi)$ corresponds to the Landau degeneracy (2.59). Therefore, the total charge does not change $\Delta Q = Q_{\text{R}} + Q_{\text{L}} = 0$, whereas the axial charge varies

$$\Delta Q_5 = \Delta Q_{\text{R}} - Q_{\text{L}} = \frac{\tau V E B}{2\pi^2}. \quad (2.64)$$

We can interpret this equation as an additional source of the classical conservation law associated with the axial charge symmetry per unit time and volume. Thus, we obtain

$$\partial_\mu j_5^\mu = \frac{EB}{2\pi^2}. \quad (2.65)$$

This equation in static electric and magnetic fields can be generalized into,

$$\partial_\mu j_5^\mu = C \mathbf{E} \cdot \mathbf{B}, \quad (2.66)$$

where

$$C \equiv \frac{1}{2\pi^2}. \quad (2.67)$$

Equation (2.66) is the same relation as that of the triangle anomalies in quantum field theories [14, 15].

We make some remarks on this triangle anomaly relation. It is exact at all orders of perturbation theory according to the Adler-Bardeen's theorem [52]. Moreover, this is an ‘‘anomalous’’ Ward-Takahashi identity, which does not depend on any perturbative calculations [53]. Therefore, the presence of gluons does not affect Eq. (2.66).

Chiral magnetic effect

Let us evaluate the currents in the presence of each chemical potential of left- or right-handed fermions, $\mu_{\text{R,L}}$. Using the Fermi-Dirac distribution function,

we obtain

$$j_{\text{R}}^z = \frac{B}{2\pi} \int_0^\infty \frac{dk_z}{2\pi} \left(\frac{1}{1 + e^{\frac{k_z - \mu_{\text{R}}}{T}}} - \frac{1}{1 + e^{\frac{k_z + \mu_{\text{R}}}{T}}} \right) = \frac{\mu_{\text{R}} B}{4\pi^2}, \quad (2.68)$$

$$j_{\text{L}}^z = -\frac{B}{2\pi} \int_0^\infty \frac{dk_z}{2\pi} \left(\frac{1}{1 + e^{\frac{k_z - \mu_{\text{L}}}{T}}} - \frac{1}{1 + e^{\frac{k_z + \mu_{\text{L}}}{T}}} \right) = -\frac{\mu_{\text{L}} B}{4\pi^2}. \quad (2.69)$$

Here the first and second terms of each equation correspond to the particle and anti-particle contributions, respectively. Note also that only the lowest Landau level contributes to the currents. By writing these in the vector form, we get

$$\mathbf{j}_{\text{R}} = \frac{\mu_{\text{R}} \mathbf{B}}{4\pi^2}, \quad (2.70)$$

$$\mathbf{j}_{\text{L}} = -\frac{\mu_{\text{L}} \mathbf{B}}{4\pi^2}. \quad (2.71)$$

Thus, the total and axial currents are

$$\mathbf{j} \equiv \mathbf{j}_{\text{R}} + \mathbf{j}_{\text{L}} = \frac{\mu_5 \mathbf{B}}{2\pi^2}, \quad (2.72)$$

$$\mathbf{j}_5 \equiv \mathbf{j}_{\text{R}} - \mathbf{j}_{\text{L}} = \frac{\mu \mathbf{B}}{2\pi^2}, \quad (2.73)$$

where $\mu_5 \equiv (\mu_{\text{R}} - \mu_{\text{L}})/2$ and $\mu \equiv (\mu_{\text{R}} + \mu_{\text{L}})/2$. The creation of the vector current \mathbf{j} and the axial current \mathbf{j}_5 are called the chiral magnetic effect (CME) [16, 17, 18, 19] and the chiral separation effect (CSE) [54, 55], respectively. As we will see in Chap. 5.2.1, we can also derive the CME and CSE in the use of the anomalous commutation relation (5.21), which is equivalent to the triangle anomaly relation (2.66).

2.3.3 Chiral magnetic wave

We here show the presence of the CME and CSE leads to the collective gapless modes called the chiral magnetic wave (CMW) [20, 21]. In the absence of the electric field, the conservation laws for the electric charge and the axial charge are

$$\frac{\partial n}{\partial t} + \nabla \cdot \mathbf{j} = 0, \quad (2.74)$$

$$\frac{\partial n_5}{\partial t} + \nabla \cdot \mathbf{j}_5 = 0. \quad (2.75)$$

The vector and the axial currents are generated by the CME and the CSE as

$$\mathbf{j} = \frac{\mu_5 \mathbf{B}}{2\pi^2} = \frac{n_5 \mathbf{B}}{2\pi^2 \chi_5}, \quad (2.76)$$

$$\mathbf{j}_5 = \frac{\mu \mathbf{B}}{2\pi^2} = \frac{n \mathbf{B}}{2\pi^2 \chi}. \quad (2.77)$$

Here we write the conserved charge densities n and n_5 into $n = \chi\mu$ and $n_5 = \chi_5\mu_5$ by using the the susceptibilities

$$\chi \equiv \frac{\partial n}{\partial \mu}, \quad \chi_5 \equiv \frac{\partial n_5}{\partial \mu_5}. \quad (2.78)$$

We substitute Eqs. (2.76) and (2.77) into Eqs. (2.74) and (2.75), respectively. Then, we obtain

$$\frac{\partial n}{\partial t} + \frac{\mathbf{B}}{2\pi^2 \chi_5} \cdot \nabla n_5 = 0, \quad (2.79)$$

$$\frac{\partial n_5}{\partial t} + \frac{\mathbf{B}}{2\pi^2 \chi} \cdot \nabla n = 0. \quad (2.80)$$

By eliminating n_5 from these equations, we find a wave function

$$\frac{\partial^2 n}{\partial t^2} = -\frac{\mathbf{B}}{2\pi^2 \chi_5} \cdot \nabla \frac{\partial n_5}{\partial t} = \frac{\mathbf{B}}{4\pi^2 \chi \chi_5} \cdot \nabla (\mathbf{B} \cdot \nabla n) = \frac{\mathbf{B}^2}{4\pi^2 \chi \chi_5} \nabla_s^2 n, \quad (2.81)$$

where we define the projection of the derivative into the direction of the magnetic field,

$$\nabla_s \equiv \frac{\mathbf{B} \cdot \nabla}{|\mathbf{B}|}. \quad (2.82)$$

We can interpret Eq. (2.81) as a propagating mode due to the fluctuation of charge density and axial charge density. This collective wave is called the CMW.

Chapter 3

Theory of dynamic critical phenomena

In this chapter, we give an overview of the theory of dynamic critical phenomena. In Sec. 3.1, we first review the dynamic universality class and explain the idea of dynamic critical phenomena. In Sec. 3.2, we formulate the static/dynamic low-energy effective theories of a general critical system. In Sec. 3.3, we also illustrate the RG analysis of the effective theories.

3.1 Dynamic universality class

Near a second-order phase transition or a critical point, the large correlation length of an order parameter, ξ , leads to unusual hydrodynamics [6]. For example, the typical time scale of diffusion becomes larger when the nuclear liquid-gas critical point is approached [56, 57, 58]. Remarkably, this critical slowing down is independent of the microscopic details of the system. In fact, several molecules, such as water, carbon dioxide, xenon, etc., exhibit experimentally the same dynamic critical behavior [59]. Moreover, as we mentioned in the introduction, relativistic fluid near the high-temperature QCD critical point also displays the same dynamic critical phenomenon as above [7, 8, 9, 10]. This shows the universality between the quark-gluon system at $T \sim \Lambda_{\text{QCD}} \sim 200$ MeV and the molecular systems at $T \sim 300$ K ~ 30 meV.

Let us look into the details of the universality of critical phenomena. We here consider the general system near a second-order phase transition or a

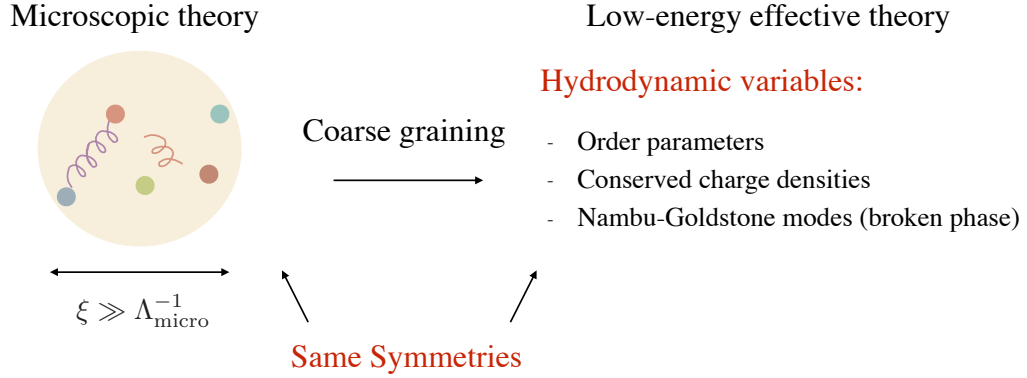


Figure 3.1: Idea of the dynamic universality class

critical point. As schematically illustrated in Fig. 3.1, the correlation length of the order parameter, ξ , is much larger than the typical microscopic length scale, $\Lambda_{\text{micro}}^{-1}$.¹ Therefore, to describe the dynamic critical phenomena characterized by ξ , we can coarse grain or integrate out microscopic degrees of freedom, such as quarks and gluons in QCD. Then, it is sufficient to use the low-energy effective theory of the hydrodynamic variables at large-length and long-time scales of the system. Typical hydrodynamic variables are order parameters (e.g., magnetization), conserved-charge densities (e.g., energy and momentum densities), and Nambu-Goldstone modes associated with spontaneously symmetry breaking (e.g., superfluid phonon). Symmetries of the low-energy effective theory must be the same as those of the microscopic theory before coarse graining or integrating out. We can classify dynamic critical phenomena based on the hydrodynamic variables and the symmetries of the systems. The classification of dynamic critical phenomena is called the dynamic universality class [6].

We summarize the conventional classification of dynamic critical phenomena studied by Hohenberg and Halperin [6] in Table 3.1. We here show, for each of the universality classes, internal symmetry, the property of order parameter (whether it is conserved or not) and conserved charge (the symmetry related by the Noether's theorem), and a typical system.

¹Note here that we consider the system not *directly* at the critical point $\xi \rightarrow \infty$, but sufficiently *near* the critical point where $\xi \gg \Lambda_{\text{micro}}^{-1}$ ($\Lambda_{\text{micro}} \neq 0$). Otherwise, the hydrodynamic description breaks down. In other words, we extrapolate the calculation on $\xi \gg \Lambda_{\text{micro}}^{-1}$ to the critical point perturbatively.

Class	Symmetry	Order Parameter	Conserved Charge	System
A	$\mathbb{Z}(2)$	Nonconserved		Ising model
B	$\mathbb{Z}(2)$	Conserved		Uniaxial Ferromagnets
C	$\mathbb{Z}(2)$	Nonconserved	Energy	Uniaxial Antiferromagnets
E	$U(1) \times \mathcal{C}$	Nonconserved	$U(1)$	Easy-plane magnets
F	$U(1)$	Nonconserved	$U(1)$	Superfluid ^4He
G	$O(N)$	Nonconserved	$O(N)$	Isotropic Antiferromagnets
H	$\mathbb{Z}(2)$	Conserved	Momentum	Liquid gas
J	$O(N)$	Conserved		Isotropic Ferromagnets

Table 3.1: Conventional dynamic universality class

3.2 Formulation

In this section, we give more details about the low-energy effective theory of critical phenomena. In Secs. 3.2.1 and 3.2.2, we formulate the Ginzburg-Landau theory/Langevin theory to describe static/critical critical phenomena, respectively. In Sec. 3.2.3, we demonstrate how to obtain the field theory equivalent to the Langevin theory derived in Sec. 3.2.2. This field theory will help us to apply the renormalization group approach in Sec. 3.3.2.

3.2.1 Ginzburg-Landau theory

The static critical phenomena and the static universality class can be determined only by the order parameters and the symmetries of the system. This notion is called the Ginzburg-Landau theory, and its idea can be summarized as follows.

Since a second-order phase transition or a critical point is/can be regarded as a continuous transition, we can consider the parameter region, e.g., temperature, with a small order parameter. Then, we can expand the free energy of the system with respect to the order parameter. Moreover, as we are interested in the long-range behavior of the system characterized by ξ , we can also expand this Ginzburg-Landau free energy with respect to the derivative.

Here we can neglect higher-order terms because such terms are suppressed by $O(\nabla/\Lambda)$. Here Λ is the momentum cutoff, which gives the upper limit of the applicability of the effective theory.² See, e.g., Refs. [60, 61, 62] for the general construction of effective field theories.

We generalize the above expansion of the order parameter to all of the hydrodynamic variables. In the Ginzburg-Landau free energy, we write down all consistent terms with the symmetries of the system from the double expansion of the derivative and the hydrodynamic variables. Let us write one of the hydrodynamic variables of the system as ψ_I ($I, J, K = 1, \dots, n$). Then, we can formally write the free energy of the system in the following form:

$$F[\psi] = \int d\mathbf{r} \left[\frac{1}{2} \psi_I \beta_{IJ}(\nabla) \psi_J + \frac{1}{3!} \beta_{IJK}(\nabla) \psi_I \psi_J \psi_K + \frac{1}{4!} \beta_{IJKL}(\nabla) \psi_I \psi_J \psi_K \psi_L + \dots \right]. \quad (3.1)$$

Here β_{IJ} , β_{IJK} , β_{IJKL} are some functions of the spatial derivative. These coefficients can also be expanded with respect to the derivative. Summation over repeated indices I, J, K , and L is implied.

Once we determine the functional of the free energy, we can calculate any correlation functions among the hydrodynamic variables by using the following definition of the expectation value:

$$\langle \mathcal{O}[\psi] \rangle = \frac{\int \prod_I \mathcal{D}\psi_I \mathcal{O}[\psi] e^{-\beta F[\psi]}}{\int \prod_I \mathcal{D}\psi_I e^{-\beta F[\psi]}}. \quad (3.2)$$

Here, $\beta \equiv T^{-1}$ is the inverse temperature, and $\mathcal{O}[\psi]$ is some product of the hydrodynamic variables. We can also calculate thermodynamic quantities related to these static correlation functions. Static critical exponents characterize the critical phenomena of these thermodynamic quantities. Systems with the same critical exponents belong to the same universality class. As we will see later, we can uniquely determine static critical exponents by using the

²Practically, we are constructing the low-energy effective theory by integrating out the microscopic degrees of freedom whose energy scale is larger than the typical energy scale of the critical phenomena, i.e., the inverse correlation length ξ^{-1} . It follows that Λ should be chosen as to satisfy $\xi^{-1} \ll \Lambda$.

renormalization group. Thus, the static universality class is only determined by the order parameter and the symmetries, which constrains the possible terms of the Ginzburg-Landau free energy.³

3.2.2 Langevin theory

The Langevin theory is the low-energy effective theory at large-length and long-time scales, including macroscopic dissipation effects. The time evolution of the hydrodynamic variable ψ_I is described by the following Langevin equation [63, 64, 65, 66]:

$$\frac{\partial \psi_I(t, \mathbf{r})}{\partial t} = -\gamma_{IJ}(\nabla) \frac{\delta F[\psi]}{\delta \psi_J(t, \mathbf{r})} - \int d\mathbf{r}' [\psi_I(t, \mathbf{r}), \psi_J(t, \mathbf{r}')] \frac{\delta F[\psi]}{\delta \psi_J(t, \mathbf{r}')} + \xi_I(t, \mathbf{r}). \quad (3.3)$$

These three terms in the right-hand side are called the dissipative term, the reversible term,⁴ and the noise term, respectively.

Dissipative term

The first term of Eq. (3.3) describes the relaxation process of the hydrodynamic variables to its equilibrium value. We consider the system slightly apart from the equilibrium. It follows that we can interpret this first term

³ You may logically think that not only the order parameter but also conserved charge densities can affect the *static* universality class. Such variables are normalized so that those mass terms in the Ginzburg-Landau free energy become unity (unlike the order parameter field) under the renormalization group. Due to this fact, the loop corrections on the fixed point structure solely determined by the order parameters tend to be irrelevant. For example, it is shown that the inclusion of the energy density does not change the static universality class governed by the Wilson-Fisher fixed-point [67, 68].

⁴Strictly speaking, there is another contribution in the reversible term at finite temperature,

$$T \frac{\delta}{\delta \psi_J(t, \mathbf{r}')} [\psi_I(t, \mathbf{r}), \psi_J(t, \mathbf{r}')]. \quad (3.4)$$

This term is required so that the Fokker-Plank equation corresponding to Eq. (3.3) yields the equilibrium distribution $\propto e^{-\beta F}$ as a steady-state solution (for more details, see, e.g., Refs. [63, 65, 66]). Nevertheless, this term is found to be zero or unimportant in most cases.

as a leading term of the expansion with respect to the variation of the free energy, $\Psi_I \equiv \delta F / \delta \psi_I$,

$$f_I[\Psi] = f_I[0] + \gamma_{IJ} \Psi_J + \dots, \quad (3.5)$$

where, $\Psi_I = 0$ at the equilibrium. Note that $f_I[0]$ and Ψ_J are some functions of ψ_I , in general. The leading term $f_I[0]$ is the 0-th order of the perturbation which may be regarded as an equilibrium. On the other hand, the left-hand side of Eq. (3.3), $\partial \psi_I / \partial t$ vanish at this 0-th order. It follows that we can set $f_I[0] = 0$. We also expand the coefficient γ_{IJ} with respect to the derivative as we are interested in the long-range behavior of the system,

$$\gamma_{ij}(\nabla) = \gamma_{ij}^{(0)} + \gamma_{ij}^{(2)} \nabla^2 + \dots. \quad (3.6)$$

Reversible term

The second term describes the reversible dynamics at a macroscopic scale. In the expression of this second term, $[A(t, \mathbf{r}), B(t, \mathbf{r}')]]$ denotes the Poisson bracket, which can be postulated from the symmetry algebra. One can obtain the expression of the Poisson bracket by computing the microscopic commutation relation of the operators corresponding to the hydrodynamic variables. We can interpret this term as the classical limit of the Heisenberg equation,

$$\int d\mathbf{r}' [\psi_I(t, \mathbf{r}), \psi_J(t, \mathbf{r}')] \frac{\delta F[\psi]}{\delta \psi_J(t, \mathbf{r}')} = [\psi_I(t, \mathbf{r}), F[\psi]]. \quad (3.7)$$

One may show this relation, order by order of the expansions in Eq. (3.1).

One distinct difference from the first dissipative term is that this second reversible term does not contribute to the time derivative of the free energy:

$$\begin{aligned} \frac{d \langle F[\psi] \rangle}{dt} &= \left\langle \frac{\delta F[\psi]}{\delta \psi_I} \frac{\partial \psi_I}{\partial t} \right\rangle \\ &= -\gamma_{IJ} \left\langle \frac{\delta F}{\delta \psi_I} \frac{\delta F}{\delta \psi_J} \right\rangle - \int d\mathbf{r}' \left\langle [\psi_I, \psi_J] \frac{\delta F}{\delta \psi_I} \frac{\delta F}{\delta \psi_J} \right\rangle + \left\langle \frac{\delta F}{\delta \psi_I} \xi \right\rangle \\ &= -\gamma_{IJ} \left\langle \frac{\delta F}{\delta \psi_I} \frac{\delta F}{\delta \psi_J} \right\rangle. \end{aligned} \quad (3.8)$$

Therefore, the second term describes the time evolution of the system without increasing the entropy. Intuitively, the dissipative term breaks the time-reversal symmetry, whereas the reversible term does not.

Noise term

The third term is the random driving force, which originates from the underlying microscopic degrees of freedom. Those statistical properties should be dictated by the nature of equilibrium as follows:

$$\langle \xi_I(t, \mathbf{r}) \rangle = 0, \quad (3.9)$$

$$\langle \xi_I(t, \mathbf{r}) \xi_J(t', \mathbf{r}') \rangle = 2T \gamma_{IJ}(\nabla) \delta(t - t') \delta^d(\mathbf{r} - \mathbf{r}'). \quad (3.10)$$

Equation (3.9) stems from the requirement that $\langle \psi_I(t, \mathbf{r}) \rangle$ should not be affected by the presence of ξ_I . The matrix γ_{IJ} in the random-force correlation (3.10) should be the same as that in the dissipative term (3.6). The relation between the dissipation effects and the random force is called the (second) fluctuation-dissipation relation.⁵

3.2.3 Dynamic perturbation theory

We here convert the Langevin theory derived in Sec. 3.2.2 into the path-integral formulation of a field theory. This formulation is called the Martin-Siggia-Rose-Janssen-de Dominicis (MSRJD) formalism [32, 33, 34] and helps us to apply the renormalization group method systematically. In this subsection, we follow the derivation in Ref. [66].

We first formally write the Langevin equation (3.3) and the fluctuation-dissipation relation (3.10) (in the unit of $T = 1$) in the following form:

$$\frac{\partial \psi_I(\mathbf{r}, t)}{\partial t} = \mathcal{F}_I[\psi] + \xi_I(\mathbf{r}, t), \quad (3.11)$$

$$\langle \xi_I(\mathbf{r}, t) \xi_J(\mathbf{r}', t') \rangle = 2\gamma_{IJ}(\nabla) \delta^d(\mathbf{r} - \mathbf{r}') \delta(t - t'). \quad (3.12)$$

Here, \mathcal{F}_I may involve all the hydrodynamic variables $\{\psi_I\}$, and the noises $\{\xi_I\}$ are assumed to obey the Gaussian white noise.

We consider the correlation functions for the hydrodynamic variables under various configurations of the noise variables,

$$\langle \mathcal{O}[\bar{\psi}] \rangle_\xi = \mathcal{N} \int \mathcal{D}\xi \mathcal{O}[\bar{\psi}] \exp \left[-\frac{1}{4} \int dt \int d\mathbf{r} \xi_I \gamma_{IJ}^{-1} \xi_J \right], \quad (3.13)$$

⁵In the context of the Brownian motion, this relation is due to the fact that both fluctuation and dissipation of the Brownian particles come from the same origin: random impact of surrounding molecules.

where $\bar{\psi}_I$ denotes the formal solution of the Langevin equations, and \mathcal{N} is a normalization factor. We can reproduce Eq. (3.12) by using the distribution (3.13). To carry out the path integral of ξ in Eq. (3.13) in the presence of the noise-dependent variable $\mathcal{O}[\bar{\psi}]$, we insert the following identity into the right-hand side of Eq. (3.13):

$$1 = \int \mathcal{D}\psi \prod_I \delta(\psi_I - \bar{\psi}_I) = \int \mathcal{D}\psi \prod_I \prod_{\mathbf{r}, t} \delta\left(\frac{\partial\psi_I}{\partial t} - \mathcal{F}_I[\psi] - \xi_I\right). \quad (3.14)$$

We here omit the Jacobian $\det(\partial_t - \delta\mathcal{F}/\delta\psi)$ in the right-hand side. We can justify this by getting rid of some unnecessary graphs containing the so-called *closed response loops* in diagrammatic calculations (see Ref. [66] for more details). Then, we can replace $\mathcal{O}[\bar{\psi}]$ by $\mathcal{O}[\psi]$ and integrate over the noise variables of Eq. (3.13). Finally, we get

$$\langle \mathcal{O}[\psi] \rangle = \mathcal{N}' \int i\mathcal{D}\tilde{\psi} \int \mathcal{D}\psi \mathcal{O}[\psi] \exp\left(-S[\tilde{\psi}, \psi]\right). \quad (3.15)$$

Here, \mathcal{N}' is a normalization factor, and we use the Fourier representation of the delta function. We introduce the pure imaginary auxiliary field $\tilde{\psi}_I$ called the response field for each hydrodynamic variable ψ_I . The MSRJD effective action $S[\tilde{\psi}, \psi]$ is given by

$$S[\tilde{\psi}, \psi] = \int dt \int d\mathbf{r} \left[\tilde{\psi}_I \left(\frac{\partial\psi_I}{\partial t} - \mathcal{F}_I[\psi] \right) - \tilde{\psi}_J \gamma_{IJ}(\nabla) \tilde{\psi}_I \right]. \quad (3.16)$$

By the use of the path-integral technique, we can calculate any correlation functions (3.15) among the hydrodynamic variables ψ_I and the response fields $\tilde{\psi}_I$.

3.3 Renormalization group analysis

The renormalization group (RG) is a powerful method to solve the theory near a second-order phase transition or a critical point. In Sec. 3.3.1, we first review the static RG for the Ginzburg-Landau free energy following Ref. [63]. Next, in Sec. 3.3.2, we move to the dynamic RG based on the MSRJD action and make remarks on its difference from the static one.

3.3.1 Statics

RG transformation

We perform static RG transformation on the path integral of the partition function:

$$Z = \int \mathcal{D}\psi e^{-\beta F_\Lambda[\psi]}, \quad (3.17)$$

with $F_\Lambda[\psi]$ being a Ginzburg-Landau free energy. The static RG consists of the following steps:

(i) Integrating over $\psi(\mathbf{q})$ in the momentum shell:

$$\Lambda/b < q < \Lambda; \quad (3.18)$$

(ii) Rescaling the momentum scale and all of the fields:

$$\mathbf{q} \rightarrow \mathbf{q}' = b\mathbf{q}; \quad (3.19)$$

$$\psi(\mathbf{q}) \rightarrow \psi'(\mathbf{q}') = [\zeta(b)]^{-1}\psi(\mathbf{q}). \quad (3.20)$$

Here, $q \equiv |\mathbf{q}|$, Λ is the momentum cutoff, $b > 1$ is the renormalization scale. We will determine the explicit form of the scaling function $\zeta(b)$ in a moment. At the second-order phase transition or the critical point, the correlation length diverges, and the typical length-scale disappears. Therefore, we expect the RG invariance of the system. This emergent symmetry brings strong constraints on the calculation.

RG of the Ginzburg-Landau free energy

To apply the RG to $F_\Lambda[\psi]$, we decompose the field $\psi(\mathbf{q})$ into the low momentum part $\psi^<$ and the high momentum part $\psi^>$:

$$\psi(\mathbf{q}) = \psi^<(\mathbf{q}) + \psi^>(\mathbf{q}), \quad (3.21)$$

where

$$\psi^<(\mathbf{q}) = \begin{cases} \psi(\mathbf{q}) & (0 < q < \Lambda/b); \\ 0 & (\Lambda/b < q < \Lambda), \end{cases} \quad (3.22)$$

$$\psi^>(\mathbf{q}) = \begin{cases} 0 & (0 < q < \Lambda/b); \\ \psi(\mathbf{q}) & (\Lambda/b < q < \Lambda). \end{cases} \quad (3.23)$$

We first integrate over the high-momentum field on the partition function:

$$\begin{aligned} Z &= \int \mathcal{D}\psi^<(\mathbf{q})\mathcal{D}\psi^>(\mathbf{q})e^{-\beta F_\Lambda[\psi^<+\psi^>]} \\ &= \int \mathcal{D}\psi^<(\mathbf{q})e^{-\beta F_{\Lambda/b}[\psi^<]}. \end{aligned} \quad (3.24)$$

Here, $\beta F_{\Lambda/b}[\psi^<(\mathbf{q})]$ is the effective action for $\psi^<$, after integrating out $\psi^>$:

$$e^{-\beta F_{\Lambda/b}[\psi^<]} \equiv \int \mathcal{D}\psi^>(\mathbf{q})e^{-\beta F_\Lambda[\psi^<+\psi^>]}. \quad (3.25)$$

Next, we rescale the momentum $\mathbf{q} \rightarrow \mathbf{q}' = b\mathbf{q}$ and the low momentum field $\psi^<(\mathbf{q})$ into the original field $\psi'(\mathbf{q})$ without the label “<” or “>,”

$$\psi^<(\mathbf{q}) \rightarrow \psi'(\mathbf{q}) = [\zeta(b)]^{-1}\psi^<(\mathbf{q}). \quad (3.26)$$

A series of these operations is the static RG transformation.

Scaling factor $\zeta(b)$

Let us determine the explicit form of $\zeta(b)$ from the RG invariance of the static correlation function.

From the translational symmetry of the system, we can generally write the static correlation function of the fields as

$$\langle \psi(\mathbf{q}_1)\psi(\mathbf{q}_2) \rangle = C(\mathbf{q}_1)(2\pi)^d \delta(\mathbf{q}_1 + \mathbf{q}_2). \quad (3.27)$$

Here, the expectation value is defined in Eq. (3.2) and $C(\mathbf{q})$ is some function of \mathbf{q} . On the other hand, the correlation function after the RG transformation is

$$\langle \psi'(\mathbf{q}'_1)\psi'(\mathbf{q}'_2) \rangle = C(\mathbf{q}'_1)(2\pi)^d \delta(\mathbf{q}'_1 + \mathbf{q}'_2) = \zeta^{-2}(b) \langle \psi(\mathbf{q}_1)\psi(\mathbf{q}_2) \rangle. \quad (3.28)$$

We plug Eq. (3.27) into Eq. (3.28) and find

$$\begin{aligned} C(\mathbf{q}'_1)(2\pi)^d \delta(\mathbf{q}'_1 + \mathbf{q}'_2) &= \zeta^{-2}(b)C(\mathbf{q}_1)(2\pi)^d \delta(\mathbf{q}_1 + \mathbf{q}_2), \\ C(b\mathbf{q}_1)b^{-d} &= \zeta^{-2}(b)C(\mathbf{q}_1). \end{aligned} \quad (3.29)$$

At the critical point $\xi \rightarrow \infty$, the anomalous dimension η characterizes the critical behavior of the correlation, $C(\mathbf{q}) = q^{2-\eta}$. We thus obtain the expression for $\zeta(b)$ as

$$\zeta(b) = b^{\frac{d+2-\eta}{2}}. \quad (3.30)$$

In particular, $\eta = 0$ for the Gaussian distribution.

Higher order terms

We here discuss the RG of the following general term:

$$\begin{aligned}\beta F_\Lambda^p[\psi] &= \int d^d \mathbf{r} u_p(\nabla) \psi^p(\mathbf{r}) \\ &= \int \prod_{i=1}^p \frac{d^d \mathbf{q}_i}{(2\pi)^3} u_p(\mathbf{q}_1, \dots, \mathbf{q}_p) \psi(\mathbf{q}_1) \cdots \psi(\mathbf{q}_p) \delta(\mathbf{q}_1 + \cdots + \mathbf{q}_p). \quad (3.31)\end{aligned}$$

In particular, the terms with $p \leq 2$ are Gaussian terms; the terms with $p > 2$ are the non-Gaussian terms.

We can expand $u_p(\nabla)$ by using the rotational symmetry of the system as

$$u_p(\nabla) = u_p + u'_p \nabla^2 + \cdots. \quad (3.32)$$

Here, u_p and u'_p are some constants. The parity symmetry under $\nabla \rightarrow -\nabla$ prohibits the term proportional to ∇ . The coefficient of the higher-order derivative acquires an additional scaling factor, b^{-2} , after rescaling the momentum and the fields. Therefore, higher-order derivative terms with fixed p are relatively suppressed under the RG procedure. In particular, we set $u'_p = 0$ for $p > 2$ from now on.

By applying the RG transformation to Eq. (3.31) we obtain

$$\beta F_\Lambda^p[\psi] = u_p b^{-pd} \zeta^p(b) b^d \int \prod_{i=1}^p \frac{d^d \mathbf{q}'_i}{(2\pi)^3} \psi'(\mathbf{q}'_1) \cdots \psi'(\mathbf{q}'_p) \delta(\mathbf{q}'_1 + \cdots + \mathbf{q}'_p). \quad (3.33)$$

The new parameter u'_p after the single RG step satisfies

$$u'_p = b^{-pd} \zeta^p(b) b^d u_p \equiv b^{\lambda_p} u_p. \quad (3.34)$$

Here, $\lambda_p \equiv p + d - p(d + \eta)/2$. We can classify terms depending on the value of λ_p ,

$$\lambda_p = \begin{cases} > 0 & \text{relevant,} \\ = 0 & \text{marginal,} \\ < 0 & \text{irrelevant.} \end{cases} \quad (3.35)$$

When u_p is a relevant parameter, it becomes larger under the RG transformation; when u_p is an irrelevant parameter, it becomes smaller under the RG transformation. Therefore, we can neglect all the irrelevant parameters from the beginning. We can define the above critical dimension $d_c(p)$ such that u_p is irrelevant when $d > d_c$. In particular, we find $d_c(3) = 6$ and $d_c(4) = 4$.

RG equation

We here show an outline of the RG of a scalar field theory (see Appendix A for details). The Ginzburg-Landau free energy is given by

$$\beta F[\psi] = \int d\mathbf{r} \left[\frac{r}{2} \psi^2 + \frac{1}{2} (\nabla \psi)^2 + u \psi^4 + h \psi \right] \quad (3.36)$$

with ψ being a scalar field. It is worth noting that Eq. (3.36) has $\mathbb{Z}(2)$ symmetry under the following transformation:

$$\psi \rightarrow -\psi. \quad (3.37)$$

This is the same symmetry as that of the Ising model, so that we can map the scalar field ψ into the magnetization m and expect the same static critical phenomena.

According to the discussion just under Eq. (3.35), relevant terms at $d = 4$ are only the Gaussian terms. On the other hand, when d is slightly smaller than 4, u grows a little bit under the RG transformation. Therefore, by working at

$$d = 4 - \epsilon \quad (3.38)$$

with the small ϵ ($0 < \epsilon \ll 1$), we can construct the perturbation theory based on the expansion with respect to u (or ϵ). Starting from this assumption, we will eventually find $u = \mathcal{O}(\epsilon)$ and check the consistency of this perturbation scheme.

We can evaluate the parameters r and u under the RG transformation. When we write these values after the RG as r' and u' , we obtain

$$r' = b^2 \left[r + 6u \int_{\mathbf{q}}^{\>} \frac{1}{r + \mathbf{q}^2} + O(u^2) \right], \quad (3.39)$$

$$u' = b^\epsilon \left[u - 36u^2 \int_{\mathbf{q}}^{\>} \frac{1}{(r + \mathbf{q}^2)^2} \right]. \quad (3.40)$$

Here, the integrals $\int^{\>}$ represent the integration over the high-momentum degrees of freedom $\psi^{\>}$ (see Eq. (A.21) for the definition of this integral); overall factors b^2 and b^ϵ come from the rescaling. See Appendix A for the derivation of Eqs. (3.39) and (3.40), which correspond to Eqs. (A.18) and (A.20), respectively.

We work on the thin momentum shell by setting $b \equiv e^l \simeq 1 + l$ with $l \ll 1$. Then, Eqs. (3.39) and (3.40) reduce to the following RG equations (for the derivation, see Eqs. (A.34) and (A.35)):

$$\frac{d\bar{r}}{dl} = 2\bar{r} + 12\bar{u} - 12\bar{r}\bar{u}, \quad (3.41)$$

$$\frac{d\bar{u}}{dl} = \epsilon\bar{u} - 36\bar{u}^2, \quad (3.42)$$

where

$$\bar{r} \equiv \frac{r}{\Lambda^2}, \quad \bar{u} \equiv \frac{u}{8\pi^2\Lambda^\epsilon}, \quad (3.43)$$

are dimensionless parameters. These equations describe the parameters under the RG transformation at a general renormalization scale $l = \ln b$. The stable fixed-point solution is called the Wilson-Fisher fixed point (its derivation is given in Appendix A.2):

$$\bar{r} = -\frac{\epsilon}{6} \quad \bar{u} = \frac{\epsilon}{36}. \quad (3.44)$$

We can calculate the critical exponents from these fixed point values.

3.3.2 Dynamics

We can also apply the dynamic RG analysis to the MSRJD action $S[\psi, \psi]$ given in Eq. (3.16). We carry out the RG transformation of $S[\psi, \psi]$ on the path integral defined in the following partition function:

$$Z = \int \mathcal{D}\tilde{\psi} \mathcal{D}\psi e^{-S[\psi, \psi]}. \quad (3.45)$$

This is analogous to the static partition function (3.17). In this subsection, we make some remark on the important differences from the static RG procedure.

Dynamic critical exponent

The first difference is the presence of time t or frequency ω . In addition to the rescaling of the space coordinate in Eq. (3.19), frequency (or time) is regarded as a parameter which scales by

$$\omega \rightarrow \omega' = b^z \omega, \quad (3.46)$$

where z is called the dynamic critical exponent which characterizes the dynamic universality class.

Response fields

The second difference is the presence of the response field $\tilde{\psi}$. In the presence of this additional field, the Green function in the field theory becomes a matrix form in $(\psi, \tilde{\psi})$ space. In particular, the bilinear term of $\tilde{\psi}$ in the MSRJD action yields the so-called noise vortex. We will look into these points explicitly in our main analysis in Sec. 5.2.2.

There is also an extension of the RG procedure. In addition to the rescaling for the hydrodynamic field ψ , Eq. (3.20), we also scale the response field as

$$\tilde{\psi}(\mathbf{r}) \rightarrow b^{\tilde{a}} \tilde{\psi}(\mathbf{r}). \quad (3.47)$$

Here, note that the scaling factor $b^{\tilde{a}}$ is generally independent of that for the hydrodynamic variable, $\zeta(b)$, in Eq. (3.30). We will see the rescaling of the response fields in our main calculation, Eqs. (5.60)–(5.62).

Frequency-dependent internal loops

The third difference can be seen in the integrating out procedure of the higher-momentum fields. In addition to the same momentum integral as that of the static RG, Eq. (3.18), we carry out frequency integrals over $-\infty < \omega < \infty$ in the dynamic formulation. Integrals in frequency space are performed by using contour integrals. These integrals pick up hydrodynamic poles of the system.

Chapter 4

Dynamic critical phenomena of the high-density QCD critical point

In this chapter, we study the static and dynamic critical phenomena near the high-density QCD critical point. In Sec. 4.1, we summarize the hydrodynamic variables of the system by following the strategy in Sec. 3.1. In Sec. 4.2, based on the general discussion in Sec. 3.2.1, we study the static universality class of the system. In Sec. 4.3, we apply the formulation in Sec. 3.2.2 and study its dynamic universality class. We conclude with Sec. 4.4 with some discussions.

4.1 Hydrodynamic variables

The hydrodynamic variables of the system can be summarized as follows:

- (i) the chiral condensate, $\sigma \equiv \bar{q}q - \langle \bar{q}q \rangle$;
- (ii) the baryon number density, $n_B \equiv \bar{q}\gamma^0 q - \langle \bar{q}\gamma^0 q \rangle$;
- (iii) the energy-momentum densities, $\varepsilon \equiv T^{00} - \langle T^{00} \rangle$ and $\pi^i \equiv \langle T^{0i} \rangle$;
- (iv) the superfluid phonon, θ .

Some remarks are in order here: the chiral condensate σ is defined as the scalar channel of the general chiral order parameter (2.27), namely Eq. (2.39); the baryon number density n_B is the conserved charge density for the baryon

number symmetry under its transformation, Eq. (2.19); the superfluid phonon θ is the Nambu-Goldstone mode associated with the spontaneous breaking of the baryon number symmetry, Eq. (2.37). The superfluid phonon θ corresponds to the phase degrees of freedom of ϕ in Eq. (2.40). Among others, σ , n_B , and ε are defined as the fluctuations around the equilibrium. Note that the hydrodynamic variables in the system near the high-temperature QCD critical point are the same as (i)–(iii) of the high-density critical point.

We note that the following variables are not hydrodynamic variables. The first one is the amplitude fluctuation of the diquark condensate, or the fluctuation of $|\phi|$ in Eq. (2.40). This is because, the high-density QCD critical point is characterized by the massless chiral condensate σ , where the diquark condensate is nonvanishing. The second ones are the Nambu-Goldstone modes associated with the chiral symmetry breaking in Eq. (2.36), e.g., the pions. As we mentioned under Eq. (2.18), the chiral symmetry is explicitly broken by the finite quark mass. It follows that the pions acquire finite masses and can be integrated out (or coarse grained) according to the general discussion in Sec. 3.1. The third ones are the gluons which are gapped due to the color Meissner effect in the color superconducting phase.

As we will give a discussion in Sec. 4.4, ε and π^i do not affect the static and dynamic critical phenomena of the system. Therefore, we first neglect ε and π^i and consider only σ , n_B , and θ as hydrodynamic variables in the following sections.

4.2 Static critical phenomena

We first construct the Ginzburg Landau theory by following the argument in Sec. 3.2.1. The general Ginzburg-Landau free energy consistent with the symmetries of the system, such as the chiral symmetry, the $U(1)_B$ symmetry, and the discrete \mathcal{CPT} symmetries (charge conjugation, parity, and time-reversal symmetries, respectively) is given by

$$F[\sigma, n_B, \theta] = \int d\mathbf{r} \left[\frac{a}{2} (\nabla\sigma)^2 + b' \nabla\sigma \cdot \nabla n_B + \frac{c}{2} (\nabla n_B)^2 + \frac{\rho}{2} (\nabla\theta)^2 + V(\sigma, n_B) \right], \quad (4.1)$$

where

$$V(\sigma, n_B) = \frac{A}{2} \sigma^2 + B\sigma n_B + \frac{C'}{2} n_B^2 + \dots \quad (4.2)$$

Here a, b', c, ρ, A, B, C' are the expansion parameters and “ \dots ” denotes higher order terms. The prime notation is used to distinguish from other characters introduced so far. Note that b' and B can be finite only when $m_q \neq 0$ and $\mu_B \neq 0$, otherwise the term $\propto \sigma n_B$ is prohibited by the chiral symmetry and the charge conjugate symmetry.

An important observation here is that the superfluid phonon θ is decoupled from the other hydrodynamic variables σ and n_B at the Gaussian level. This is because the time-reversal symmetry prohibits the mixing between θ and σ (or n_B). Beyond the mean-field level, one can find that the nonlinear couplings between σ and θ , e.g., $\sigma^2(\nabla\theta)^2$ are irrelevant at the Wilson-Fisher fixed point at $d = 3$.¹ Therefore, the static property of the system is only determined by σ and n_B , even when one takes into account higher-order terms. It follows that the static universality class of the high-density critical point is the same as that of the high-temperature critical point. In particular, we obtain the following static correlation functions:

$$\langle \sigma(\mathbf{r})\sigma(\mathbf{0}) \rangle = \frac{1}{4\pi r} e^{-r/\xi}, \quad (4.3)$$

$$\chi_B \equiv \frac{\partial n_B}{\partial \mu_B} = \frac{1}{VT} \langle n_B^2 \rangle_{\mathbf{q} \rightarrow \mathbf{0}} = \frac{A}{\Delta}, \quad (4.4)$$

where V and T being spatial volume and temperature of the system, respectively. We also define

$$\xi \sim \Delta^{-\frac{1}{2}}, \quad \Delta \equiv AC' - B^2. \quad (4.5)$$

The critical point is characterized by $\Delta \rightarrow 0$, so that the correlation length of σ , ξ , diverges. Because of the mixing between σ and n_B mentioned under Eq. (4.2), χ_B and the susceptibility for the chiral condensate, χ_{m_q} , diverge as

$$\chi_B \sim \xi^{2-\eta}, \quad (4.6)$$

$$\chi_{m_q} \equiv \frac{\partial \sigma}{\partial m_q} \sim \xi^{2-\eta}. \quad (4.7)$$

Here, the anomalous dimension η is determined by the static universality class of the system ($\eta \simeq 0.04$ including non-Gaussian effects [63]).

¹Note that the couplings between θ and σ or n_B contain the derivative due to the $U(1)_B$ symmetry of the system, i.e., the invariance under $\theta \rightarrow \theta + \alpha_B$.

We here give the reason why the high-density QCD critical point belongs to the same static universality class as that of the Ising model. Since σ and n_B are mixed in the potential, it is useful to change the basis in the (σ, n_B) plane. We chose the basis such that the flat direction, $n'_B \propto -B\sigma + An_B$, appears at the critical point $\Delta \rightarrow 0$. After integrating out the gapped degrees of freedom orthogonal to n'_B , we can obtain the free energy of the system as

$$F[\tilde{n}'_B] = \int d\mathbf{r} \left[\frac{a}{2} (\nabla n'_B)^2 + \frac{A'}{2} n_B'^2 + v n_B'^3 + u' n_B'^4 \right], \quad (4.8)$$

with some parameters A' , v , and u' . By taking the particular complete of square, we can map this functional into the same functional as that of the Ising model, namely, Eq. (3.36).

4.3 Dynamic critical phenomena

In this section, we study the dynamic critical phenomena of the system in the vicinity of the high-density QCD critical point. First, in Sec. 4.3.1, we construct the nonlinear-Langevin equations of the high-density QCD critical point. Next, in Sec. 4.3.2, we solve the linearized Langevin equation and obtain the hydrodynamic modes of the system. Then, in Sec. 4.3.3, we calculate the dynamic critical exponent, which determines the dynamic universality class.

4.3.1 Langevin theory

We can write down the Langevin equation of the system by following Eq. (3.3) as

$$\frac{\partial \sigma}{\partial t} = -\Gamma \frac{\delta F}{\delta \sigma} + \tilde{\lambda} \nabla^2 \frac{\delta F}{\delta n_B} + \xi_\sigma, \quad (4.9)$$

$$\frac{\partial n_B}{\partial t} = \tilde{\lambda} \nabla^2 \frac{\delta F}{\delta \sigma} + \lambda \nabla^2 \frac{\delta F}{\delta n_B} - \int_V [n_B, \theta] \frac{\delta F}{\delta \theta} + \xi_{n_B}, \quad (4.10)$$

$$\frac{\partial \theta}{\partial t} = - \int_V [\theta, n_B] \frac{\delta F}{\delta n_B} - \zeta \frac{\delta F}{\delta \theta} + \xi_\theta. \quad (4.11)$$

Here, we use the simplified notation of the integral,

$$\int_V [A, B] \frac{\delta F}{\delta B} \equiv \int d\mathbf{r}' [A(t, \mathbf{r}), B(t, \mathbf{r}')] \frac{\delta F}{\delta B(t, \mathbf{r}')}. \quad (4.12)$$

The kinetic coefficients Γ , λ , and $\tilde{\lambda}$ originate from the expansion (3.6) and are related to the noise terms ξ_σ , ξ_n , and ξ_θ by the fluctuation-dissipation relations corresponding to Eq. (3.10),

$$\langle \xi_\sigma(t, \mathbf{r}) \xi_\sigma(t, \mathbf{r}') \rangle = 2T\Gamma \delta(t-t') \delta^d(\mathbf{r}-\mathbf{r}'), \quad (4.13)$$

$$\langle \xi_{n_B}(t, \mathbf{r}) \xi_{n_B}(t, \mathbf{r}') \rangle = -2T\lambda \nabla^2 \delta(t-t') \delta^d(\mathbf{r}-\mathbf{r}'), \quad (4.14)$$

$$\langle \xi_\sigma(t, \mathbf{r}) \xi_{n_B}(t, \mathbf{r}') \rangle = -2T\tilde{\lambda} \nabla^2 \delta(t-t') \delta^d(\mathbf{r}-\mathbf{r}'), \quad (4.15)$$

$$\langle \xi_\theta(t, \mathbf{r}) \xi_\theta(t, \mathbf{r}') \rangle = 2T\zeta \delta(t-t') \delta^d(\mathbf{r}-\mathbf{r}'). \quad (4.16)$$

Here, d denotes the spatial dimension.

We postulate the following Poisson bracket,

$$[\theta(t, \mathbf{r}), n_B(t', \mathbf{r}')] = \delta(t-t') \delta^d(\mathbf{r}-\mathbf{r}'), \quad (4.17)$$

so that n_B and θ satisfy the canonical conjugate relation. The reason why these variables are canonical conjugate can be understood as follows. We start from the QCD Lagrangian at finite baryon chemical potential,

$$\mathcal{L}'_{\text{QCD}} = \mathcal{L}_{\text{QCD}} + \mu_B \bar{q} \gamma^0 q. \quad (4.18)$$

We regard μ_B as an auxiliary gauge field $a^\mu = (\mu_B, \mathbf{0})$, and rewrite the Lagrangian into

$$\mathcal{L}'_{\text{QCD}} = \mathcal{L}_{\text{QCD}} + a_\mu \bar{q} \gamma^\mu q, \quad (4.19)$$

which has the gauge invariance under the local $U(1)_B$ transformation,

$$a_\mu \rightarrow a_\mu - \partial_\mu \alpha_B, \quad \theta \rightarrow \theta + \alpha_B. \quad (4.20)$$

Next, we consider the effective Lagrangian \mathcal{L}_{eff} of the superfluid phonon θ . Since \mathcal{L}_{eff} should also possess the local gauge symmetry (4.20), the expression of \mathcal{L}_{eff} is dictated by the covariant derivative

$$D_\mu \theta = (\partial_t \theta + a^0, \nabla \theta). \quad (4.21)$$

Thus, we find [69, 70]

$$\mathcal{L}_{\text{eff}} = \mathcal{L}_{\text{eff}} \left(\frac{\partial \theta}{\partial t} + \mu_B, \nabla \theta \right), \quad (4.22)$$

which yields the canonical conjugation relation between n_B and θ ,

$$n_B \equiv \frac{\delta \mathcal{L}_{\text{eff}}}{\delta \mu_B} = \frac{\delta \mathcal{L}_{\text{eff}}}{\delta \dot{\theta}}, \quad \dot{\theta} \equiv \frac{\partial \theta}{\partial t}. \quad (4.23)$$

Some remarks on the Langevin equations (4.9)–(4.11) are in order here. The derivative expansions for the first two terms of Eq. (4.10) start from ∇^2 so that the total baryon number is conserved $\dot{n}_B \rightarrow 0$, ($\mathbf{q} \rightarrow \mathbf{0}$). The coefficient of the second term of Eq. (4.9) should have the same kinetic coefficient as that of the first term in Eq. (5.13), according to the Onsager's principle (see Ref. [71] for the derivation of the Onsager's principle).

By substituting Eq. (4.17) and the variation of the free energy to the linear level of hydrodynamic variables,

$$\frac{\delta F}{\delta \sigma} = (A - a\nabla^2)\sigma + (B - b'\nabla^2)n_B, \quad (4.24)$$

$$\frac{\delta F}{\delta n_B} = (B - b'\nabla^2)\sigma + (C' - c\nabla^2)n_B, \quad (4.25)$$

$$\frac{\delta F}{\delta \theta} = -\rho\nabla^2\theta, \quad (4.26)$$

into Eqs. (4.9)–(4.11), we obtain the Langevin equations to the order of $O(\mathbf{q}^2)$ in frequency-momentum space (ω, \mathbf{q}) ,

$$\mathcal{M} \begin{pmatrix} \sigma \\ n \\ \theta \end{pmatrix} = 0, \quad (4.27)$$

where

$$\mathcal{M} \equiv \begin{pmatrix} i\omega - \Gamma A - (\Gamma a + \tilde{\lambda} B)\mathbf{q}^2 & -\Gamma B - (\Gamma b' + \tilde{\lambda} C')\mathbf{q}^2 & 0 \\ -(\tilde{\lambda} A + \lambda B)\mathbf{q}^2 & i\omega - (\tilde{\lambda} B + \lambda C')\mathbf{q}^2 & \rho\mathbf{q}^2 \\ -B - b'\mathbf{q}^2 & -C' - c\mathbf{q}^2 & i\omega - \zeta\rho\mathbf{q}^2 \end{pmatrix}. \quad (4.28)$$

We here omit the noise terms because these are not important in the following argument, where we only need the expressions of hydrodynamic modes.

4.3.2 Hydrodynamic modes

We obtain the hydrodynamic modes of the system by solving the proper equation, $\det \mathcal{M} = 0$. This equation reduces to

$$\omega^3 + i(x_1 + x_2\mathbf{q}^2)\omega^2 - y\mathbf{q}^2\omega - iz\mathbf{q}^2 = 0, \quad (4.29)$$

where

$$\begin{aligned}
x_1 &\equiv \Gamma A, \\
x_2 &\equiv \Gamma a + 2\tilde{\lambda}B + \lambda C' + \zeta\rho, \\
y &\equiv \Gamma\lambda\Delta + C'\rho + \Gamma\zeta A\rho, \\
z &\equiv \Gamma\rho\Delta.
\end{aligned} \tag{4.30}$$

In Eq. (4.29), we ignore the higher-order terms of \mathbf{q} . At this order, the left-hand side of Eq. (4.29) can be factorized as

$$\begin{aligned}
&\left[\omega + ix_1 + i \left(x_2 - \frac{y}{x_1} + \frac{z}{x_1^2} \right) \mathbf{q}^2 + O(\mathbf{q}^3) \right] \\
&\times \left[\omega - \sqrt{\frac{z}{x_1}} |\mathbf{q}| + \frac{i}{2} \left(\frac{y}{x_1} - \frac{z}{x_1^2} \right) \mathbf{q}^2 + O(\mathbf{q}^3) \right] \\
&\times \left[\omega + \sqrt{\frac{z}{x_1}} |\mathbf{q}| + \frac{i}{2} \left(\frac{y}{x_1} - \frac{z}{x_1^2} \right) \mathbf{q}^2 + O(\mathbf{q}^3) \right] = 0.
\end{aligned} \tag{4.31}$$

Form this factorized form, one can find three hydrodynamic modes of the system near the high-density QCD critical point: the relaxation mode and the pair of the superfluid phonons with the dispersion relations,

$$\omega_1 = -i\Gamma A + O(\mathbf{q}^2), \tag{4.32}$$

$$\omega_{2,3} = \pm c_s |\mathbf{q}| + O(\mathbf{q}^2), \tag{4.33}$$

respectively. Here,

$$c_s \equiv \sqrt{\frac{\rho}{\chi_B}} \tag{4.34}$$

is the speed of the superfluid phonon, whose existence is dictated by the spontaneously symmetry breaking of the $U(1)_B$ symmetry, Eq. (2.37). We here find the critical slowing down of the speed of the superfluid phonon, $c_s \rightarrow 0$. Note that we have shown the divergence of χ_B when the critical point is approached $\xi \rightarrow \infty$, in Eq. (4.6).

4.3.3 Dynamic critical exponent

We can estimate the dynamic critical exponent z from $\omega \sim \xi^{-z}$ by using Eq. (4.33),

$$c_s \sim \xi^{1-z}. \tag{4.35}$$

Here, we use the matching condition at $\xi q \sim 1$ between the critical regime ($\xi q \gg 1$) and the hydrodynamic regime ($\xi q \ll 1$).

To determine the value of z , we use the following ξ dependences of ρ and χ_B near the high-density QCD critical point:

$$\rho \sim \xi^0, \quad \chi_B \sim \xi^{2-\eta}. \quad (4.36)$$

Here, ρ is the stiffness parameter (or the “decay constant” for the superfluid phonon). Note that it does not depend on ξ near the high-density critical point, which is generally away from the superfluid phase transition characterized by the amplitude mode of the diquark condensate.

From Eqs. (4.34), (4.35), and (4.36), we find the dynamic critical exponent z as

$$z = 2 - \frac{\eta}{2}. \quad (4.37)$$

This dynamic critical exponent is different from all the exponents reported in the conventional classification by Hohenberg and Halperin [6]. In this sense, we find that the high-density QCD critical point belongs to a new dynamic universality class.

4.4 Conclusion and discussion

So far, we have constructed the low-energy effective theory near the high-density QCD critical point and studied its static and dynamic critical phenomena. We have first shown that the static universality class of the system is the same as that of the high-temperature critical point, in Sec. 4.2. From the speed of the superfluid phonon, c_s , obtained in Eq. (4.34), we found the critical slowing down of c_s in the vicinity of the critical point. Furthermore, we have calculated the dynamic critical exponent of the system, z , in Eq. (4.37), and found that the high-density QCD critical point belongs to a new dynamic universality class beyond the conventional Hohenberg and Halperin’s classification [6].

Let us discuss nonlinear effects on the dynamic critical phenomena. In general, there are nonlinear corrections to kinetic coefficients when a critical point is approached. Nevertheless, we can argue that the expression for the dynamic critical exponent (4.37) is an exact relation, which does not receive

any renormalization effects due to $U(1)_B$ symmetry of the system. In fact, when we rewrite (4.17) with some coupling constant g_0

$$[\theta(\mathbf{r}), n(\mathbf{r}')] = g_0 \delta(\mathbf{r} - \mathbf{r}'), \quad (4.38)$$

the speed of the superfluid phonon, Eq. (4.34) becomes

$$c_s \equiv \sqrt{\frac{g_0^2 \rho}{\chi_B}}. \quad (4.39)$$

Since Eq. (4.38) is related to the $U(1)_B$ symmetry, g_0 is not affected by any renormalization effects. Thus, the dynamic critical exponent obtained by using c_s is an exact relation. As is also shown in Appendix B, the speed of the superfluid phonon, Eq. (B.50), does not include any kinetic coefficients when the energy and momentum densities are taken into account.

Why the high-density QCD critical point belongs to a new dynamic universality class beyond the conventional classification? First, the presence of the superfluid phonon in the high-density critical point leads to a different dynamic universality class from that of the high-temperature QCD critical point. We next compare with the superfluid λ transition of ^4He , where the superfluid phonon also exists. Nevertheless, the interplay between the superfluid phonon and the chiral order parameter cannot be found in this condensed matter system. In fact, the second-order phase transition of the λ transition is characterized by the massless superfluid gap.²

Our findings suggest that the static quantities cannot distinguish two possible critical points in the QCD phase diagram, whereas the dynamic critical phenomena can distinguish them. Moreover, since the uniqueness of the dynamic critical phenomena of the high-density critical point is due to the presence of the superfluid phonon, observation of the critical slowing down of the superfluid phonon in the future heavy-ion collisions would provide indirect evidence of superfluidity of high-density QCD matter.

Other than the high-density QCD critical point, systems near critical points associated with $\mathcal{G}_1 = \mathbb{Z}_2$ symmetry breaking under $\mathcal{G}_2 = U(1)$ spontaneously symmetry breaking can also belong to this new dynamic universality

²Quantitatively, one can see a difference in the correlation length dependence of the stiffness parameter ρ , Eq. (4.36). Unlike the high-density QCD critical point, the phase transition is characterized by the superfluid gap in the helium system, so that the stiffness parameter depends on ξ as $\rho \sim \xi^{-1}$ [6].

class with appropriate background fields. The generalization of $\mathcal{G}_{1,2}$ enables us to classify the dynamic critical phenomena involving a general interplay between order parameters and Nambu-Goldstone modes.

Chapter 5

Dynamic critical phenomena induced by the chiral magnetic effect in QCD

In this chapter, we study the interplay between the dynamic critical phenomena and the CME in QCD. In Sec. 5.1, we first explain our setup and summarize the symmetries and the hydrodynamic modes of the system. In Sec. 5.2, we construct the Ginzburg-Landau theory and the nonlinear Langevin equation to describe the static and dynamic critical phenomena, respectively. We also give the MSRJD action corresponding to the Langevin theory and summarize its Feynman rules. In Sec. 5.3, we study the Ginzburg-Landau free energy and the MSRJD action by using the static and dynamic RG, respectively. We also show the results in Sec. 5.3. We conclude with Sec. 5.4.

5.1 Setup

5.1.1 Symmetries

We consider two-flavor QCD with massless up and down quarks at finite temperature T and isospin chemical potential μ_I in an external magnetic field \mathbf{B} . In this setup, there are two additional terms in the quark sector of massless two-flavor QCD Lagrangian. One is the finite isospin density term (the first term of Eq. (5.1)); the other is the coupling to the background

electromagnetic gauge field A^μ (the second term of Eq. (5.1)):

$$\mathcal{L}'_{\text{quark}} = \mathcal{L}_{\text{quark}} + \mu_{\text{I}} \bar{q} \gamma^0 \tau^3 q + A_\mu \bar{q} \gamma^\mu Q_e q \quad (5.1)$$

$$= \mathcal{L}_{\text{quark}} + \frac{\mu_{\text{I}}}{2} (q_{\text{u}}^\dagger q_{\text{u}} - q_{\text{d}}^\dagger q_{\text{d}}) + \frac{2}{3} A_\mu \bar{q}_{\text{u}} \gamma^\mu q_{\text{u}} - \frac{1}{3} A_\mu \bar{q}_{\text{d}} \gamma^\mu q_{\text{d}}. \quad (5.2)$$

Here, $\mathcal{L}_{\text{quark}}$ is the same Lagrangian given in Eq. (2.2) except for $m_{\text{u}} = m_{\text{d}} = 0$ in the present case; $n_{\text{I}} = \bar{q} \gamma^0 \tau^3 q$ and μ_{I} are the isospin¹ conserved-charge density and the isospin chemical potential, respectively; the third component of the generators for the SU(2) algebra, τ^3 acts on the vector in the flavor space. In Eq. (5.2), we write the Dirac fields for the up and down quarks as q_{u} and q_{d} , by using the vector notation of the flavor space:

$$q = \begin{pmatrix} q_{\text{u}} \\ q_{\text{d}} \end{pmatrix}. \quad (5.3)$$

The electric charge matrix Q_e in Eq. (5.1) are

$$Q_e = \begin{pmatrix} \frac{2}{3} & 0 \\ 0 & -\frac{1}{3} \end{pmatrix}. \quad (5.4)$$

Note here that the up and down quarks possess the electric charge $2/3$ and $-1/3$ in the unit of the elementary charge.

In the presence of the electromagnetic gauge field (and/or the isospin chemical potential), the chiral symmetry Eq. (2.16) is explicitly broken into its subgroup [72]

$$\text{SU}(2)_{\text{L}} \times \text{SU}(2)_{\text{R}} \rightarrow \text{U}(1)_{\text{L}}^{\tau^3} \times \text{U}(1)_{\text{R}}^{\tau^3}. \quad (5.5)$$

Here we call $\text{U}(1)_{\text{L}}^{\tau^3} \times \text{U}(1)_{\text{R}}^{\tau^3}$ the partial chiral symmetry, which corresponds to the invariance under the following particular chiral transformation (corresponding to τ^3),²

$$q_{\text{L}} \rightarrow V_{\text{L}}^{\tau^3} q_{\text{L}}, \quad q_{\text{R}} \rightarrow V_{\text{R}}^{\tau^3} q_{\text{R}}, \quad V_{\text{L,R}}^{\tau^3} \equiv e^{-i\theta_{\text{L,R}} \tau^3} q_{\text{L,R}}, \quad (5.7)$$

¹The flavor space at $N_{\text{f}} = 2$ is specially called the isospin space in an analogy to the spin $1/2$.

²This transformation can be also written as

$$q \rightarrow q' = e^{-i\alpha_{\text{V}} \tau^3} e^{-i\alpha_{\text{A}} \tau^3 \gamma^5} q, \quad (5.6)$$

where α_{V} and α_{A} denote the phase-rotating angles associated with $\text{U}(1)_{\text{V}}^{\tau^3}$ and $\text{U}(1)_{\text{A}}^{\tau^3}$ symmetries, respectively.

with $\theta_{L,R}$ being the independent parameters.

Some remarks on our setup are in order here. First, we assume massless quarks so that possible quark-mass corrections to the CME can be ignored. Second, we consider finite μ_I instead of baryon chemical potential μ_B , because both n_I and n_{I5} are conserved in massless QCD, so that μ_I and μ_{I5} are well-defined. On the other hand, the conservation of the axial charge is violated by the axial anomaly, even in massless QCD, Eq. (2.22).

5.1.2 Hydrodynamic variables

We here order the hydrodynamic variables of the system. First one is the two-component order parameter field characterizing the symmetry breaking of the partial chiral symmetry $U(1)_L^{\tau^3} \times U(1)_R^{\tau^3}$, ϕ_α ($\alpha = 1, 2$), i.e.,

$$\phi = \begin{pmatrix} \sigma \\ \pi^3 \end{pmatrix}, \quad (5.8)$$

with $\sigma = \bar{q}\tau^0 q$ and $\pi^3 = \bar{q}i\gamma^5\tau^3 q$ being the chiral condensate and the neutral pion, respectively ($\tau^0 = 1/2$). We can show that the other variables in the chiral order parameter Φ in Eq. (2.27) are not hydrodynamic modes as follows. At $N_f = 2$, the chiral order parameter Φ can be decomposed

$$\Phi = \sigma\tau^0 + i\eta\tau^0 + \delta^a\tau^a + i\pi^a\tau^a, \quad (5.9)$$

where $\sigma = \bar{q}\tau^0 q$, $\eta = \bar{q}i\gamma_5\tau^0 q$, $\delta^a = \bar{q}\tau^a q$, and $\pi^a = \bar{q}i\gamma^5\tau^a q$; we take the sum over repeated indices. In the absence of the magnetic field, σ and π^a become massless near the second-order chiral phase transition, while η and δ^a acquire finite masses due to the $U(1)_A$ anomaly [73].³ When we switch on the magnetic field, the charged pions $\pi^{1,2}$ also acquire a mass proportional to

³Actually, in the presence of the $U(1)_A$ anomaly, the Ginzburg-Landau potential for the chiral order parameter Φ includes the so-called Kobayashi-Maskawa-'t Hooft interaction [39, 40],

$$-\frac{c}{2}(\det \Phi + \det \Phi^\dagger) = -\frac{c}{2}[\sigma^2 + (\pi^a)^2] + \frac{c}{2}[\eta^2 + (\delta^a)^2], \quad (5.10)$$

with c being some positive parameter. By taking into account the mass terms

$$\frac{a}{2}\text{Tr}\Phi^\dagger\Phi = \frac{a}{2}[\sigma^2 + (\pi^a)^2 + \eta^2 + (\delta^a)^2], \quad (5.11)$$

only σ and π^a can be massless at the phase transition point.

$\sqrt{|\mathbf{B}|}$ due to the explicit chiral symmetry breaking (5.5). We can integrate out such massive degrees of freedom.

The second hydrodynamic variable is the conserved charge densities. We here only take into account the conserved charge densities associated with the symmetry $U(1)_L^{\tau^3} \times U(1)_R^{\tau^3}$ which are coupled to ϕ_α , i.e., n_I and the axial isospin density $n_{I5} = \bar{q}\gamma^0\gamma_5\tau^3q$. Although the energy and momentum densities can be also coupled to these hydrodynamic variables, we only focus on ϕ_α , n_I , and n_{I5} .

From now on, we omit the subscripts of n_I , n_{I5} , μ_I , and μ_{I5} and rewrite these variables into n , n_5 , and μ for notational simplicity.

5.2 Formulation

In this section, we give the formulation to study the static and the dynamic universality classes of the system. In Sec. 5.2.1, we first derive the nonlinear Langevin equations following general arguments in Sec. 3.2.2. We also construct the Ginzburg-Landau theory in Sec. 5.2.1. In Sec. 5.2.2, we show the MSRJD field theory equivalent to the derived Langevin equations with the help of Sec. 3.2.3.

5.2.1 Langevin theory

Applying the general formation of the Langevin equation (3.3) to this system, we obtain the nonlinear Langevin equations for the hydrodynamic variables ϕ_α , n , and n_5 as follows:

$$\frac{\partial\phi_\alpha}{\partial t} = -\Gamma\frac{\delta F}{\delta\phi_\alpha} - g\int_V[\phi_\alpha, n_5]\frac{\delta F}{\delta n_5} + \xi_\alpha, \quad (5.12)$$

$$\frac{\partial n}{\partial t} = \lambda\nabla^2\frac{\delta F}{\delta n} - \int_V[n, n_5]\frac{\delta F}{\delta n_5} + \zeta, \quad (5.13)$$

$$\frac{\partial n_5}{\partial t} = \lambda_5\nabla^2\frac{\delta F}{\delta n_5} - g\int_V[n_5, \phi_\alpha]\frac{\delta F}{\delta\phi_\alpha} - \int_V[n_5, n]\frac{\delta F}{\delta n} + \zeta_5, \quad (5.14)$$

We here use the simplified notation of the integrals (4.12). The Ginzburg-Landau free energy F is given by

$$F = \int d\mathbf{r} \left[\frac{r}{2}(\phi_\alpha)^2 + \frac{1}{2}(\nabla\phi_\alpha)^2 + u(\phi_\alpha)^2(\phi_\beta)^2 + \frac{1}{2\chi}n^2 + \frac{1}{2\chi_5}n_5^2 + \gamma n\phi_\alpha^2 \right], \quad (5.15)$$

where we take the summations over repeated indices; r, u and γ are some expansion parameters; the isospin and axial isospin susceptibilities, χ and χ_5 , are defined as

$$\chi \equiv \frac{\partial n}{\partial \mu}, \quad \chi_5 \equiv \frac{\partial n_5}{\partial \mu_5}. \quad (5.16)$$

The last term of Eq. (5.15), $\gamma n \phi_\alpha^2$, is forbidden at $\mu = 0$ by the charge conjugation symmetry, whereas it can appear at $\mu \neq 0$. Returning to the Langevin equations (5.12)–(5.14), Γ, λ , and λ_5 are the kinetic coefficients obtained by the derivative expansion (3.6), and g is the coupling constant between ϕ_α and n_5 . The noise terms ξ_α, ζ , and ζ_5 satisfy the fluctuation-dissipation relations:

$$\langle \xi_\alpha(\mathbf{r}, t) \xi_\beta(\mathbf{r}', t') \rangle = 2\Gamma \delta_{\alpha\beta} \delta(t - t') \delta^d(\mathbf{r} - \mathbf{r}'), \quad (5.17)$$

$$\langle \zeta(\mathbf{r}, t) \zeta(\mathbf{r}', t') \rangle = -2\lambda \nabla^2 \delta(t - t') \delta^d(\mathbf{r} - \mathbf{r}'), \quad (5.18)$$

$$\langle \zeta_5(\mathbf{r}, t) \zeta_5(\mathbf{r}', t') \rangle = -2\lambda_5 \nabla^2 \delta(t - t') \delta^d(\mathbf{r} - \mathbf{r}'), \quad (5.19)$$

and $\langle \xi_\alpha \zeta \rangle = \langle \xi_\alpha \zeta_5 \rangle = \langle \zeta \zeta_5 \rangle = 0$. We here postulate the following Poisson brackets from the symmetry algebra:

$$[n_5(\mathbf{r}, t), \phi_\alpha(\mathbf{r}', t)] = \varepsilon_{\alpha\beta} \phi_\beta \delta(t - t') \delta^d(\mathbf{r} - \mathbf{r}'), \quad (5.20)$$

$$[n(\mathbf{r}, t), n_5(\mathbf{r}', t)] = C \mathbf{B} \cdot \nabla \delta(t - t') \delta^d(\mathbf{r} - \mathbf{r}'). \quad (5.21)$$

Here, $\varepsilon_{\alpha\beta}$ denotes the anti-symmetric tensor in the order parameter space (5.8), and C is usually related to the anomaly coefficient (2.67) or the CME coefficient. However, in our analysis near the second-order phase transition, we regard C as a free parameter, which will be determined by the RG equation of the system. Since nonlinear fluctuations of massless σ can potentially renormalize C , it is a nontrivial question whether C is exactly fixed, related to the nonrenormalization away from the second-order phase transition mentioned under Eq. (2.67). Nevertheless, in Sec. 5.3.2, we will show that this anomaly coefficient or the CME coefficient does not receive the renormalization at the one-loop level.

5.2.2 Dynamic perturbation theory

We here summarize the MSRJD formulation of our Langevin theory. The field theoretical MSRJD action corresponding to the Langevin theory in

Sec. 5.2.1 is

$$S = \int dt \int d\mathbf{r} (\mathcal{L}_\phi + \mathcal{L}_n + \mathcal{L}_{\phi n}), \quad (5.22)$$

whose general form is given by Eq. (3.16). We will explain each of the Lagrangian in Eq. (5.22) and its brief derivation by assuming Eq. (3.16) (see Sec. 3.1 for the derivation of Eq. (3.16) itself).

First, \mathcal{L}_ϕ represents the kinetic term of the order parameters ϕ_α and the 4-point interaction term:

$$\mathcal{L}_\phi = \tilde{\phi}_\alpha \left(\frac{\partial}{\partial t} + \Gamma(r - \nabla^2) \right) \phi_\alpha - \Gamma \tilde{\phi}_\alpha^2 + 4\Gamma u \tilde{\phi}_\alpha \phi_\alpha \phi_\beta^2, \quad (5.23)$$

where $\tilde{\phi}_\alpha$ denotes the responsible field for ϕ_α . Almost all of the terms come from $\mathcal{F}_{\phi_\alpha}[\psi]$ corresponding to the right-hand side of Eq. (5.12) (see Eq. (3.11) for the definition of $\mathcal{F}_I[\psi]$ with $\psi_I = \phi_\alpha, n, n_5$), but the bilinear of the response field, $-\Gamma \tilde{\phi}_\alpha^2$, comes from the last term of Eq. (3.16). The form of $\gamma_{IJ}(\nabla)$ in Eq. (3.16) can be obtained by comparing the original definition of $\gamma_{IJ}(\nabla)$, Eq. (3.12) and Eq. (5.17).

Next, \mathcal{L}_n represents the bilinear part of the conserved charge densities n and n_5 , which are coupled to each other in the presence of the CME:

$$\mathcal{L}_n = \frac{1}{2}(\tilde{n}, n, \tilde{n}_5, n_5) \mathcal{M} \begin{pmatrix} \tilde{n} \\ n \\ \tilde{n}_5 \\ n_5 \end{pmatrix}, \quad (5.24)$$

where

$$\mathcal{M} \equiv \begin{pmatrix} 2\lambda \nabla^2 & \frac{\partial}{\partial t} - \frac{\lambda}{\chi} \nabla^2 & 0 & \frac{C}{\chi_5} \mathbf{B} \cdot \nabla \\ -\frac{\partial}{\partial t} - \frac{\lambda}{\chi} \nabla^2 & 0 & -\frac{C}{\chi} \mathbf{B} \cdot \nabla & 0 \\ 0 & \frac{C}{\chi} \mathbf{B} \cdot \nabla & 2\lambda_5 \nabla^2 & \frac{\partial}{\partial t} - \frac{\lambda_5}{\chi_5} \nabla^2 \\ -\frac{C}{\chi_5} \mathbf{B} \cdot \nabla & 0 & -\frac{\partial}{\partial t} - \frac{\lambda_5}{\chi_5} \nabla^2 & 0 \end{pmatrix} \quad (5.25)$$

and \tilde{n} and \tilde{n}_5 are the response fields for n and n_5 , respectively. Almost all terms come from $\mathcal{F}_n[\psi]$ and $\mathcal{F}_{n_5}[\psi]$ corresponding to the linear terms of

the right-hand sides of Eqs. (5.13) and (5.14), respectively. Meanwhile, the bilinear terms of \tilde{n} and \tilde{n}_5 originate from the last term of Eq. (3.16). Here, Eqs. (5.18) and (5.19) give $\gamma_{nn} = \lambda \nabla^2$ and $\gamma_{n_5 n_5} = \lambda_5 \nabla^2$, respectively.

The last term of Eq. (5.22), $\mathcal{L}_{\phi n}$ represents the 3-point interaction between the order parameters ϕ_α and the conserved charge densities n and n_5 :

$$\begin{aligned} \mathcal{L}_{\phi n} = & -\frac{g\varepsilon_{\alpha\beta}}{\chi_5} \left(\tilde{\phi}_\alpha \phi_\beta n_5 + \chi_5 \tilde{n}_5 (\nabla^2 \phi_\alpha) \phi_\beta \right) \\ & + 2\gamma \Gamma \tilde{\phi}_\alpha \phi_\alpha n - \gamma \lambda \tilde{n} (\nabla^2 \phi_\alpha^2) + \gamma C \tilde{n}_5 \mathbf{B} \cdot (\nabla \phi_\alpha^2). \end{aligned} \quad (5.26)$$

We obtain these terms from $\mathcal{F}_I[\psi]$ corresponding to the nonlinear terms among ϕ_α , n , and n_5 in the Langevin equations (5.12)–(5.14).

We make some remarks on the interaction term $\mathcal{L}_{\phi n}$. There are two types of interactions: the first line of Eq. (5.26) ($\propto g$) originates from the Poisson bracket (5.20), the second line of Eq. (5.26) ($\propto \gamma$) originates from the non-Gaussian term $\gamma n \phi_\alpha^2$ in the Ginzburg-Landau free energy (5.15). The former ($\propto g$) exists even at $\mu = 0$ and gives the couplings between different components of the order parameters field reflecting $\varepsilon_{\alpha\beta}$ in the interaction vortex; the latter ($\propto \gamma$) exists as long as $\mu \neq 0$ and gives the couplings between the same order parameter components. Note also that the last term of Eq. (5.26) may potentially generate the nonlinear corrections to the anomaly coefficient C . Nevertheless, we will show that this is not the case from the explicit computation.

Feynman rules

We here summarize the Feynman rules for the action (5.22) (see Ref. [66] to obtain the Feynman rules from the MSRJD action. See also standard textbooks of quantum field theory, e.g., Ref. [74] for getting the Feynman rules from a field theoretical action)

The bare propagator of the order parameter, $G_{\alpha\beta}^0$, is obtained by calculating the 2-point correlation $\langle \phi_\alpha \tilde{\phi}_\beta \rangle$ from the Gaussian part of \mathcal{L}_ϕ in momentum space:

$$G_{\alpha\beta}^0(\mathbf{k}, \omega) = G^0(\mathbf{k}, \omega) \delta_{\alpha\beta} \equiv \frac{\delta_{\alpha\beta}}{-i\omega + \Gamma(r + \mathbf{k}^2)}, \quad (5.27)$$

which is diagonal with respect to α and β . The bare propagator of the conserved fields, D_{ij}^0 , is obtained by calculating the 2-point correlation $\langle n_i \tilde{n}_j \rangle$

from \mathcal{L}_n , where $n_i = n, n_5$. In particular, the inverse matrix of D_{ij}^0 has the following expression:

$$[D^0(\mathbf{k}, \omega)]^{-1} = \begin{pmatrix} -i\omega + \frac{\lambda}{\chi} \mathbf{k}^2 & i \frac{C}{\chi_5} \mathbf{B} \cdot \mathbf{k} \\ i \frac{C}{\chi} \mathbf{B} \cdot \mathbf{k} & -i\omega + \frac{\lambda_5}{\chi_5} \mathbf{k}^2 \end{pmatrix}, \quad (5.28)$$

which has off-diagonal components with respect to i and j because of the CME.

As we have briefly mentioned in Sec. 3.3.2, there is a 2-point noise vortex corresponding to the bilinear of the response fields in the action. In particular, from the bilinear term of the response field of the order parameter $\tilde{\psi}_\alpha$ in \mathcal{L}_ϕ , we obtain the bare noise vertex of the order parameter as $2\Gamma\delta_{\alpha\beta}$. Similarly, we get the bare noise vertex of the conserved charge densities as

$$L^0(\mathbf{k}) = \begin{pmatrix} 2\lambda \mathbf{k}^2 & 0 \\ 0 & 2\lambda_5 \mathbf{k}^2 \end{pmatrix}, \quad (5.29)$$

which is related to the bare correlation function of the conserved charge densities, B_{ij}^0 , through the following equation:

$$B_{ij}^0(\mathbf{k}, \omega) = D_{il}^0(\mathbf{k}, \omega) L_{lk}^0(\mathbf{k}) [D^0(-\mathbf{k}, -\omega)]_{kj}^T = D_{il}^0(\mathbf{k}, \omega) L_{lk}^0(\mathbf{k}) [D^0(\mathbf{k}, \omega)]_{kj}^\dagger. \quad (5.30)$$

Here, B_{ij}^0 can be calculated explicitly by the 2-point correlation $\langle n_i n_j \rangle$ from \mathcal{L}_n as follows:

$$B_{11}^0(\mathbf{k}, \omega) = \frac{2\lambda \mathbf{k}^2 (\omega^2 + \lambda_5^2 \mathbf{k}^4 / \chi_5^2) + 2\lambda_5 \mathbf{k}^2 (C \mathbf{B} \cdot \mathbf{k} / \chi_5)^2}{|\det[D^0(\mathbf{k}, \omega)]^{-1}|^2}, \quad (5.31)$$

$$B_{12}^0(\mathbf{k}, \omega) = B_{21}^0(\mathbf{k}, \omega) = \frac{2(\lambda/\chi + \lambda_5/\chi_5) \mathbf{k}^2 C (\mathbf{B} \cdot \mathbf{k}) \omega}{|\det[D^0(\mathbf{k}, \omega)]^{-1}|^2}, \quad (5.32)$$

$$B_{22}^0(\mathbf{k}, \omega) = \frac{2\lambda_5 \mathbf{k}^2 (\omega^2 + \lambda^2 \mathbf{k}^4 / \chi^2) + 2\lambda \mathbf{k}^2 (C \mathbf{B} \cdot \mathbf{k} / \chi)^2}{|\det[D^0(\mathbf{k}, \omega)]^{-1}|^2}. \quad (5.33)$$

The 4-point interaction vertex is obtained from \mathcal{L}_ϕ as

$$U_{\alpha;\beta\gamma\delta}^0 = -4u\Gamma\delta_{\alpha\beta}\delta_{\gamma\delta}, \quad (5.34)$$

where the indices $\alpha; \beta\gamma\delta$ are the shorthand notation of the fields $\tilde{\phi}_\alpha\phi_\beta\phi_\gamma\phi_\delta$. The 3-point interaction vertices are obtained as

$$V_{\alpha;\beta i}^0 = \begin{pmatrix} -2\gamma\Gamma\delta_{\alpha\beta} \\ g\varepsilon_{\alpha\beta}/\chi_5 \end{pmatrix}, \quad (5.35)$$

$$V_{i;\alpha\beta}^0(\mathbf{k}, \mathbf{p}) = \begin{pmatrix} -2\gamma\lambda\mathbf{k}^2\delta_{\alpha\beta} \\ g[(\mathbf{k} - \mathbf{p})^2 - \mathbf{p}^2]\varepsilon_{\alpha\beta} - 2i\gamma C\mathbf{B} \cdot \mathbf{k}\delta_{\alpha\beta} \end{pmatrix}, \quad (5.36)$$

where we use the vector notation for the label i which classifies $n_i = n, n_5$. The indices $\alpha; \beta i$ and $i; \alpha\beta$ are the shorthand notation of $\tilde{\phi}_\alpha\phi_\beta n_i$ and $\tilde{n}_i\phi_\alpha\phi_\beta$, respectively. The vertex $V_{i;\alpha\beta}^0(\mathbf{k}, \mathbf{p})$ is the function of the outgoing momentum \mathbf{k} of n_i and the ingoing momentum \mathbf{p} of ϕ_α (see also Fig. 5.2(c) for the configuration of the external momentum).

We next summarize the diagrammatic representations of the above propagators, the noise- and interaction- vortices. First, we depict $G_{\alpha\beta}^0$ by the plane line, and D_{ij}^0 by the wavy line with the outgoing and ingoing components i and j . Since $G_{\alpha\beta}^0$ is diagonal with respect to α, β as one can confirm in Eq. (5.27), we omit writing both of the outgoing and ingoing indices α and β in the diagram for $G_{\alpha\beta}^0$. Instead, we shall write α alone at the center of plane lines. Each noise vertex of the order parameters and the conserved charge densities can be understood as the diagrams with two outgoing lines as represented in Fig. 5.1. Note that the number of ingoing and outgoing lines in one of the diagrams corresponds to the power of the hydrodynamic variable $\psi = \phi_\alpha, n_i$ and the response field $\tilde{\psi} = \tilde{\phi}_\alpha, \tilde{n}_i$ in the action, respectively [66]. As is shown in Fig 5.2, each of the interaction vertices has one outgoing and three or two ingoing lines.

Ordinary Feynman rules are applied to obtain full n -point correlations. Among others, we obtain the full propagators $G_{\alpha\beta}$ and D_{ij} by using the self-energies of the order parameter, $\Sigma_{\alpha\beta}$, and those of the conserved charge densities, Π_{ij} , as

$$G_{\alpha\beta}^{-1}(\mathbf{k}, \omega) = [G_{\alpha\beta}^0(\mathbf{k}, \omega)]^{-1} - \Sigma_{\alpha\beta}(\mathbf{k}, \omega), \quad (5.37)$$

$$D_{ij}^{-1}(\mathbf{k}, \omega) = [D_{ij}^0(\mathbf{k}, \omega)]^{-1} - \Pi_{ij}(\mathbf{k}, \omega). \quad (5.38)$$

We also get the three-point vertex function $V_{\alpha;\beta i}(\mathbf{k}_1, \mathbf{k}_2, \omega_1, \omega_2)$ by computing one-particle irreducible diagrams with outgoing ϕ_α and ingoing ϕ_β, n_i . Here, \mathbf{k}_1 and ω_1 denote the ingoing momentum and frequency of ϕ_β , and \mathbf{k}_2 and ω_2 denote the ingoing momentum and frequency of n_i . From the energy and

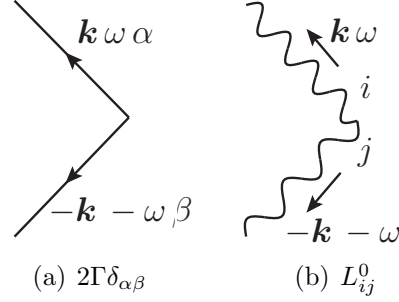


Figure 5.1: Noise vertices

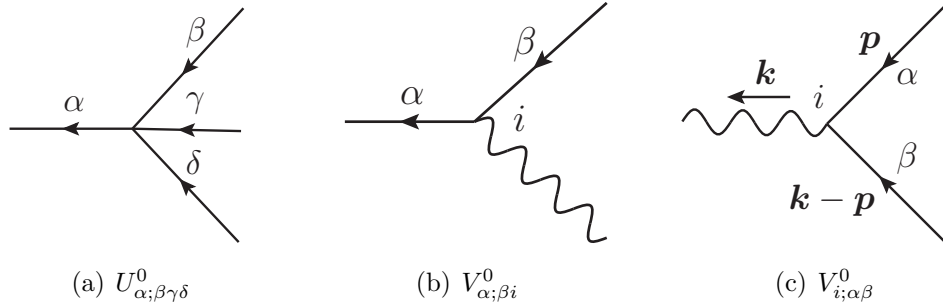


Figure 5.2: Interaction vertices

momentum conservation laws, $\tilde{\phi}_\beta$ has the outgoing momentum $\mathbf{k}_3 = \mathbf{k}_1 + \mathbf{k}_2$ and the frequency $\omega_3 = \omega_1 + \omega_2$. For later purposes, it is convenient to divide $V_{\alpha;\beta i}$ into its bare contribution $V_{\alpha;\beta i}^0$ and the correction term $\mathcal{V}_{\alpha;\beta i}$ as follows:

$$V_{\alpha;\beta i}(\mathbf{k}_1, \mathbf{k}_2, \omega_1, \omega_2) = V_{\alpha;\beta i}^0 + \mathcal{V}_{\alpha;\beta i}(\mathbf{k}_1, \mathbf{k}_2, \omega_1, \omega_2). \quad (5.39)$$

5.3 Renormalization-group analysis

In this section, we apply the RG to the effective theories derived in Sec. 5.2. In Sec. 5.3.1, we apply the static RG to the Ginzburg-Landau free energy (5.15) within the ϵ expansion. In Sec. 5.3.2, we study the MSRJD action (5.22) by using the dynamic RG with the help of Appendix C. We remark those results in Sec. 5.3.3.

5.3.1 Statics

In a single RG transformation, we integrate out the degrees of freedom in the momentum shell $\Lambda/b < q < \Lambda$ (with Λ being the momentum cutoff and $b > 1$, $q \equiv |\mathbf{q}|$), and we rescale the coordinate and the fields in the following way (For the details about the static RG, see Sec. 3.3):

$$\mathbf{r} \rightarrow \mathbf{r}' = b^{-1}\mathbf{r}, \quad (5.40)$$

$$\phi_\alpha(\mathbf{r}) \rightarrow \phi'_\alpha(\mathbf{r}') = b^a \phi_\alpha(\mathbf{r}), \quad (5.41)$$

$$n(\mathbf{r}) \rightarrow n'(\mathbf{r}') = b^c n(\mathbf{r}), \quad (5.42)$$

$$n_5(\mathbf{r}) \rightarrow n'_5(\mathbf{r}') = b^{c_5} n_5(\mathbf{r}). \quad (5.43)$$

Here a , c , and c_5 are some constants computed in the calculation below. Hereafter, we work with the spatial dimension $d \equiv 4 - \epsilon$ with small ϵ and perform the calculation to leading orders in the expansion of ϵ as we remarked around Eq. (3.38).

Let us write the static parameters at the l th stage of the renormalization procedure, r_l , u_l , χ_l and γ_l . Then, these parameters satisfy the same recursion relation as that of the so-called model C for the system with a single (two-component) order parameter and the conserved charge densities [67]. In particular, we quote Eqs. (4.5)–(4.8) in Ref. [67]. The recursion relations for the static parameters in the leading-order of ϵ are given as

$$r_{l+1} = b^{d-2a} \{r_l + 8\bar{u}_l [\Lambda^2(1 - b^{-2}) - 2r_l \ln b]\}, \quad (5.44)$$

$$\bar{u}_{l+1} = b^{d-4a} \bar{u}_l (1 - 40\bar{u}_l \ln b), \quad (5.45)$$

$$\chi_{l+1}^{-1} = b^{d-2c} \chi_l^{-1} (1 - 4v_l \ln b), \quad (5.46)$$

$$(\chi_5)_{l+1}^{-1} = b^{d-2c_5} (\chi_5)_l^{-1}, \quad (5.47)$$

$$\gamma_{l+1} = b^{2-c} \gamma_l [1 - (16\bar{u}_l + 4v_l) \ln b]. \quad (5.48)$$

Here, the left-hand sides are the parameters at the $(l+1)$ -th step of the RG, and we introduced the following quantities,

$$v \equiv \frac{\gamma^2 \chi \Lambda^{-\epsilon}}{8\pi^2}, \quad \bar{u} \equiv \frac{u \Lambda^{-\epsilon}}{8\pi^2}. \quad (5.49)$$

Note that one may not find the equation corresponding to Eq. (5.47) in Ref. [67] which we quoted. Nevertheless, Eq. (5.47) can be readily introduced because there is only Gaussian term for n_5 in the Ginzburg-Landau free

energy (5.15) and $(\chi_5)_l$ is affected only by the trivial scale transformation (5.43). From the condition that $(\chi_5)_l$ remains finite at the fixed point, we find the value of c from Eq. (5.47) as

$$c_5 = \frac{d}{2}. \quad (5.50)$$

It is also worth writing that the recursion relations (5.45)–(5.48) are the extension of Eqs. (3.39) and (3.40) to include the effects of the conserved charge density n and n_5 . In particular, v characterizes the nonlinear coupling between the order parameter and the conserved-charge density n .

Let us now compute a and c . Because the anomalous dimension η is zero to the order of ϵ [63], the exponent a is solely determined by Eq. (3.30) as

$$a = \frac{d-2}{2}. \quad (5.51)$$

To determine c , we evaluate the interplay of the RG flow between v and \bar{u} . Combining Eqs. (5.46) and (5.48), we obtain the recursion relation for v_l ,

$$v_{l+1} = b^\epsilon v_l [1 - (32\bar{u}_l + 4v_l) \ln b]. \quad (5.52)$$

The RG equations corresponding to Eqs. (5.45) and (5.52) become⁴

$$\frac{d\bar{u}_l}{dl} = (d - 4a - 40\bar{u}_l)\bar{u}_l. \quad (5.53)$$

$$\frac{dv_l}{dl} = (\epsilon - 32\bar{u}_l - 4v_l)v_l, \quad (5.54)$$

where Eq. (5.53) is the two-component order parameter version of Eq. (3.42), and Eq. (5.54) is the RG equation that evaluates the coupling between the order parameter ϕ_α and the conserved charge density n .

⁴ The derived recursion relations typically have the following form:

$$A_{l+1} = b^{c_A} A_l (1 + B_l \ln b).$$

with A_l and B_l being the variables and c_A being some constant. One can derive the RG equation for A_l by setting $b = e^l$ and taking the limit $l \rightarrow 0$ as

$$\frac{dA_l}{dl} = (c_A + B_l)A_l$$

Equations (5.53)-(5.54) tell us the fixed-point values of \bar{u}_l and v_l as [67]

$$\bar{u}_\infty = \frac{\epsilon}{40}, \quad v_\infty = \frac{\epsilon}{20}. \quad (5.55)$$

Returning to Eq. (5.46), we arrive at

$$c = \frac{3d-2}{5}. \quad (5.56)$$

Static critical exponents

The physical parameters near the transition temperature T_c are solely given by the loop-correction terms proportional to $\ln b$ in the static recursion relations [75]. In particular, we obtain the renormalized isospin charge susceptibility $\chi(T)$ by taking into account the correction calculated in Eq. (5.46) to the bare value χ_0 at the cutoff scale Λ ,

$$\chi(T) = \chi_0[1 + 4v_\infty \ln(\Lambda\xi)] \sim \xi^{\epsilon/5}, \quad (5.57)$$

where we use the relation $1 + x \ln \Lambda\xi + O(x^2) = (\Lambda\xi)^x$ for $x \ll 1$, by regarding $x = 4v_\infty$ as a small parameter when $\epsilon \ll 1$. Defining the critical exponents ν and α in the usual manner,

$$\xi \sim \tau^{-\nu}, \quad \chi \sim \tau^{-\alpha}, \quad (5.58)$$

with $\tau \equiv (T - T_c)/T_c$ being the reduced temperature, we obtain

$$\frac{\alpha}{\nu} = \frac{\epsilon}{5}. \quad (5.59)$$

5.3.2 Dynamics

As we mentioned it around Eq. (3.47), we also need to rescale the response fields $\tilde{\psi} = \tilde{\phi}_\alpha, \tilde{n}_i$ in addition to those for the hydrodynamic variables $\psi = \phi_\alpha, n_i$, (5.41)–(5.43) in the dynamic RG:

$$\tilde{\phi}_\alpha(\mathbf{r}) \rightarrow \tilde{\phi}'_\alpha(\mathbf{r}') = b^{\tilde{a}} \tilde{\phi}_\alpha(\mathbf{r}), \quad (5.60)$$

$$\tilde{n}(\mathbf{r}) \rightarrow \tilde{n}'(\mathbf{r}') = b^{\tilde{c}} \tilde{n}(\mathbf{r}), \quad (5.61)$$

$$\tilde{n}_5(\mathbf{r}) \rightarrow \tilde{n}'_5(\mathbf{r}') = b^{\tilde{c}_5} \tilde{n}_5(\mathbf{r}). \quad (5.62)$$

We will determine \tilde{a} , \tilde{c} , and \tilde{c}_5 in the following calculations.

We compute the full inverse propagators at the $(l + 1)$ th renormalization step. Then, we get the recursion relations of the dynamic parameters Γ_l , λ_l , λ_5 , and C_l , in an analogy to those of the static quantities, (5.45)–(5.48). In particular, we here demonstrate the derivation of the recursion relation for Γ_l as an example. First, we calculate the full inverse propagator for the order parameter as

$$\begin{aligned} [G_{\alpha\alpha}(\mathbf{k}', \omega')]_{l+1}^{-1} &= [G_{\alpha\alpha}(\mathbf{k}, \omega)]_l^{-1} b^{-\tilde{a}-a} \\ &= \left[-i\omega \left(1 - i \frac{\partial \Sigma_{\alpha\alpha}(\mathbf{0}, \omega)}{\partial \omega} \Big|_{\omega \rightarrow 0} \right) + \Gamma_l r_l - \Sigma_{\alpha\alpha}(\mathbf{0}, 0) \right. \\ &\quad \left. + \left(\Gamma_l - \frac{1}{2} \frac{\partial^2 \Sigma_{\alpha\alpha}(\mathbf{k}, 0)}{\partial \mathbf{k}^2} \Big|_{\mathbf{k} \rightarrow \mathbf{0}} \right) \mathbf{k}^2 + \dots \right] b^{-\tilde{a}-a}. \end{aligned} \quad (5.63)$$

Here, we use Eq. (5.37) and expand $\Sigma_{\alpha\alpha}$ with respect to the frequency ω and wave number \mathbf{k} . By regarding the term proportional to \mathbf{k}^2 on the right-hand side as $\Gamma_{l+1} \mathbf{k}'^2$ and including the overall factor b^{z+d} coming from rescaling the measure of the action, we obtain the recursion relation for Γ_l ,

$$\Gamma_{l+1} = \Gamma_l \left(1 - \frac{1}{2\Gamma_l} \frac{\partial^2 \Sigma_{\alpha\alpha}(\mathbf{k}, 0)}{\partial \mathbf{k}^2} \Big|_{\mathbf{k} \rightarrow \mathbf{0}} \right) b^{d+z-\tilde{a}-a-2}. \quad (5.64)$$

Furthermore, we normalize the term proportional to $-i\omega$ including the overall factor,

$$1 = \left(1 - i \frac{\partial \Sigma_{\alpha\alpha}(\mathbf{0}, \omega)}{\partial \omega} \Big|_{\omega \rightarrow 0} \right) b^{d-\tilde{a}-a}. \quad (5.65)$$

Similarly, we can derive the following recursion relations by computing the inverse propagator for conserved charge densities, $[D_{ij}(\mathbf{k}', \omega')]_{l+1}^{-1}$, and three-point vertex $[V_{\alpha;\beta i}(\mathbf{k}_1, \mathbf{k}_2, \omega_1, \omega_2)]_{l+1}$ instead of $[G_{\alpha\alpha}(\mathbf{k}', \omega')]_{l+1}^{-1}$ as we

used in Eq. (5.63):

$$\frac{\lambda_{l+1}}{\chi_{l+1}} = \frac{\lambda_l}{\chi_l} \left(1 - \frac{\chi_l}{2\lambda_l} \frac{\partial^2 \Pi_{11}(\mathbf{k}, 0)}{\partial \mathbf{k}^2} \Big|_{\mathbf{k} \rightarrow \mathbf{0}} \right) b^{d+z-\tilde{c}-c-2}, \quad (5.66)$$

$$\frac{(\lambda_5)_{l+1}}{(\chi_5)_{l+1}} = \frac{(\lambda_5)_l}{(\chi_5)_l} \left(1 - \frac{(\chi_5)_l}{2(\lambda_5)_l} \frac{\partial^2 \Pi_{22}(\mathbf{k}, 0)}{\partial \mathbf{k}^2} \Big|_{\mathbf{k} \rightarrow \mathbf{0}} \right) b^{d+z-\tilde{c}_5-c_5-2}, \quad (5.67)$$

$$\frac{C_{l+1}}{\chi_{l+1}} \mathbf{B} = \left(\frac{C_l}{\chi_l} \mathbf{B} + i \frac{\partial \Pi_{21}(\mathbf{k}, 0)}{\partial \mathbf{k}} \Big|_{\mathbf{k} \rightarrow \mathbf{0}} \right) b^{d+z-\tilde{c}_5-c-1}, \quad (5.68)$$

$$\frac{C_{l+1}}{(\chi_5)_{l+1}} \mathbf{B} = \left(\frac{C_l}{(\chi_5)_l} \mathbf{B} + i \frac{\partial \Pi_{12}(\mathbf{k}, 0)}{\partial \mathbf{k}} \Big|_{\mathbf{k} \rightarrow \mathbf{0}} \right) b^{d+z-\tilde{c}-c_5-1}, \quad (5.69)$$

$$\frac{g_{l+1}}{(\chi_5)_{l+1}} \varepsilon_{\alpha\beta} = \frac{g_l}{(\chi_5)_l} \left(\varepsilon_{\alpha\beta} + \frac{(\chi_5)_l}{g_l} \mathcal{V}_{\alpha;\beta 2}(\mathbf{k}_1, \mathbf{k}_2, \omega_1, \omega_2) \Big|_{\mathbf{k}_{1,2} \rightarrow \mathbf{0}, \omega_{1,2} \rightarrow 0} \right) b^{d+z-\tilde{a}-a-c_5}, \quad (5.70)$$

with the following constraints,

$$1 = \left(1 - i \frac{\partial \Pi_{11}(\mathbf{0}, \omega)}{\partial \omega} \Big|_{\omega \rightarrow 0} \right) b^{d-\tilde{c}-c}, \quad (5.71)$$

$$1 = \left(1 - i \frac{\partial \Pi_{22}(\mathbf{0}, \omega)}{\partial \omega} \Big|_{\omega \rightarrow 0} \right) b^{d-\tilde{c}_5-c_5}. \quad (5.72)$$

Therefore, once we can evaluate the self-energies $\Sigma_{\alpha\alpha}(\mathbf{k}, \omega)$, $\Pi_{ij}(\mathbf{k}, \omega)$ and vertex function corrections $V_{\alpha;\beta 2}(\mathbf{k}_1, \mathbf{k}_2, \omega_1, \omega_2)$, we obtain the recursion relations for the dynamic parameters in the MSRJD action. We put the details of the calculations on $\Sigma_{\alpha\alpha}$, Π_{ij} , and $\mathcal{V}_{\alpha;\beta 2}$ in Appendix C.

In the calculations of Appendix C, the following parameters are introduced:

$$f \equiv \frac{g^2 \Lambda^{-\epsilon}}{8\pi^2 \lambda_5 \Gamma}, \quad w \equiv \frac{\Gamma \chi}{\lambda}, \quad w_5 \equiv \frac{\Gamma \chi_5}{\lambda_5}, \quad h \equiv \frac{CB}{\sqrt{\lambda \lambda_5 \Lambda}}, \quad (5.73)$$

$$X \equiv \frac{2}{\sqrt{(1+w)(1+w_5)+h^2} + \sqrt{(1+w)(1+w_5)}} \sqrt{\frac{1+w}{1+w_5}}, \quad X' \equiv \frac{1+w_5}{1+w} X, \quad (5.74)$$

where $B \equiv |\mathbf{B}|$. By using these new parameters and based on the detailed analysis in appendix C, we can obtain the recursion relations for the dynamic

parameters Γ_l , λ_l , λ_5 , C_l and g_l at the one-loop level:

$$\Gamma_{l+1} = b^{z-2}\Gamma_l [1 - (4v_l w_l X'_l - f_l X_l) \ln b], \quad (5.75)$$

$$\lambda_{l+1} = b^{z-d+2c-2}\lambda_l, \quad (5.76)$$

$$(\lambda_5)_{l+1} = b^{z-d+2c_5-2}(\lambda_5)_l \left(1 + \frac{f_l}{2} \ln b\right), \quad (5.77)$$

$$C_{l+1} = b^{z+c+c_5-d-1}C_l, \quad (5.78)$$

$$g_{l+1} = b^{z-d+c_5}g_l. \quad (5.79)$$

Here, Eqs. (5.75), (5.76)–(5.78), (5.79) are derived in Appendix C.2, C.1, C.3, respectively. Among these recursion relations, Eq. (5.78) shows that the CME coefficient C is not renormalized by the critical fluctuations of the order parameter in this order. This may be viewed as an extension of the nonrenormalization theorem for the CME coefficient at the second-order chiral phase transition, where σ becomes massless.

To obtain the fixed point solutions of the recursion relations, it is useful to obtain the recursion relations for the parameters defined in Eq. (5.73). By using the recursion relations for the dynamic parameters (5.75)–(5.79) and the static parameters (5.46)–(5.48), we reach

$$f_{l+1} = b^\epsilon f_l \left[1 + \left(4v_l w_l X'_l - f_l X_l - \frac{1}{2}f_l\right) \ln b\right], \quad (5.80)$$

$$(w_5)_{l+1} = (w_5)_l \left[1 - \left(4v_l w_l X'_l - f_l X_l + \frac{1}{2}f_l\right) \ln b\right], \quad (5.81)$$

$$w_{l+1} = w_l [1 - (4v_l w_l X'_l - f_l X_l - 4v_l) \ln b], \quad (5.82)$$

$$h_{l+1} = b h_l \left(1 - \frac{f_l}{4} \ln b\right). \quad (5.83)$$

The dynamic RG equations corresponding to Eqs. (5.80)–(5.83) can be derived in a way similar to Eqs. (5.53)–(5.54) as (see also the footnote under

Eq. (5.53) for the derivation of the RG equation from the recursion relation)

$$\frac{df_l}{dl} = \left(\epsilon + 4v_l w_l X'_l - f_l X_l - \frac{1}{2} f_l \right) f_l, \quad (5.84)$$

$$\frac{d(w_5)_l}{dl} = \left(-4v_l w_l X'_l + f_l X_l - \frac{1}{2} f_l \right) (w_5)_l, \quad (5.85)$$

$$\frac{dw_l}{dl} = (-4v_l w_l X'_l + f_l X_l + 4v_l) w_l, \quad (5.86)$$

$$\frac{dh_l}{dl} = \left(1 - \frac{f_l}{4} \right) h_l, \quad (5.87)$$

from which we find four possible nontrivial fixed-point values of f , w_5 , w , h :⁵

$$(i) \quad f_\infty = \epsilon, \quad (w_5)_\infty = 1, \quad w_\infty = h_\infty = 0; \quad (5.88)$$

$$(ii) \quad f_\infty = \frac{2}{3}\epsilon, \quad (w_5)_\infty = w_\infty = h_\infty = 0; \quad (5.89)$$

$$(iii) \quad f_\infty = \epsilon, \quad (w_5)_\infty = \frac{3}{7}, \quad w_\infty = h_\infty = \infty; \quad (5.90)$$

$$(iv) \quad f_\infty = 2\epsilon, \quad (w_5)_\infty = 0, \quad w_\infty = h_\infty = \infty. \quad (5.91)$$

Some remarks on the fixed points above are in order here. Since the magnetic field is external ($B \neq 0$), the fixed points (i) and (ii) with $h_\infty = 0$ should be interpreted as $C = 0$. We should note that the RG equations (5.84)–(5.86) are nonuniform in the limits $w \rightarrow \infty$ and $h^2 \rightarrow \infty$. If one takes $w \rightarrow \infty$ first by fixing h^2 to some particular value, the fixed point (iii) is obtained; if one takes $h^2 \rightarrow \infty$ first by fixing w to some particular value, the fixed point (iv) is obtained. In other words, the fixed point (iii) corresponds to the case $w_\infty \gg h_\infty^2 \gg 1$, and the fixed point (iv) corresponds to the case $h_\infty^2 \gg w_\infty \gg 1$. The competition between $w \rightarrow \infty$ and $h^2 \rightarrow \infty$ in Eq. (5.74) are characterized by the strength of the following parameter,

$$\frac{h^2}{w} = \frac{C^2 B^2}{\lambda_5 \Gamma \chi \Lambda^2}. \quad (5.92)$$

From the expression of Eq. (5.92), we can see which parameters among C , λ and λ_5 are dominant near the fixed points, for a finite kinetic coefficient of the

⁵Besides, there is a trivial fixed point, $f_\infty = (w_5)_\infty = w_\infty = h_\infty = 0$, which is stable only for $\epsilon < 0$, and is not considered here.

order parameter, Γ , and finite static susceptibilities, χ and χ_5 .⁶ By looking at f_∞ , $(w_5)_\infty$, and the fixed-point value of (5.92), one can see the fixed point (iii) corresponds to $C \rightarrow 0$ and $\lambda \rightarrow 0$ with finite λ_5 , where the CME can be neglected compared to the diffusion effect; the fixed point (iv) corresponds to $C \rightarrow \infty$, $\lambda \rightarrow 0$, and $\lambda_5 \rightarrow \infty$ with $C^2/\lambda_5 \rightarrow \infty$, where the diffusion effect can be neglected compared to the CME. In short, we can regard the competition between the two limits $w \rightarrow \infty$ and $h^2 \rightarrow \infty$ as the competition between the CME and the diffusion of the axial isospin density n_5 .

Stability of fixed points

We here summarize the stability analysis of the fixed points (i)–(iv). In order to investigate the influence of the CME, we study the stability of the fixed points at $C = 0$, namely the fixed points (i) and (ii). For this purpose, we consider the linear perturbations around these fixed points,

$$f_l = f_\infty + \delta f, \quad (w_5)_l = (w_5)_\infty + \delta w_5, \quad w_l = \delta w, \quad h_l = \delta h. \quad (5.93)$$

Substituting these expressions into Eqs. (5.84)–(5.87) and setting $v_l = v_\infty = \epsilon/20$ from Eq. (5.55),⁷ the linearized equations with respect to δf , δw_5 , δw , and δh read

$$\frac{d}{dl} \begin{pmatrix} \delta f \\ \delta w_5 \\ \delta w \\ \delta h \end{pmatrix} = \mathcal{M}' \begin{pmatrix} \delta f \\ \delta w_5 \\ \delta w \\ \delta h \end{pmatrix}, \quad (5.94)$$

where we define

$$\mathcal{M}' \equiv \begin{pmatrix} -f_\infty \left(\theta_\infty + \frac{1}{2} \right) & f_\infty^2 \theta_\infty^2 & 4v_\infty f_\infty & 0 \\ (w_5)_\infty \left(\theta_\infty - \frac{1}{2} \right) & f_\infty \left[\theta_\infty - \frac{1}{2} - (w_5)_\infty \theta_\infty^2 \right] & -4v_\infty (w_5)_\infty & 0 \\ 0 & 0 & f_\infty \theta_\infty + 4v_\infty & 0 \\ 0 & 0 & 0 & 1 - \frac{f_\infty}{4} \end{pmatrix} \quad (5.95)$$

⁶One can confirm the finiteness of Γ , χ , and χ_5 by putting back the fixed-point values of v , f , w_5 , w , and h to the recursion relations (5.46), (5.47), and (5.75) with the help of Eqs. (5.50) and (5.56).

⁷Here we can ignore the fluctuation of v_l , because all of the fluctuation of v_l will be multiplied by $O(\delta w)$ in Eqs. (5.84)–(5.87) if we try to substitute $v_l = v_\infty + \delta v$.

and

$$\theta_\infty \equiv \frac{1}{1 + (w_5)_\infty} = \begin{cases} \frac{1}{2} & \text{for the case (i),} \\ 1 & \text{for the case (ii).} \end{cases} \quad (5.96)$$

We can test the stability of the fixed points (i) and (ii) by substituting each of the fixed point values into \mathcal{M}' . Because of $(w_5)_\infty (\theta_\infty - 1/2) = 0$ for both cases (i) and (ii), the matrix \mathcal{M}' defined in Eq. (5.94) is reduced to an upper triangular matrix. Thus, the eigenvalues of \mathcal{M}' are just given by its diagonal components for each fixed point:

$$(i) \quad \left(-\epsilon, -\frac{\epsilon}{4}, \frac{7}{10}\epsilon, 1 - \frac{\epsilon}{4}\right) \quad \text{and} \quad (ii) \quad \left(-\epsilon, \frac{\epsilon}{3}, \frac{13}{15}\epsilon, 1 - \frac{\epsilon}{6}\right). \quad (5.97)$$

From this result, we find that the fixed point (ii) is unstable in the w_5 di-

$$(v_l, w_l, h_l) = (v_\infty, w_\infty, h_\infty) = (\epsilon/20, 0, 0)$$

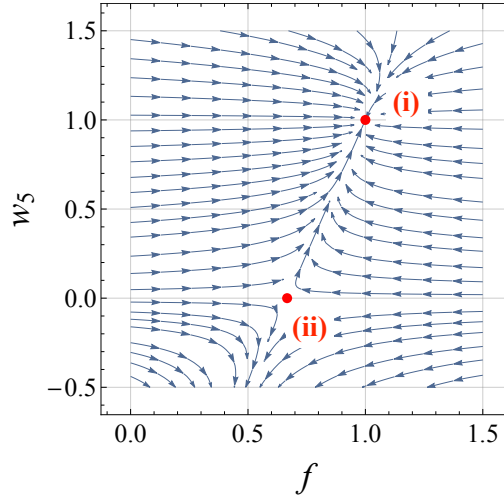


Figure 5.3: RG flow of the parameters f and w_5 for fixed w and h ($\epsilon = 1$), which shows the fixed points (i) and (ii).

rection and that the RG flow runs to the fixed point (i) (see also Fig. 5.3 showing the RG flows in the (f, w_5) plane at $w = h = 0$). We also find that the fixed points (i) and (ii) are unstable in the directions of w and h , showing that λ and C are relevant. It follows that small but nonzero values of w and h grow around the fixed point (i).

There are two possibilities of the final destination of the flow from the fixed point (i): the fixed point (iii) and the fixed point (iv). Let us first qualitatively understand the conditions for obtaining each of the fixed points (iii) and (iv) by using RG flow diagrams. For this purpose, we first forcibly fix w and h to some finite values and investigate the RG flows in the (f, w_5) plane. As one can see in the RG flows in Figs. 5.4(a) and 5.4(b), f and w_5 flow to the fixed point (iii) when $w \gg h^2 \gg 1$, while they flow to the fixed point (iv) when $h^2 \gg w \gg 1$, related to the properties of the fixed points (iii) and (iv) noted under Eq. (5.91). On the other hand, Fig. 5.4(c) shows that (f, w_5) flow to the intermediate values between the fixed-point values of (iii) and (iv) when $w \sim h^2$. Next, we vary w and h around those values of the fixed point (i) with fixed f and w_5 , and study which one is more relevant (iii) or (iv) around the fixed points (i). As is shown in Fig. 5.5, the points in the (w, h) plane flow in the direction along the h axis unless $w \gg h$. Therefore, the system eventually flows to the fixed point (iv) for most of the parameter region around the fixed point (i).

Next, we consider the RG flows in all the parameter space (f, w_5, w, h) without fixing the parameters. Here, we first set the initial parameters near the fixed point (i) and consider the flow equations at a finite flow time. As is shown within the linear-stability analysis in Appendix D, the initial parameter region that flows to the fixed point (iv) is much broader than the region that flows to the fixed point (iii) in the (w, h) plane. Therefore, in the almost whole region of the (w, h) plane near the fixed point (i), the fixed point (iv) is favorable rather than the fixed point (iii). We can also study the RG flow from the initial values near the fixed point (iii). Expect for the case of the RG evolution, starting from the parameters exactly at the fixed point (iii), all the parameters will eventually take the fixed-point values of (iv). This is because h grows much more rapidly than w due to the additional scaling factor b in the recursion relation (5.83) for h , compared to the relation (5.82) for w . From the above discussion, it follows that the fixed point (iv) is stable in the almost whole region at finite w and h , while generally at a finite flow time there is a small parameter region that flows to the fixed point (iii).

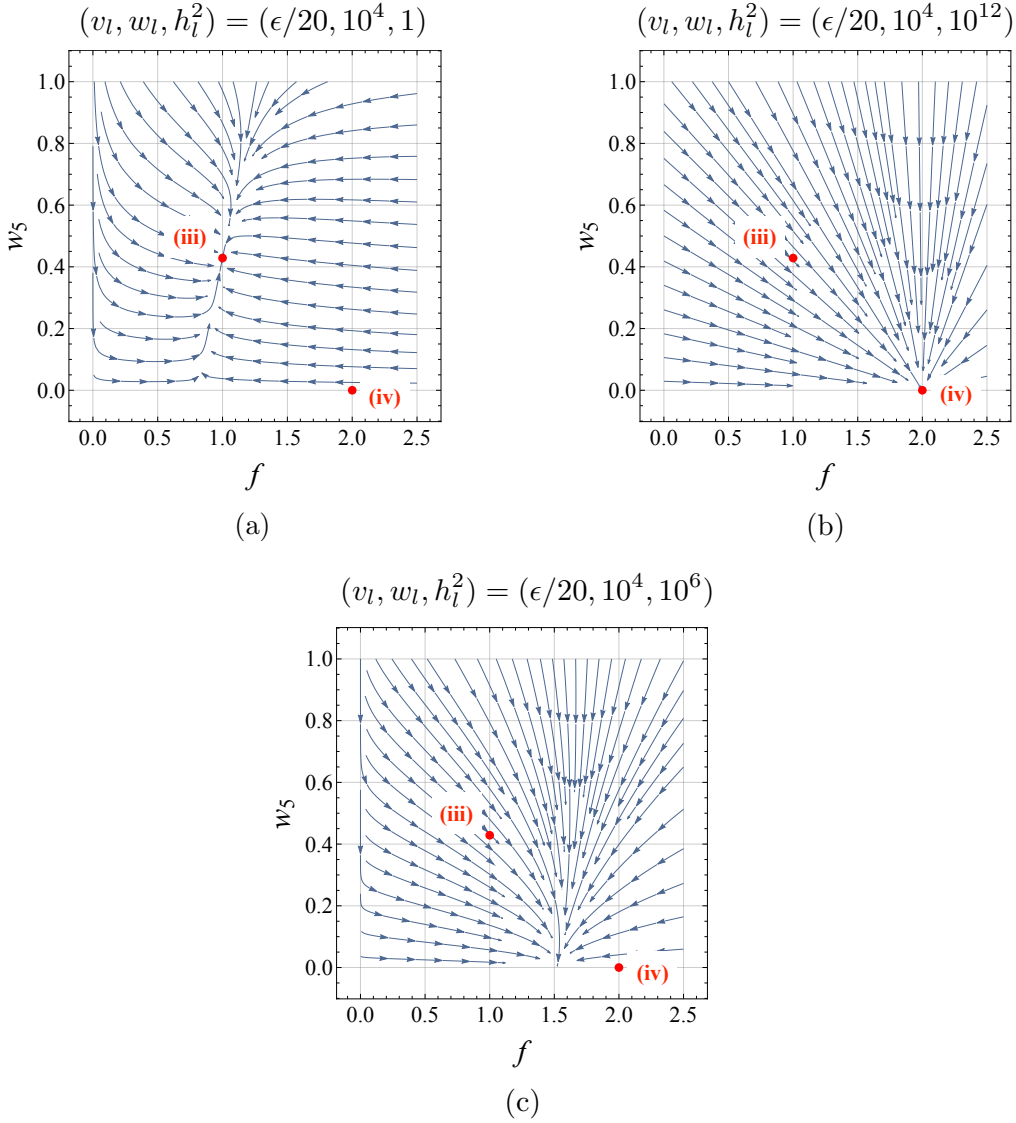


Figure 5.4: RG flows of f and w_5 ($\epsilon = 1$). We fix the values of w and h^2 in several cases: (a) $w \gg h^2 \gg 1$, (b) $h^2 \gg w \gg 1$, and (c) $w \sim h^2$. These figures show the existence of the fixed points (iii) and (iv), and the flow to their intermediate values.

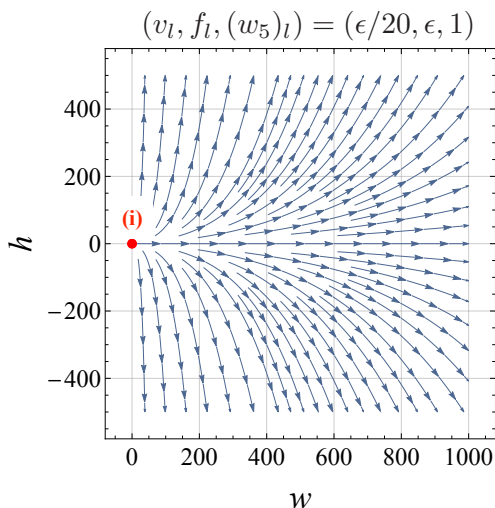


Figure 5.5: RG flow of w and h with fixing f and w_5 to those values at the fixed point (i) ($\epsilon = 1$).

5.3.3 Physical consequences

Dynamic universality class

From the fixed point values (i)–(iv) obtained in Eqs. (5.88)–(5.91), we can evaluate the dynamic critical exponent which characterizes the dynamic universality class of the system. Practically, we substitute the fixed point values into the recursion relation (5.75) for Γ_l , in each case of the fixed-point values (i)–(iv).

The fixed points (i) and (iii) have the dynamic critical exponent of model E, $z = d/2$. As is also summarized in Tab. 3.1 the dynamic universality class of model E is generally determined only by two-component order parameter (mapped into $U(1)$) and *one* conserved density that are coupled through the Poisson brackets. In our case, the order parameter field ϕ_α and the axial isospin density n_5 are essential, whereas the isospin density n does not affect the dynamic universality class.⁸

On the other hand, the fixed point (iv) has the dynamic critical exponent $z = 2$. Up to $O(\epsilon)$, this exponent is the same as that of model A, which is the

⁸The difference between n and n_5 can be seen in the Poisson brackets: there is a nonzero Poisson bracket among n_5 and ϕ_α in Eq. (5.20), whereas there are no nontrivial Poisson brackets among n and ϕ_α .

simplest class determined only by nonconserved order parameters (see also Tab. 3.1). In the system near the fixed point (iv), the internal-momentum loop dominated by the CMW (the wavy lines in Fig. C.2) is suppressed, so that not only n but also n_5 do not affect the dynamic universality class. One can confirm that the factors X and wX' stemming from Fig. C.2 vanish.

Now we remind the stability analysis in Sec. 5.3.2: the small fluctuation of the fixed point (i) in the absence of the CME can lead to the fixed point (iv). We find that the inclusion of the CME can change the dynamic universality class from model E into model A, corresponding to the stable fixed point (i) and (iv), respectively. Strictly speaking, there is a small parameter region that leads to model E, even $\mathbf{B} \neq \mathbf{0}$ and $C \neq 0$ as we also noted in 5.3.2. Nevertheless, such a region is small compared to the region that leads to model A.

Critical attenuation of the CMW

As a result of the static critical behavior, Eq. (5.58), we find the critical attenuation of the CMW: in the vicinity of the second-order chiral phase transition, the speed of the CMW tends to zero as

$$v_{\text{CMW}}^2 \equiv \frac{C^2 B^2}{\chi \chi_5} \sim \xi^{-\frac{\alpha}{\nu}}, \quad (5.98)$$

where v_{CMW} is the speed of the CMW [20] which have been already seen in its wave equation (2.81). We have already obtained the ratio α/ν in Eq. (5.59). This phenomenon is analogous to the critical attenuation of the speed of sound near the critical point associated with the liquid-gas phase transition [35].

5.4 Conclusion and discussion

In this chapter, we have studied the critical dynamics near the second-order chiral phase transition in massless two-flavor QCD under an external magnetic field and investigated the influence of the CME on the dynamic critical phenomena in QCD. We found that the inclusion of the CME and the resulting CMW can change the dynamic universality class of the system from the model E into model A. We also found the critical attenuation of the CMW analogous to that of the sound wave in the liquid-gas phase transition.

We now discuss the analogy of the critical attenuation between the CMW and the sound wave of the compressive fluids near the liquid-gas critical point. Let us first recall the critical attenuation of sounds near the critical point associated with the liquid-gas phase transition, where the order parameter ψ_{LG} is a linear combination of the energy density ε and the mass density ρ_m . In this case, the speed of sound, c_s , is attenuated with the correlation-length dependence [35],

$$c_s^2 \equiv \left(\frac{\partial P}{\partial \rho_m} \right)_S = \frac{T \left(\frac{\partial P}{\partial T} \right)_{\rho_m}^2}{\rho_m^2 C_V \left(1 - \frac{C_V}{C_P} \right)} \sim \xi^{-\frac{\alpha}{\nu}}, \quad (5.99)$$

where P and S are the pressure and total entropy per unit mass of the fluids, respectively. To obtain the last expression of Eq. (5.99), we use some thermodynamic relations and the fact that the specific heat with constant volume $C_V \equiv T(\partial S/\partial T)_\rho$, and that with constant pressure $C_P \equiv T(\partial S/\partial T)_P$, diverge near the critical point as $C_V \sim \xi^{\frac{\alpha}{\nu}}$ and $C_P \sim \xi^{\frac{\gamma}{\nu}}$, respectively. Here, the critical exponents ν , α , and γ defined by Eq. (5.58) and $\psi_{\text{LG}} \sim \tau^\gamma$ are determined by the static universality class of the 3D Ising model, $\alpha \approx 0.1$, $\nu \approx 0.6$, $\gamma \approx 1.2$. We also use the approximation $C_V/C_P \ll 1$ near the critical point. Remarkably, Eq. (5.99) takes exactly the same form as that of the CMW which we obtained in Eq. (5.98), although the values of α and ν themselves are different due to the difference of the static universality classes.

When the reduced temperature τ is sufficiently larger than $\bar{m}_q \equiv m_q/T_c$, quark mass effects on the critical phenomena can be negligible. Our analysis in the chiral limit would be relevant to such a parameter region around the high-temperature QCD critical point under an external magnetic field.

Chapter 6

Summary and outlook

In this thesis, we have studied the novel dynamic critical phenomena induced by superfluidity and the CME in QCD.

In Sec. 4 we have first elucidated the influence of the superfluidity on the critical phenomena near the high-density QCD critical point. In particular, we have found that the static universality class is the same as that of the high-temperature critical point, independently of the existence of the superfluid phonon. On the other hand, we have found that the superfluid phonon exhibits the critical slowing down when the critical point is approached. Furthermore, we have found that the dynamic universality class of the high-density critical point is not only different from that of the high-temperature critical point but also all of the conventional classes studied by Hohenberg and Halperin [6].

Experimental signatures related to the dynamic critical phenomenon in the heavy-ion collisions can distinguish the possible two QCD critical points. Though the *vanishing* speed of the superfluid phonon characterizes the high-density critical point, little research has considered the superfluid phonon itself in the context of the heavy-ion collisions. It would be essential to investigate the role of the superfluid phonon on the evolution of the hot and dense medium created in the heavy-ion collisions.

In Sec. 5 we have studied the interplay between the dynamic critical phenomena and the CME in QCD. For this purpose, we considered the dynamic critical phenomena of the second-order chiral phase transition under an external magnetic field. Then, we have found that the inclusion of the CME and the resulting CMW can change the dynamic universality class of the system from the model E into model A within the conventional classification.

We have also found that the speed of the CMW tends to vanish near the phase transition point and that the speed can be characterized by the same static critical exponents as those of the sound wave in the vicinity of the liquid-gas critical point.

While we have limited our analysis in Sec. 5 to the background magnetic field, dynamical electromagnetic fields may affect the critical dynamics in QCD. In massless QCD coupled to dynamical electromagnetic fields in an external magnetic field, there appears a nonrelativistic photon with a quadratic dispersion relation due to the quantum anomaly [77]. At finite temperature, such a novel gapless mode will be crucial for dynamic critical phenomena near the second-order chiral phase transition. This study will be reported in detail elsewhere.

Appendix A

Static RG of the scalar field theory

In this appendix, we show the detailed RG analysis on the (one component) scalar field theory (3.36). In particular, we derive the RG equations (3.41) and (3.42), and the Wilson-Fisher fixed-point solution (3.43).

A.1 Perturbative RG equation

To derive the RG equations of the Ginzburg-Landau free energy (3.36), we first construct its perturbation theory. We start by decomposing the free energy into the following form:

$$\beta F_\Lambda[\psi] = \beta F_{0\Lambda}[\psi] + \beta F'_\Lambda[\psi] + \int d\mathbf{r} h\psi, \quad (\text{A.1})$$

where the free part and the perturbative part are given by

$$\begin{aligned} \beta F_{0\Lambda}[\psi] &= \int d\mathbf{r} \left[\frac{r}{2}\psi^2(\mathbf{r}) + \frac{1}{2}(\nabla\psi(\mathbf{r}))^2 \right] \\ &= \int_{\mathbf{q}} \frac{1}{2}(r + \mathbf{q}^2)\psi(\mathbf{q})\psi(-\mathbf{q}), \end{aligned} \quad (\text{A.2})$$

$$\begin{aligned} \beta F'_\Lambda[\psi] &= u \int d\mathbf{r} \psi^4(\mathbf{r}) \\ &= u \int_{\mathbf{q}_1} \int_{\mathbf{q}_2} \int_{\mathbf{q}_3} \int_{\mathbf{q}_4} \psi(\mathbf{q}_1)\psi(\mathbf{q}_2)\psi(\mathbf{q}_3)\psi(\mathbf{q}_4)\delta(\mathbf{q}_1 + \mathbf{q}_2 + \mathbf{q}_3 + \mathbf{q}_4), \end{aligned} \quad (\text{A.3})$$

respectively. Here, we use the simple notation of the momentum integral,

$$\int_{\mathbf{q}} \equiv \int \frac{d^d \mathbf{q}}{(2\pi)^d}. \quad (\text{A.4})$$

Using Eqs. (3.21) and (A.1), we can write the partition function as

$$Z = \int \mathcal{D}\psi^> \mathcal{D}\psi^< e^{-\beta F_{\Lambda}[\psi]} = \int \mathcal{D}\psi^< e^{-\beta F_{\Lambda/b}[\psi^<]}, \quad (\text{A.5})$$

with $\beta F_{\Lambda/b}[\psi^<]$ being the effective free energy of the low-momentum field $\psi^<$:

$$e^{-\beta F_{\Lambda/b}[\psi^<]} \equiv \int \mathcal{D}\psi^> e^{-\beta F_{0\Lambda}[\psi] - \beta F'_{\Lambda}[\psi] - \beta \int d\mathbf{r} h \psi}. \quad (\text{A.6})$$

One can write this effective free energy by using the generating functional $\mathcal{Z}[h]$,

$$\mathcal{Z}[h] \equiv \left\langle e^{-\beta \int d\mathbf{r} h \psi^>} \right\rangle, \quad (\text{A.7})$$

with the expectation value defined in the following form;

$$\langle O[\psi^<, \psi^>] \rangle \equiv (Z^>)^{-1} \int \mathcal{D}\psi^> e^{-\beta F_{0\Lambda}[\psi] - \beta F'_{\Lambda}[\psi]} O[\psi^<, \psi^>], \quad (\text{A.8})$$

$$Z^> \equiv \int \mathcal{D}\psi^> e^{-\beta F_{0\Lambda}[\psi] - \beta F'_{\Lambda}[\psi]}. \quad (\text{A.9})$$

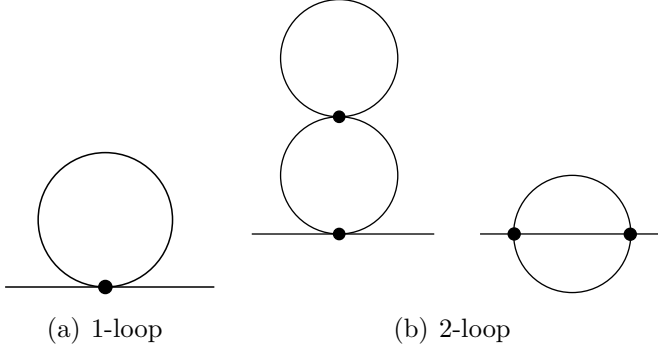
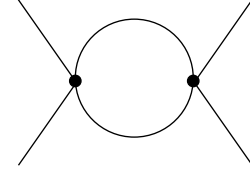
In fact, we rewrite Eq. (A.6) into

$$e^{-\beta F_{\Lambda/b}[\psi^<] + \beta \int d\mathbf{r} h \psi^<} = \int \mathcal{D}\psi^> e^{-\beta F_{0\Lambda}[\psi] - \beta F'_{\Lambda}[\psi] - \beta \int d\mathbf{r} h \psi^>} = \mathcal{Z}[h]. \quad (\text{A.10})$$

Then, we find that $\beta F_{\Lambda/b}[\psi^<]$ satisfies

$$\beta F_{\Lambda/b}[\psi^<] = -\ln \mathcal{Z}[h] + \beta \int d\mathbf{r} h \psi^<. \quad (\text{A.11})$$

This relation means that the generating functional obtained from integrating over $\psi^>$ gives the effective free energy for $\psi^<$. Therefore, we can get the

Figure A.1: Σ Figure A.2: V

effective free energy by calculating the sum of each vortex function,

$$\begin{aligned}
& \beta F_{\Lambda/b}[\psi^<] \\
&= \int_{\mathbf{q}} \frac{\delta(\beta F_{\Lambda/b}[\psi^<])}{\delta\psi^<(\mathbf{q})\delta\psi^<(-\mathbf{q})} \psi^<(\mathbf{q})\psi^<(-\mathbf{q}) \\
&+ \int_{\mathbf{q}_1 \dots \mathbf{q}_4} \frac{\delta(\beta F_{\Lambda/b}[\psi^<])}{\delta\psi^<(\mathbf{q}_1)\delta\psi^<(\mathbf{q}_2)\delta\psi^<(\mathbf{q}_3)\delta\psi^<(\mathbf{q}_4)} \psi^<(\mathbf{q}_1)\psi^<(\mathbf{q}_2)\psi^<(\mathbf{q}_3)\psi^<(\mathbf{q}_4) \\
&\quad \times \delta(\mathbf{q}_1 + \dots + \mathbf{q}_4) + \dots, \tag{A.12}
\end{aligned}$$

where the 2- and 4- points vortex functions are given by

$$\frac{\delta(\beta F_{\Lambda/b}[\psi^<])}{\delta\psi^<(\mathbf{q})\delta\psi^<(-\mathbf{q})} = \frac{1}{2}(r + \mathbf{q}^2) + \Sigma(\mathbf{q}), \tag{A.13}$$

$$\frac{\delta(\beta F_{\Lambda/b}[\psi^<])}{\delta\psi^<(\mathbf{q}_1)\delta\psi^<(\mathbf{q}_2)\delta\psi^<(\mathbf{q}_3)\delta\psi^<(\mathbf{q}_4)} = u + V(\mathbf{q}), \tag{A.14}$$

respectively. Here, Σ and V are the 1-particle irreducible diagrams including the internal momentum loops of $\psi^>$. The lowest-loop contributions can be obtained as Figs. A.1 and A.2. The rules for calculating these diagrams are summarized as follows:

(i) Assign momentums for each of internal and external lines satisfying the momentum conservation laws;

(ii) Multiply the free propagator $\frac{1}{r + \mathbf{q}^2}$ for each of the internal lines;

(iii) Multiply the free 4-point vortex function u for each of the vertices (black dots);

- (iv) Integrate over the momentum of the internal lines;
- (v) Multiply some numerical factor.¹

Next we carry out the rescaling of the vortex functions (A.13) and (A.14) and complete the RG transformation. Writing the vortex functions after one RG step as

$$\frac{\delta(\beta F_\Lambda[\psi'])}{\delta\psi'(\mathbf{q}')\delta\psi'(-\mathbf{q}')} = \frac{1}{2}(r' + K'\mathbf{q}'^2) + O(\mathbf{q}'^4), \quad (\text{A.16})$$

$$\frac{\delta(\beta F_\Lambda[\psi'])}{\delta\psi'(\mathbf{q}'_1)\delta\psi'(\mathbf{q}'_2)\delta\psi'(\mathbf{q}'_3)\delta\psi'(\mathbf{q}'_4)} = u' + O(\mathbf{q}'^2), \quad (\text{A.17})$$

we obtain the parameters one step after the RG,

$$r' = b^2 \left[r + 6u \int_{\mathbf{q}}^> \frac{1}{r + \mathbf{q}^2} + O(u^2) \right], \quad (\text{A.18})$$

$$K' = 1 + O(u^2), \quad (\text{A.19})$$

$$u' = b^\epsilon \left[u - 36u^2 \int_{\mathbf{q}}^> \frac{1}{(r + \mathbf{q}^2)^2} \right]. \quad (\text{A.20})$$

Here, the overall factors b^2 and b^ϵ come from the rescaling. The short-hand notation

$$\int_{\mathbf{q}}^> \equiv \int_{\Lambda/b}^\Lambda \frac{d^d \mathbf{q}}{(2\pi)^d} \quad (\text{A.21})$$

denotes the integration over the high momentum loop. We can carry out the

¹For the given diagram with N_v vertices, the numerical factor is given by

$$\frac{N_v!}{N_{\text{sym}}} \times \prod_{i=1}^{N_v} \frac{4!}{N_{i>}!N_{i<}!}, \quad (\text{A.15})$$

where $N_{i>}$ and $N_{i<}$ are the number of the internal and the external lines connecting to the i -th vortex, and N_{sym} is the geometrical symmetry factor.

integrals in Eqs. (A.18) and (A.20) as

$$\begin{aligned}
\int_{\mathbf{q}}^> \frac{1}{r + \mathbf{q}^2} &= \int_{\mathbf{q}}^> \frac{1}{\mathbf{q}^2} \frac{1}{1 + r/\mathbf{q}^2} \\
&\simeq \int_{\mathbf{q}}^> \frac{1}{\mathbf{q}^2} \left(1 - \frac{r}{\mathbf{q}^2} \right) \\
&= \int_{\Lambda/b}^{\Lambda} \frac{d^d \mathbf{q}}{(2\pi)^d} \frac{1}{\mathbf{q}^2} - r \int_{\Lambda/b}^{\Lambda} \frac{d^d \mathbf{q}}{(2\pi)^d} \frac{1}{\mathbf{q}^4} \\
&= \frac{\Lambda^{2-\epsilon}}{8\pi^2} \left(1 - \frac{1}{b^2} \right) - r \frac{\Lambda^{-\epsilon}}{8\pi^2} \ln b, \tag{A.22}
\end{aligned}$$

$$\begin{aligned}
\int_{\mathbf{q}}^> \frac{1}{(r + \mathbf{q}^2)^2} &\simeq \int_{\mathbf{q}}^> \frac{1}{\mathbf{q}^4} \\
&= \frac{\Lambda^{-\epsilon}}{8\pi^2} \ln b. \tag{A.23}
\end{aligned}$$

Here, we consider the system sufficiently near the phase transition point and set $r \ll 1$. We also use the formulas (A.39) and (A.40). Then, we can write Eqs. (A.18) and (A.20) into

$$r' = b^2 \left[r + 6uK_d\Lambda^{2-\epsilon} \left(1 - \frac{1}{b^2} - \frac{r}{\Lambda^2} \ln b \right) \right], \tag{A.24}$$

$$u' = b^\epsilon (u - 36u^2K_d\Lambda^{-\epsilon} \ln b). \tag{A.25}$$

By defining the dimension less parameters,

$$\bar{r} \equiv \frac{r}{\Lambda^2}, \quad \bar{u} \equiv \frac{K_d u}{\Lambda^\epsilon}, \tag{A.26}$$

with

$$K_d \equiv \frac{1}{8\pi^2}, \tag{A.27}$$

we can rewrite these into

$$\bar{r}' = b^2 \left[\bar{r} + 6\bar{u} \left(1 - \frac{1}{b^2} - \bar{r} \ln b \right) \right], \tag{A.28}$$

$$\bar{u}' = b^\epsilon (\bar{u} - 36\bar{u}^2 \ln b). \tag{A.29}$$

These are the recursion relations which relate the parameters before and after the RG procedure (at a single step).

We will next derive the differential equations equivalent to the recursion relation. In order to do this, we consider the thin momentum shell with $0 < l \ll 1$,

$$b \equiv e^l \simeq 1 + l. \quad (\text{A.30})$$

Then, Eqs. (A.28) and (A.29) reduce to

$$\bar{r}' = (1 + 2l)(\bar{r} + 24\bar{u}l - 6\bar{u}\bar{r}l) = \bar{r} + 24\bar{u}l - 6\bar{u}\bar{r}l + 2\bar{r}l + O(l^2), \quad (\text{A.31})$$

$$\bar{u}' = (1 + \epsilon l)(\bar{u} - 36\bar{u}^2l) = \bar{u} - 36\bar{u}^2l + \epsilon\bar{u}l. \quad (\text{A.32})$$

By writing

$$\frac{d\bar{r}}{dl} \equiv \lim_{l \rightarrow 0} \frac{\bar{r}' - \bar{r}}{l}, \quad \frac{d\bar{u}}{dl} \equiv \lim_{l \rightarrow 0} \frac{\bar{u}' - \bar{u}}{l}, \quad (\text{A.33})$$

we obtain the RG equations,

$$\frac{d\bar{r}}{dl} = 2\bar{r} + 12\bar{u} - 12\bar{r}\bar{u}, \quad (\text{A.34})$$

$$\frac{d\bar{u}}{dl} = \epsilon\bar{u} - 36\bar{u}^2, \quad (\text{A.35})$$

which give Eqs. (3.41) and (3.42).

A.2 Wilson-Fisher fixed point

We first assume r and u are order of ϵ near the critical point. Then we can neglect the last term in the right-hand side of Eq. (A.34) and any other higher-order terms coming from the perturbation expansion of u . Since the typical length scale disappear at the critical point, the RG invariance emerges in the system. Therefore, we can set

$$\frac{d\bar{r}}{dl} = \frac{d\bar{u}}{dl} = 0, \quad (\text{A.36})$$

which yields two fixed-point solutions: one is the Gaussian fixed point:

$$\bar{r} = \bar{u} = 0, \quad (\text{A.37})$$

and the other is the so-called Wilson-Fisher fixed point (we get Eq. (3.43)):

$$\bar{r} = -\frac{\epsilon}{6} \quad \bar{u} = \frac{\epsilon}{36}. \quad (\text{A.38})$$

This solution is consistent with the assumption at the beginning of this subsection. From the linear stability analysis, the Gaussian fixed point is unstable with respect to \bar{u} , whereas the Wilson-Fisher fixed point is stable [63].

A.3 Useful intergrals

$$\begin{aligned} \int_{\Lambda/b}^{\Lambda} \frac{d^d \mathbf{q}}{(2\pi)^d} \frac{1}{\mathbf{q}^2} &= \frac{1}{(2\pi)^d} \int d\theta \int d\varphi_1 \int d\varphi_2 \dots \int_{\Lambda/b}^{\Lambda} dq q^{d-3} \sin^{d-2} \theta \sin^{d-3} \varphi_1 \dots \\ &= \frac{\Lambda^{d-2}}{(2\pi)^d} \int d\theta \int d\varphi_1 \int d\varphi_2 \dots \int_{1/b}^1 dx x^{d-3} \sin^{d-2} \theta \sin^{d-3} \varphi_1 \dots \\ &\simeq \frac{\Lambda^{2-\epsilon}}{(2\pi)^4} \int_0^\pi d\theta \sin^2 \theta \int_0^\pi d\varphi_1 \sin \varphi_1 \int_0^{2\pi} d\varphi_2 \int_{1/b}^1 dx \\ &= \frac{\Lambda^{2-\epsilon}}{8\pi^2} \left(1 - \frac{1}{b^2}\right), \end{aligned} \quad (\text{A.39})$$

$$\begin{aligned} \int_{\Lambda/b}^{\Lambda} \frac{d^d \mathbf{q}}{(2\pi)^d} \frac{1}{\mathbf{q}^4} &= \frac{1}{(2\pi)^d} \int d\theta \int d\varphi_1 \int d\varphi_2 \dots \int_{\Lambda/b}^{\Lambda} dq q^{d-5} \sin^{d-2} \theta \sin^{d-3} \varphi_1 \dots \\ &= \frac{\Lambda^{d-4}}{(2\pi)^d} \int d\theta \int d\varphi_1 \int d\varphi_2 \dots \int_{1/b}^1 dx x^{d-3} \sin^{d-2} \theta \sin^{d-3} \varphi_1 \dots \\ &\simeq \frac{\Lambda^{-\epsilon}}{(2\pi)^4} \int_0^\pi d\theta \sin^2 \theta \int_0^\pi d\varphi_1 \sin \varphi_1 \int_0^{2\pi} d\varphi_2 \int_{1/b}^1 dx \frac{1}{x} \\ &= \frac{\Lambda^{-\epsilon}}{8\pi^2} \ln b. \end{aligned} \quad (\text{A.40})$$

Appendix B

Coupling to energy-momentum densities

In Secs. 4.2 and 4.3, we have ignored the contributions of the energy and momentum densities, ε and $\boldsymbol{\pi}$. In this appendix, we show that these contributions do not affect the static and dynamic universality classes of the high-density QCD critical point studied in Secs. 4.2 and 4.3. In particular, we obtain the expression of the superfluid phonon in the presence of ε and $\boldsymbol{\pi}$, Eq. (B.50), which will be mentioned in the discussion in Sec. 4.4.

B.1 Statics

Let us first consider the Ginzburg-Landau functional in terms of σ , n_B , ε , $\boldsymbol{\pi}$, and θ , up to the second-order expansion. Similarly to the argument in Sec. 4.2, the time reversal symmetry \mathcal{T} prohibits the mixing between $x_i \equiv \sigma, n_B, \varepsilon$ and $\boldsymbol{\pi}, \theta$:

$$F[\sigma, n_B, \varepsilon, \boldsymbol{\pi}, \theta] = F[\sigma, n_B, \varepsilon] + F[\boldsymbol{\pi}, \theta]. \quad (\text{B.1})$$

The presence of m_q and μ_B generally allows the mixing among σ, n_B , and ε in the \mathcal{T} -even sector as

$$F[\sigma, n_B, \varepsilon] = \frac{1}{2} \int d\mathbf{r} x_i \beta_{ij}(\boldsymbol{\nabla}) x_j, \quad (\text{B.2})$$

$$\beta_{ij}(\boldsymbol{\nabla}) = V_{ij} - v_{ij} \boldsymbol{\nabla}^2. \quad (\text{B.3})$$

Here, the subscripts i, j are the shorthand notations for x_i, x_j , respectively. The \mathcal{T} -odd sector is given by

$$F[\boldsymbol{\pi}, \theta] = \frac{1}{2} \int d\mathbf{r} [V_{\pi\pi} \boldsymbol{\pi}^2 + 2V_{\pi\theta} \boldsymbol{\pi} \cdot \boldsymbol{\nabla}\theta + V_{\theta\theta} (\boldsymbol{\nabla}\theta)^2]. \quad (\text{B.4})$$

We call $V_{ij}, v_{ij}, V_{\pi\pi}, V_{\pi\theta}$, and $V_{\theta\theta}$ the Ginzburg-Landau parameters.

By completing the square, Eq. (B.4) can be written as

$$F[\boldsymbol{\pi}, \theta] = \frac{1}{2} \int d\mathbf{r} [V_{\pi\pi} (\boldsymbol{\pi}')^2 + V'_{\theta\theta} (\boldsymbol{\nabla}\theta)^2], \quad (\text{B.5})$$

where $\boldsymbol{\pi}' \equiv \boldsymbol{\pi} + V_{\pi\theta} \boldsymbol{\nabla}\theta / V_{\pi\pi}$ and $V'_{\theta\theta} \equiv V_{\theta\theta} - V_{\pi\theta}^2 / V_{\pi\pi}$. We assume $V'_{\theta\theta} > 0$ and redefine $\boldsymbol{\pi}'$ and $V'_{\theta\theta}$ as $\boldsymbol{\pi}$ and $V_{\theta\theta}$ for simplicity in the following calculation.

In a similar manner to Eq. (4.3) when the ε and $\boldsymbol{\pi}$ are absent, the correlation length ξ is defined from the correlation function of σ . The form of the correlation function (4.5) can be generalized into

$$\xi \sim (\det V)^{-\frac{1}{2}} \quad (\text{B.6})$$

in the present case with V being the 3×3 matrix in $x_i \equiv \sigma, n_B, \varepsilon$ space. Thus, the critical point is characterized by the condition, $\det V = 0$, analogously to the condition $\Delta = 0$ in Eq. (4.5). At the critical point, only one of the linear combinations of σ, n_B , and ε becomes massless. This number of the gapless mode is the same as that in the absence of the ε and π as we discussed around Eq. (4.8), the static universality class remains the same as that of Sec. 4.2.

We define the generalized susceptibilities,

$$\chi_{ij} \equiv \left. \frac{\delta \langle x_i \rangle_{X_j}}{\delta X_j} \right|_{X_j=0}, \quad (\text{B.7})$$

where $\langle x_i \rangle_{X_j}$ is the the expectation value of x_i in the same definition of Eq. (3.2) except for the replacement $\beta F \rightarrow \beta F + \int d\mathbf{r} x_j X_j$ (where the summation over the index j is *not* implied). Here, $X_\varepsilon \equiv -\beta$, $X_n \equiv \beta \mu_B$, and $X_\sigma \equiv \beta m_q$ with β denotes the inverse temperature. Here and from now on, we omit the subscript of n_B when n_B is in the subscript of some character, e.g., X_n rather than X_{n_B} . One can show the following relation between χ_{ij}

and V_{ij}

$$\chi_{\varepsilon\varepsilon} = \frac{1}{\mathcal{V}} \langle \varepsilon^2 \rangle_{\mathbf{q} \rightarrow \mathbf{0}} = T(V^{-1})_{\varepsilon\varepsilon}, \quad (\text{B.8})$$

$$\chi_{\varepsilon n} = \frac{1}{\mathcal{V}} \langle \varepsilon n_{\text{B}} \rangle_{\mathbf{q} \rightarrow \mathbf{0}} = T(V^{-1})_{\varepsilon n}, \quad (\text{B.9})$$

$$\chi_{nn} = \frac{1}{\mathcal{V}} \langle n_{\text{B}}^2 \rangle_{\mathbf{q} \rightarrow \mathbf{0}} = T(V^{-1})_{nn}, \quad (\text{B.10})$$

where $(V^{-1})_{ij}$ denotes the (i, j) component of the inverse matrix of V . Since $(V^{-1})_{ij} \propto (\det V)^{-1}$, one finds

$$\chi_{\varepsilon\varepsilon} \sim \chi_{\varepsilon n} \sim \chi_{nn} \sim \xi^{2-\eta}, \quad (\text{B.11})$$

which can be regarded as a generalization of Eq. (4.6).

B.2 Dynamics

B.2.1 Full Langevin equations

We next construct the Langevin equations of the full hydrodynamic variables $x_i = \sigma, n_{\text{B}}, \varepsilon$ and $\boldsymbol{\pi}, \theta$. The Langevin equations read

$$\frac{\partial x_i}{\partial t} = -\gamma_{ij}(\boldsymbol{\nabla}) \frac{\delta F}{\delta x_j} - \int_V [\tilde{x}_i, \boldsymbol{\pi}] \cdot \frac{\delta F}{\delta \boldsymbol{\pi}} - \int_V [\tilde{x}_i, \theta] \frac{\delta F}{\delta \theta} + \xi_i, \quad (\text{B.12})$$

$$\frac{\partial \boldsymbol{\pi}}{\partial t} = \Gamma_{\pi\pi} \boldsymbol{\nabla} \boldsymbol{\nabla} \cdot \frac{\delta F}{\delta \boldsymbol{\pi}} + \Gamma'_{\pi\pi} \boldsymbol{\nabla}^2 \frac{\delta F}{\delta \boldsymbol{\pi}} - \Gamma_{\pi\theta} \boldsymbol{\nabla} \frac{\delta F}{\delta \theta} - \int_V [\boldsymbol{\pi}, \tilde{x}_i] \frac{\delta F}{\delta x_i} + \boldsymbol{\xi}_\pi, \quad (\text{B.13})$$

$$\frac{\partial \theta}{\partial t} = -\Gamma_{\pi\theta} \boldsymbol{\nabla} \cdot \frac{\delta F}{\delta \boldsymbol{\pi}} - \Gamma_{\theta\theta} \frac{\delta F}{\delta \theta} - \int_V [\theta, \tilde{x}_i] \frac{\delta F}{\delta x_i} + \xi_\theta, \quad (\text{B.14})$$

where we use the shorthand notation of the integrals, Eq. (4.12). Summation over repeated indices i, j is also understood. Here

$$\gamma_{ij}(\boldsymbol{\nabla}) \equiv \begin{pmatrix} \Gamma_{\sigma\sigma} & -\Gamma_{\sigma n} \boldsymbol{\nabla}^2 & -\Gamma_{\sigma\varepsilon} \boldsymbol{\nabla}^2 \\ -\Gamma_{\sigma n} \boldsymbol{\nabla}^2 & -\Gamma_{nn} \boldsymbol{\nabla}^2 & -\Gamma_{n\varepsilon} \boldsymbol{\nabla}^2 \\ -\Gamma_{\sigma\varepsilon} \boldsymbol{\nabla}^2 & -\Gamma_{n\varepsilon} \boldsymbol{\nabla}^2 & -\Gamma_{\varepsilon\varepsilon} \boldsymbol{\nabla}^2 \end{pmatrix}, \quad (\text{B.15})$$

Γ_{ab} ($a, b = x_i, \pi, \theta$), and $\Gamma'_{\pi\pi}$ are the kinetic coefficients. We also define the net variables $\tilde{\sigma} \equiv \bar{q}q$, $\tilde{n}_{\text{B}} \equiv \bar{q}\gamma^0 q$, and $\tilde{\varepsilon} \equiv T^{00}$. On the other hand, we note again that $\sigma = \tilde{\sigma} - \sigma_{\text{eq}}$, $n_{\text{B}} = \tilde{n}_{\text{B}} - (n_{\text{B}})_{\text{eq}}$, $\varepsilon \equiv \tilde{\varepsilon} - \varepsilon_{\text{eq}}$ are the fluctuations

around the equilibrium values σ_{eq} , $(n_{\text{B}})_{\text{eq}}$, and ε_{eq} . The noise terms ξ_i , ξ_{π} , and ξ_{θ} above are not important in the following calculation. In order to write down the above Langevin equations, we use the momentum conservation law and the Onsager's principle, similarly to the derivation in Sec. 3.3.2.

We postulate the following Poisson brackets, in addition to Eqs. (4.17),

$$[\boldsymbol{\pi}(\mathbf{r}), \tilde{\sigma}(\mathbf{r}')] = \tilde{\sigma}(\mathbf{r}') \nabla \delta(\mathbf{r} - \mathbf{r}'), \quad (\text{B.16})$$

$$[\boldsymbol{\pi}(\mathbf{r}), \tilde{n}_{\text{B}}(\mathbf{r}')] = \tilde{n}_{\text{B}}(\mathbf{r}') \nabla \delta(\mathbf{r} - \mathbf{r}'), \quad (\text{B.17})$$

$$[\boldsymbol{\pi}(\mathbf{r}), \tilde{s}(\mathbf{r}')] = \tilde{s}(\mathbf{r}') \nabla \delta(\mathbf{r} - \mathbf{r}'), \quad (\text{B.18})$$

$$[\theta(\mathbf{r}), \tilde{s}(\mathbf{r}')] = 0, \quad (\text{B.19})$$

where $\tilde{s}(\mathbf{r})$ denotes the entropy density. The Poisson brackets concerning $\tilde{\varepsilon}(\mathbf{r})$ can be derived as

$$[\boldsymbol{\pi}(\mathbf{r}), \tilde{\varepsilon}(\mathbf{r}')] = (T\tilde{s}(\mathbf{r}) + \mu_{\text{B}}\tilde{n}_{\text{B}}(\mathbf{r})) \nabla \delta(\mathbf{r} - \mathbf{r}'), \quad (\text{B.20})$$

$$[\theta(\mathbf{r}), \tilde{\varepsilon}(\mathbf{r}')] = \mu_{\text{B}}\delta(\mathbf{r} - \mathbf{r}'). \quad (\text{B.21})$$

Here, we used the thermodynamic relation $d\varepsilon = Tds + \mu_{\text{B}}dn_{\text{B}}$ and the definition of the Poisson brackets $[\boldsymbol{\pi}(\mathbf{r}), \tilde{y}_i(\mathbf{r}')] \equiv \delta\tilde{y}_i(\mathbf{r}')/\delta\mathbf{u}(\mathbf{r})$ for $\tilde{y}_i \equiv \tilde{n}_{\text{B}}, \tilde{s}, \tilde{\varepsilon}$, with $\mathbf{u}(\mathbf{r})$ being the infinitesimal translation of the coordinate, $\mathbf{r} \rightarrow \mathbf{r} + \mathbf{u}(\mathbf{r})$. (See, e.g., Ref. [78] for the details of the Poisson brackets.)

We consider the small fluctuations of variables around the equilibrium values, $\sigma(\mathbf{r}) = \tilde{\sigma}(\mathbf{r}) - \sigma_{\text{eq}}$, $n_{\text{B}}(\mathbf{r}) = \tilde{n}_{\text{B}}(\mathbf{r}) - (n_{\text{B}})_{\text{eq}}$, and $s(\mathbf{r}) = \tilde{s}(\mathbf{r}) - s_{\text{eq}}$. Then, the linearized Langevin equations neglecting the higher order fluctuations become:

$$\frac{\partial \sigma}{\partial t} = -(\Gamma_{\sigma\sigma}V_{\sigma i} - \Gamma_{\sigma j}v_{ji}\nabla^2)x_i - \sigma_{\text{eq}}V_{\pi\pi}\nabla \cdot \boldsymbol{\pi}, \quad (\text{B.22})$$

$$\frac{\partial n_{\text{B}}}{\partial t} = \Gamma_{nj}v_{ji}\nabla^2x_i - (n_{\text{B}})_{\text{eq}}V_{\pi\pi}\nabla \cdot \boldsymbol{\pi} - V_{\theta\theta}\nabla^2\theta, \quad (\text{B.23})$$

$$\frac{\partial \varepsilon}{\partial t} = \Gamma_{\varepsilon j}v_{ji}\nabla^2x_i - w_{\text{eq}}V_{\theta\theta}\nabla \cdot \boldsymbol{\pi} - \mu V_{\theta\theta}\nabla^2\theta, \quad (\text{B.24})$$

$$\frac{\partial \boldsymbol{\pi}}{\partial t} = -[\sigma_{\text{eq}}V_{\sigma i} + (n_{\text{B}})_{\text{eq}}V_{ni} + w_{\text{eq}}V_{\varepsilon i}]\nabla x_i + \Gamma_{\pi\pi}V_{\pi\pi}\nabla\nabla \cdot \boldsymbol{\pi} + \Gamma'_{\pi\pi}V_{\pi\pi}\nabla^2\boldsymbol{\pi}, \quad (\text{B.25})$$

$$\frac{\partial \theta}{\partial t} = -[(V_{ni} + \mu_{\text{B}}V_{\varepsilon i}) - (v_n + \mu_{\text{B}}v_{\varepsilon i})\nabla^2]x_i - \Gamma_{\pi\theta}V_{\pi\pi}\nabla \cdot \boldsymbol{\pi} + \Gamma_{\theta\theta}V_{\theta\theta}\nabla^2\theta, \quad (\text{B.26})$$

where $w_{\text{eq}} = Ts_{\text{eq}} + \mu_{\text{B}}(n_{\text{B}})_{\text{eq}}$.

B.2.2 Decomposition of momentum density

In this section, we decompose the momentum density π^i into the longitudinal and transverse parts with respect to momentum \mathbf{q} in (t, \mathbf{q}) space,

$$\pi^i = \pi_L^i + \pi_T^i, \quad \pi_L^i = (P_L)^{ij} \pi^j, \quad \pi_T^i = (P_T)^{ij} \pi^j, \quad (\text{B.27})$$

where $P_{L,T}$ are the longitudinal and transverse projection operators defined by

$$(P_L)^{ij} \equiv \frac{q^i q^j}{|\mathbf{q}|^2}, \quad (P_T)^{ij} \equiv \delta_{ij} - \frac{q^i q^j}{|\mathbf{q}|^2}. \quad (\text{B.28})$$

In the following calculation, we show that the dynamics of π_T^i is decoupled from that of the other hydrodynamic variables. We first write the linearized Langevin equations (B.22)–(B.26) to the leading order of \mathbf{q} , formally as

$$\frac{\partial x_k}{\partial t} = A_{x_k}(\mathbf{q} \cdot \boldsymbol{\pi}) + f(x_k, \theta), \quad (\text{B.29})$$

$$\frac{\partial \boldsymbol{\pi}}{\partial t} = A_\pi \mathbf{q}(\mathbf{q} \cdot \boldsymbol{\pi}) + B_\pi |\mathbf{q}|^2 \boldsymbol{\pi} + \mathbf{q}g(x_k), \quad (\text{B.30})$$

$$\frac{\partial \theta}{\partial t} = A_\theta(\mathbf{q} \cdot \boldsymbol{\pi}) + h(x_k, \theta), \quad (\text{B.31})$$

where $f(x_k, \theta)$, $g(x_k)$ and $h(x_k, \theta)$ are some functions which may involve x_k and θ , but not involve $\boldsymbol{\pi}$. The coefficients A_{x_k} , A_π , A_θ , and B_π are the parameters which depend on the Ginzburg-Landau parameters V_{ij} , v_{ij} , kinetic coefficients, and equilibrium values of the thermodynamic quantities. The explicit forms of these functions (f , g , and h) and the coefficients (A_{x_k} , A_π , A_θ , and B_π) are not important for our purpose. By using $\boldsymbol{\pi}_{L,T}$, we can write Eqs. (B.29)–(B.31) into

$$\frac{\partial x_k}{\partial t} = A_{x_k}(\mathbf{q} \cdot \boldsymbol{\pi}_L) + f(x_k, \theta), \quad (\text{B.32})$$

$$\frac{\partial \boldsymbol{\pi}_L}{\partial t} = (A_\pi + B_\pi) |\mathbf{q}|^2 \boldsymbol{\pi}_L + \mathbf{q}g(x_k), \quad (\text{B.33})$$

$$\frac{\partial \boldsymbol{\pi}_T}{\partial t} = B_\pi |\mathbf{q}|^2 \boldsymbol{\pi}_T, \quad (\text{B.34})$$

$$\frac{\partial \theta}{\partial t} = A_\theta(\mathbf{q} \cdot \boldsymbol{\pi}_L) + h(x_k, \theta). \quad (\text{B.35})$$

One can confirm that the dynamics of π_L^i and π_T^i are decoupled from each other at the mean-field level.

B.2.3 Hydrodynamic modes

Thanks to the decomposition in the previous section, we can readily obtain the hydrodynamic mode for $\boldsymbol{\pi}_T$,

$$(i\omega - B_\pi \mathbf{q}^2) \boldsymbol{\pi}_T = 0, \quad B_\pi = \Gamma'_{\pi\pi} V_{\pi\pi}, \quad (\text{B.36})$$

which is a diffusion mode.

The other Langevin equations which involve $\boldsymbol{\pi}_L$ (but not $\boldsymbol{\pi}_T$) can be expressed in the form of the matrix equation,

$$\mathcal{M}_{\text{EM}} \begin{pmatrix} \sigma \\ n_{\text{B}} \\ \varepsilon \\ \boldsymbol{\pi}_{\text{L}} \\ \theta \end{pmatrix} = 0, \quad (\text{B.37})$$

where

$$\mathcal{M}_{\text{EM}} \equiv \begin{pmatrix} i\omega - A_{\sigma\sigma} - a_{\sigma\sigma}\mathbf{q}^2 & -A_{\sigma n} - a_{\sigma n}\mathbf{q}^2 & -A_{\sigma\varepsilon} - a_{\sigma\varepsilon}\mathbf{q}^2 & -ia_{\sigma\pi}\mathbf{q} & 0 \\ & -a_{n\sigma}\mathbf{q}^2 & i\omega - a_{nn}\mathbf{q}^2 & -a_{n\varepsilon}\mathbf{q}^2 & -a_{n\theta}\mathbf{q}^2 \\ & -a_{\varepsilon\sigma}\mathbf{q}^2 & -a_{\varepsilon n}\mathbf{q}^2 & i\omega - a_{\varepsilon\varepsilon}\mathbf{q}^2 & -a_{\varepsilon\theta}\mathbf{q}^2 \\ & -ia_{\pi\sigma}\mathbf{q} & -ia_{\pi n}\mathbf{q} & -ia_{\pi\varepsilon}\mathbf{q} & i\omega - a_{\pi\pi}\mathbf{q}^2 \\ -A_{\theta\sigma} - a_{\theta\sigma}\mathbf{q}^2 & -A_{\theta n} - a_{\theta n}\mathbf{q}^2 & -A_{\theta\varepsilon} - a_{\theta\varepsilon}\mathbf{q}^2 & -ia_{\theta\pi}\mathbf{q} & i\omega - a_{\theta\theta}\mathbf{q}^2 \end{pmatrix}. \quad (\text{B.38})$$

Here A_{ab} and a_{ab} are the parameters depending on V_{ij} , v_{ij} , kinetic coefficients, and thermodynamic quantities. Note here that A_{ab} , a_{ab} are not symmetric with respect to a and b . The eigenfrequencies of Eq. (B.37) can be found from $\det \mathcal{M} = 0$, which yields

$$\begin{aligned} \omega^5 + i(A_{\sigma\sigma} + g_4\mathbf{q}^2)\omega^4 - [g_3\mathbf{q}^2 + O(\mathbf{q}^4)]\omega^3 - i[g_2\mathbf{q}^2 + O(\mathbf{q}^4)]\omega^2 \\ + [g_1\mathbf{q}^4 + O(\mathbf{q}^6)]\omega + i[g_0\mathbf{q}^4 + O(\mathbf{q}^6)] = 0, \end{aligned} \quad (\text{B.39})$$

where g_0, \dots, g_4 are some functions of A_{ab} and a_{ab} . Among others, we give the explicit expressions only for $A_{\sigma\sigma}$, g_2 , and g_0 which will be used in the following arguments,

$$A_{\sigma\sigma} \equiv \Gamma_{\sigma\sigma}, \quad (\text{B.40})$$

$$\begin{aligned} g_2 \equiv \Gamma_{\sigma\sigma} [(n_{\text{B}})_{\text{eq}}^2 V_{\pi\pi} + V_{\theta\theta}] & \begin{vmatrix} V_{\sigma\sigma} & V_{\sigma n} \\ V_{\sigma n} & V_{nn} \end{vmatrix} \\ & + 2\Gamma_{\sigma\sigma} [(n_{\text{B}})_{\text{eq}} w_{\text{eq}} V_{\pi\pi} + \mu_{\text{B}} V_{\theta\theta}] \begin{vmatrix} V_{\sigma\sigma} & V_{\sigma n} \\ V_{\sigma\varepsilon} & V_{n\varepsilon} \end{vmatrix} \\ & + \Gamma_{\sigma\sigma} (w_{\text{eq}}^2 V_{\pi\pi} + \mu_{\text{B}}^2 V_{\theta\theta}) \begin{vmatrix} V_{\sigma\sigma} & V_{\sigma\varepsilon} \\ V_{\sigma\varepsilon} & V_{\varepsilon\varepsilon} \end{vmatrix}, \end{aligned} \quad (\text{B.41})$$

$$g_0 \equiv \Gamma_{\sigma\sigma} V_{\pi\pi} V_{\theta\theta} T^2 s_{\text{eq}}^2 \det V. \quad (\text{B.42})$$

Equation (B.39) can be factorized as

$$\begin{aligned} & \left[\omega + iA_{\sigma\sigma} + i \left(g_4 - \frac{g_3}{A_{\sigma\sigma}} + \frac{g_2}{A_{\sigma\sigma}^2} \right) \mathbf{q}^2 \right] \\ & \times \left[\omega - s_+ |\mathbf{q}| + i \frac{t_+}{2} \mathbf{q}^2 \right] \left[\omega + s_+ |\mathbf{q}| + i \frac{t_+}{2} \mathbf{q}^2 \right] \\ & \times \left[\omega - s_- |\mathbf{q}| + i \frac{t_-}{2} \mathbf{q}^2 \right] \left[\omega + s_- |\mathbf{q}| + i \frac{t_-}{2} \mathbf{q}^2 \right] = 0, \end{aligned} \quad (\text{B.43})$$

where s_{\pm} and t_{\pm} satisfy

$$s_+^2 + s_-^2 = \frac{g_2}{A_{\sigma\sigma}}, \quad (\text{B.44})$$

$$s_+^2 s_-^2 = \frac{g_0}{A_{\sigma\sigma}}, \quad (\text{B.45})$$

$$t_+ + t_- = \frac{g_3}{A_{\sigma\sigma}} - \frac{g_2}{A_{\sigma\sigma}^2}, \quad (\text{B.46})$$

$$s_+^2 t_- + s_-^2 t_+ = \frac{g_1}{A_{\sigma\sigma}} - \frac{g_0}{A_{\sigma\sigma}^2}. \quad (\text{B.47})$$

From Eq. (B.43), we find the hydrodynamic modes of the system other than the diffusion mode described by Eq. (B.36): one relaxation mode and two pairs of phonons. The speeds of phonons s_{\pm} can be obtained from the solution of

$$s^4 - \frac{g_2}{A_{\sigma\sigma}} s^2 + \frac{g_0}{A_{\sigma\sigma}} = 0. \quad (\text{B.48})$$

Note here that Eq. (B.42) shows that $g_0 \rightarrow 0$ when the critical point is approached $\det V \rightarrow 0$. Therefore, near the critical point, we obtain

$$s_+^2 = \frac{g_2}{A_{\sigma\sigma}} - \frac{g_0}{g_2}, \quad s_-^2 = \frac{g_0}{g_2}. \quad (\text{B.49})$$

B.2.4 Dynamic critical exponent

From the results above, we can show that one of the phonons with the speed $c_s \equiv s_-$ exhibits the critical slowing down. By using Eqs. (B.41) and (B.42), together with Eqs. (B.8)–(B.10), we have

$$c_s^2 = \frac{V_{\pi\pi} V_{\theta\theta} T^3 s_{\text{eq}}^2}{\kappa_{nn} \chi_{nn} + 2\kappa_{n\epsilon} \chi_{n\epsilon} + \kappa_{\epsilon\epsilon} \chi_{\epsilon\epsilon}}, \quad (\text{B.50})$$

where

$$\kappa_{nn} \equiv (n_{\text{B}})_{\text{eq}}^2 V_{\pi\pi} + V_{\theta\theta}, \quad (\text{B.51})$$

$$\kappa_{n\varepsilon} \equiv (n_{\text{B}})_{\text{eq}} w_{\text{eq}} V_{\pi\pi} + \mu_{\text{B}} V_{\theta\theta}, \quad (\text{B.52})$$

$$\kappa_{\varepsilon\varepsilon} \equiv w_{\text{eq}}^2 V_{\pi\pi} + \mu_{\text{B}}^2 V_{\theta\theta}. \quad (\text{B.53})$$

Using Eq. (B.11), $V_{\pi\pi} \sim \xi^0$, and $V_{\theta\theta} \sim \xi^0$ near the critical point, we obtain

$$c_{\text{s}}^2 \sim \xi^{-2+\eta}. \quad (\text{B.54})$$

Comparing Eq. (B.54) with Eq. (4.35), we obtain the same dynamic critical exponent z as that given by Eq. (4.37). Therefore, the dynamic universality class remains the same as that without ε and $\boldsymbol{\pi}$ in Sec. 3.3.2.

Appendix C

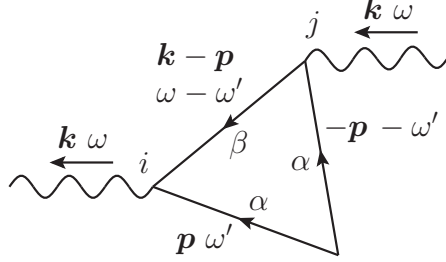
Calculation of the self-energies and the vertex function

As we mentioned under Eq. (5.72), in this appendix, we evaluate the self-energies of the order parameter, $\Sigma_{\alpha\beta}(\mathbf{k}, \omega)$, and those of the conserved charge densities, $\Pi_{ij}(\mathbf{k}, \omega)$, to the first order of ϵ , namely at the one-loop level. From these expressions, we can derive the recursion relations for the dynamic parameters, Eqs. (5.75)–(5.78). In particular, we calculate Π_{ij} and derive Eqs. (5.76)–(5.78) in Sec. C.1; we calculate $\Sigma_{\alpha\alpha}$ and derive Eq. (5.75) in Sec. C.2. We also evaluate the three-point vertex function used in Eq. (5.70) at the one-loop level, and derive Eq. (5.79).

C.1 Self-energy Π

Let us begin with the self-energy for the conserved-charge densities, $\Pi_{ij}(\mathbf{k}, \omega)$, which corresponds to the diagrams with outgoing \tilde{n}_i and ingoing n_j . The leading diagram is given by Fig. C.1. According to the Feynman rules on the analytic translation of the diagrams of the (plane and wavy) lines and the noise vortices (Fig. 5.1) and the interaction vortices (Fig. 5.2), summarized in Sec. 5.2.2, we can calculate Fig. C.1 as

$$\begin{aligned}\Pi_{ij}(\mathbf{k}, \omega) &= \int \frac{d\omega'}{2\pi} \int \frac{d^d p}{(2\pi)^d} V_{i;\alpha\beta}^0(\mathbf{k}, \mathbf{p}) G^0(\mathbf{k} - \mathbf{p}, \omega - \omega') |G^0(\mathbf{p}, \omega')|^2 2\Gamma V_{\beta;\alpha j}^0 \\ &= \int \frac{d^d p}{(2\pi)^d} \frac{F_{ij}}{\{-i\omega + \Gamma[r + (\mathbf{k} - \mathbf{p})^2] + \Gamma(r + \mathbf{p}^2)\}(r + \mathbf{p}^2)}, \quad (\text{C.1})\end{aligned}$$

Figure C.1: Diagram for Π_{ij} at one-loop level

where we defined F_{ij} as the components of the following matrix:

$$F \equiv \begin{pmatrix} 8\gamma^2\Gamma\lambda\mathbf{k}^2 & 0 \\ 8i\gamma^2C\Gamma\mathbf{B} \cdot \mathbf{k} & -2g^2[(\mathbf{k} - \mathbf{p})^2 - \mathbf{p}^2]/\chi_5 \end{pmatrix}. \quad (\text{C.2})$$

From this expression of the self energy Π_{ij} , we can calculate its derivatives which are required in the recursion relations (5.66)–(5.69) and the normalization conditions (5.71) and (5.72).

It is easy to calculate the latter conditions. Because $\Pi_{ij}(\mathbf{0}, \omega) = 0$, the normalization conditions (5.71) and (5.72) reduce to

$$\tilde{c} = d - c, \quad \tilde{c}_5 = d - c_5. \quad (\text{C.3})$$

Let us calculate the derivatives needed in the recursion relations (5.66)–(5.69),

$$i \frac{\partial \Pi_{21}(\mathbf{k}, 0)}{\partial \mathbf{k}} \Big|_{\mathbf{k} \rightarrow \mathbf{0}} = -4\gamma^2 C \mathbf{B} \int \frac{d^d p}{(2\pi)^d} \left(\frac{1}{\mathbf{p}^4} + O(\epsilon) \right) = -\frac{\gamma^2 C \mathbf{B} \Lambda^{-\epsilon}}{2\pi^2} \ln b, \quad (\text{C.4})$$

$$\frac{1}{2} \frac{\partial^2 \Pi_{11}(\mathbf{k}, 0)}{\partial \mathbf{k}^2} \Big|_{\mathbf{k} \rightarrow \mathbf{0}} = 4\gamma^2 \lambda \int \frac{d^d p}{(2\pi)^d} \left(\frac{1}{\mathbf{p}^4} + O(\epsilon) \right) = \frac{\gamma^2 \lambda \Lambda^{-\epsilon}}{2\pi^2} \ln b, \quad (\text{C.5})$$

where we carried out the integral over \mathbf{p} in the shell $\Lambda/b < |\mathbf{p}| < \Lambda$ using the standard formula in the dimensional regularization:

$$\int \frac{d^d p}{(2\pi)^d} \frac{1}{\mathbf{p}^4} = \frac{\Lambda^{-\epsilon}}{8\pi^2} \ln b. \quad (\text{C.6})$$

We also compute

$$\frac{1}{2} \left. \frac{\partial^2 \Pi_{22}(\mathbf{k}, 0)}{\partial \mathbf{k}^2} \right|_{\mathbf{k} \rightarrow \mathbf{0}} = \frac{g^2}{\chi_5 \Gamma} \int \frac{d^d p}{(2\pi)^d} \left(\frac{\cos 2\theta}{\mathbf{p}^4} + O(\epsilon) \right) = -\frac{g^2 \Lambda^{-\epsilon}}{16\pi^2 \chi_5 \Gamma} \ln b, \quad (\text{C.7})$$

where we parameterize \mathbf{p} in the limit of $d \rightarrow 4$ by

$$(p_1, p_2, p_3, p_4) = p(\cos \theta, \sin \theta \cos \phi, \sin \theta \sin \phi \cos \varphi, \sin \theta \sin \phi \sin \varphi) \quad (\text{C.8})$$

with $\mathbf{k} = (1, 0, 0, 0)$ and use

$$\int \frac{d^d p}{(2\pi)^d} \frac{\cos 2\theta}{\mathbf{p}^4} = -\frac{\Lambda^{-\epsilon}}{16\pi^2} \ln b. \quad (\text{C.9})$$

Now it is ready to rewrite the recursion relations (5.66)–(5.69). By using Eqs. (C.3)–(C.5), and (C.7), we obtain

$$\frac{\lambda_{l+1}}{\chi_{l+1}} = b^{z-2} \frac{\lambda_l}{\chi_l} (1 - 4v_l \ln b), \quad (\text{C.10})$$

$$\frac{(\lambda_5)_{l+1}}{(\chi_5)_{l+1}} = b^{z-2} \frac{(\lambda_5)_l}{(\chi_5)_l} \left(1 + \frac{f_l}{2} \ln b \right), \quad (\text{C.11})$$

$$\frac{C_{l+1}}{\chi_{l+1}} = b^{z+c_5-c-1} \frac{C_l}{\chi_l} (1 - 4v_l \ln b), \quad (\text{C.12})$$

$$\frac{C_{l+1}}{(\chi_5)_{l+1}} = b^{z+c-c_5-1} \frac{C_l}{(\chi_5)_l}. \quad (\text{C.13})$$

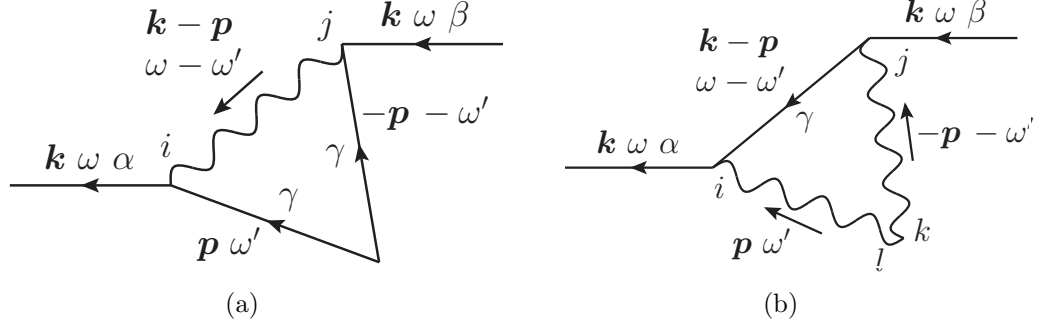
Then, we can derive Eqs. (5.76)–(5.78) by using Eqs. (5.46), (5.47), and (C.10)–(C.12).

C.2 Self-energy Σ

Next, let us evaluate the self-energy of the order parameter field ϕ_α , $\Sigma_{\alpha\beta}(\mathbf{k}, \omega)$, whose diagrams are shown in Fig. C.2,

$$\Sigma_{\alpha\beta}(\mathbf{k}, \omega) = \Sigma_{\alpha\beta}^{(a)}(\mathbf{k}, \omega) + \Sigma_{\alpha\beta}^{(b)}(\mathbf{k}, \omega), \quad (\text{C.14})$$

where $\Sigma^{(a)}$ and $\Sigma^{(b)}$ correspond to figures C.2(a) and C.2(b), respectively. Similarly to the expression for Eq. (C.1), the diagonal ($\alpha\alpha$) components

Figure C.2: Diagrams for $\Sigma_{\alpha\beta}$ at one-loop level

used in the recursion relation (5.64) and the normalization condition (5.65) are given by

$$\begin{aligned}
& \Sigma_{\alpha\alpha}^{(a)}(\mathbf{k}, \omega) \\
&= \int \frac{d\omega'}{2\pi} \int \frac{d^d p}{(2\pi)^d} V_{\alpha;\gamma i}^0 D_{ij}^0(\mathbf{k} - \mathbf{p}, \omega - \omega') |G^0(\mathbf{p}, \omega')|^2 2\Gamma V_{j;\gamma\alpha}(\mathbf{k} - \mathbf{p}, -\mathbf{p}) \\
&= 4\gamma^2 \Gamma \int \frac{d^d p}{(2\pi)^d} \frac{\lambda(\mathbf{k} - \mathbf{p})^2 [-i\omega + \Gamma(r + \mathbf{p})^2 + \lambda_5(\mathbf{k} - \mathbf{p})^2/\chi_5] + C^2[\mathbf{B} \cdot (\mathbf{k} - \mathbf{p})]^2/\chi_5}{(r + \mathbf{p}^2) \det[D^0(\mathbf{k} - \mathbf{p}, \omega + i\Gamma(r + \mathbf{p}^2))]^{-1}} \\
&+ \frac{g^2}{\chi_5} \int \frac{d^d p}{(2\pi)^d} \frac{(\mathbf{p}^2 - \mathbf{k}^2) [-i\omega + \Gamma(r + \mathbf{p})^2 + \lambda(\mathbf{k} - \mathbf{p})^2/\chi]}{(r + \mathbf{p}^2) \det[D^0(\mathbf{k} - \mathbf{p}, \omega + i\Gamma(r + \mathbf{p}^2))]^{-1}}, \quad (\text{C.15})
\end{aligned}$$

$$\begin{aligned}
& \Sigma_{\alpha\alpha}^{(b)}(\mathbf{k}, \omega) \\
&= \int \frac{d\omega'}{2\pi} \int \frac{d^d p}{(2\pi)^d} V_{\alpha;\gamma i}^0 G^0(\mathbf{k} - \mathbf{p}, \omega - \omega') B_{ij}^0(\mathbf{p}, \omega') V_{\gamma;\alpha j} \\
&= 8\gamma^2 \Gamma^2 \int \frac{d\omega'}{2\pi} \int \frac{d^d p}{(2\pi)^d} \frac{\lambda \mathbf{p}^2 (\omega'^2 + \kappa_5 \mathbf{p}^2) + \lambda_5 (C\mathbf{B} \cdot \mathbf{p})^2 / \chi_5^2}{|\det[D^0(\mathbf{p}, \omega')]^{-1}|^2 \{-i(\omega - \omega') + \Gamma[r + (\mathbf{k} - \mathbf{p})^2]\}} \\
&- \frac{2g^2}{\chi_5^2} \int \frac{d\omega'}{2\pi} \int \frac{d^d p}{(2\pi)^d} \frac{\lambda_5 \mathbf{p}^2 (\omega'^2 + \kappa \mathbf{p}^2) + \lambda (C\mathbf{B} \cdot \mathbf{p})^2 / \chi^2}{|\det[D^0(\mathbf{p}, \omega')]^{-1}|^2 \{-i(\omega - \omega') + \Gamma[r + (\mathbf{k} - \mathbf{p})^2]\}}. \quad (\text{C.16})
\end{aligned}$$

Note that we do not take a sum over α here.

The integral over ω' in Eq. (C.16) can be performed by closing contour below and picking up the poles on a lower half plane,

$$\det[D^0(\mathbf{p}, \omega')]^{-1} = [-i\omega' + \kappa_+ \mathbf{p}^2 + i\Omega(\mathbf{p})] [-i\omega' + \kappa_+ \mathbf{p}^2 - i\Omega(\mathbf{p})] = 0, \quad (\text{C.17})$$

where we defined

$$\Omega(\mathbf{p}) \equiv \sqrt{\frac{(C\mathbf{B} \cdot \mathbf{p})^2}{\chi\chi_5} - \kappa_-^2 \mathbf{p}^4}, \quad \kappa_{\pm} \equiv \frac{1}{2} \left(\frac{\lambda}{\chi} \pm \frac{\lambda_5}{\chi_5} \right). \quad (\text{C.18})$$

The result of the contour integral is given by

$$\begin{aligned} \Sigma_{\alpha\alpha}^{(b)}(\mathbf{k}, \omega) &= -2\gamma^2 \Gamma^2 \int \frac{d^d p}{(2\pi)^d} \left(\frac{-\lambda\kappa_- \mathbf{p}^4 + (C\mathbf{B} \cdot \mathbf{p})^2 / \chi_5}{i\Omega(\mathbf{p})} K_-(\mathbf{p}, \mathbf{k}) - \lambda \mathbf{p}^2 K_+(\mathbf{p}, \mathbf{k}) \right) \\ &\quad + \frac{g^2}{2\chi_5^2} \int \frac{d^d p}{(2\pi)^d} \left(\frac{\lambda_5 \kappa_- \mathbf{p}^4 + (C\mathbf{B} \cdot \mathbf{p})^2 / \chi}{i\Omega(\mathbf{p})} K_-(\mathbf{p}, \mathbf{k}) - \lambda_5 \mathbf{p}^2 K_+(\mathbf{p}, \mathbf{k}) \right), \end{aligned} \quad (\text{C.19})$$

where we introduced

$$\begin{aligned} K_{\pm}(\mathbf{p}, \mathbf{k}) &\equiv \frac{1}{[\kappa_+ \mathbf{p}^2 + i\Omega(\mathbf{p})] [-i\omega + \Delta_+(\mathbf{p}, \mathbf{k}) + i\Omega(\mathbf{p})]} \\ &\quad \pm \frac{1}{[\kappa_+ \mathbf{p}^2 - i\Omega(\mathbf{p})] [-i\omega + \Delta_+(\mathbf{p}, \mathbf{k}) - i\Omega(\mathbf{p})]}, \end{aligned} \quad (\text{C.20})$$

$$\Delta_+(\mathbf{p}, \mathbf{k}) \equiv \Gamma[r + (\mathbf{k} - \mathbf{p})^2] + \kappa_+ \mathbf{p}^2. \quad (\text{C.21})$$

By using an identity,

$$\det[D^0(\mathbf{p}, \omega + i\Gamma[r + (\mathbf{k} - \mathbf{p})^2])]^{-1} = [-i\omega + \Delta_+(\mathbf{p}, \mathbf{k})]^2 + \Omega(\mathbf{p})^2, \quad (\text{C.22})$$

together with some straightforward calculations, we obtain

$$\begin{aligned} \Sigma_{\alpha\alpha}^{(b)}(\mathbf{k}, \omega) &= 4\gamma^2 \chi \Gamma^2 \int \frac{d^d p}{(2\pi)^d} \frac{-i\omega + \lambda_5 \mathbf{p}^2 / \chi_5 + \Gamma[r + (\mathbf{k} - \mathbf{p})^2]}{\det[D^0(\mathbf{p}, \omega + i\Gamma[r + (\mathbf{k} - \mathbf{p})^2])]^{-1}} \\ &\quad - \frac{g^2}{\chi_5} \int \frac{d^d p}{(2\pi)^d} \frac{-i\omega + \lambda \mathbf{p}^2 / \chi + \Gamma[r + (\mathbf{k} - \mathbf{p})^2]}{\det[D^0(\mathbf{p}, \omega + i\Gamma[r + (\mathbf{k} - \mathbf{p})^2])]^{-1}}. \end{aligned} \quad (\text{C.23})$$

Combining Eqs. (C.15) and (C.23), we find

$$\begin{aligned} \Sigma_{\alpha\alpha}(\mathbf{k}, \omega) = & 4\gamma^2\chi\Gamma \int \frac{d^d p}{(2\pi)^d} \frac{\Theta(\mathbf{p}, \mathbf{k}, 0)\Theta_5(\mathbf{p}, \mathbf{k}, \omega) + [C\mathbf{B} \cdot (\mathbf{k} - \mathbf{p})]^2/(\chi\chi_5)}{(r + \mathbf{p}^2)[\Theta(\mathbf{p}, \mathbf{k}, \omega)\Theta_5(\mathbf{p}, \mathbf{k}, \omega) + (C\mathbf{B} \cdot \mathbf{p})^2/(\chi\chi_5)]} \\ & - \frac{g^2}{\chi_5} \int \frac{d^d p}{(2\pi)^d} \frac{(r + \mathbf{k}^2)\Theta(\mathbf{p}, \mathbf{k}, \omega)}{(r + \mathbf{p}^2)[\Theta(\mathbf{p}, \mathbf{k}, \omega)\Theta_5(\mathbf{p}, \mathbf{k}, \omega) + (C\mathbf{B} \cdot \mathbf{p})^2/(\chi\chi_5)]}, \end{aligned} \quad (\text{C.24})$$

where $\Theta(\mathbf{p}, \mathbf{k}, \omega)$ and $\Theta_5(\mathbf{p}, \mathbf{k}, \omega)$ are defined by

$$\Theta(\mathbf{p}, \mathbf{k}, \omega) \equiv -i\omega + \Gamma(r + \mathbf{p}^2) + \lambda(\mathbf{k} - \mathbf{p})^2/\chi, \quad (\text{C.25})$$

$$\Theta_5(\mathbf{p}, \mathbf{k}, \omega) \equiv -i\omega + \Gamma(r + \mathbf{p}^2) + \lambda_5(\mathbf{k} - \mathbf{p})^2/\chi_5. \quad (\text{C.26})$$

Note that $\Sigma_{11} = \Sigma_{22}$ and the first term on the right-hand side of Eq. (C.24) is independent of \mathbf{k} when $\omega = 0$. From the expression (C.24), we obtain

$$\begin{aligned} & \frac{1}{2} \left. \frac{\partial^2 \Sigma_{\alpha\alpha}(\mathbf{k}, 0)}{\partial \mathbf{k}^2} \right|_{\mathbf{k} \rightarrow \mathbf{0}} \\ &= -\frac{g^2}{\chi_5} \int \frac{d^d p}{(2\pi)^d} \left(\frac{\Theta(\mathbf{p}, \mathbf{0}, 0)}{(r + \mathbf{p}^2)[\Theta(\mathbf{p}, \mathbf{0}, 0)\Theta_5(\mathbf{p}, \mathbf{0}, 0) + (C\mathbf{B} \cdot \mathbf{p})^2/(\chi\chi_5)]} + O(\epsilon) \right), \end{aligned} \quad (\text{C.27})$$

$$\begin{aligned} & i \left. \frac{\partial \Sigma_{\alpha\alpha}(\mathbf{0}, \omega)}{\partial \omega} \right|_{\omega \rightarrow 0} \\ &= -4\gamma^2\chi\Gamma \int \frac{d^d p}{(2\pi)^d} \frac{\Theta_5(\mathbf{p}, \mathbf{0}, 0)}{(r + \mathbf{p}^2)\{\Theta(\mathbf{p}, \mathbf{0}, 0)\Theta_5(\mathbf{p}, \mathbf{0}, 0) + (C\mathbf{B} \cdot \mathbf{p})^2/(\chi\chi_5)\}} \\ & \quad + \frac{g^2}{\chi_5} \int \frac{d^d p}{(2\pi)^d} \frac{r[\Theta^2(\mathbf{p}, \mathbf{0}, 0) - (C\mathbf{B} \cdot \mathbf{p})^2/(\chi\chi_5)^2]}{(r + \mathbf{p}^2)[\Theta(\mathbf{p}, \mathbf{0}, 0)\Theta_5(\mathbf{p}, \mathbf{0}, 0) + (C\mathbf{B} \cdot \mathbf{p})^2/(\chi\chi_5)]^2}. \end{aligned} \quad (\text{C.28})$$

The $O(\epsilon)$ terms in Eq. (C.27) proportional to r are irrelevant for the following discussion. Let us carry out the integral over \mathbf{p} in the shell $\Lambda/b < |\mathbf{p}| < \Lambda$. Setting $\mathbf{B} = (1, 0, 0, 0)$ and using the parameterization (C.8), we obtain

$$\begin{aligned} & \frac{1}{2\Gamma} \left. \frac{\partial^2 \Sigma_{\alpha\alpha}(\mathbf{k}, 0)}{\partial \mathbf{k}^2} \right|_{\mathbf{k} \rightarrow \mathbf{0}} \\ &= -\frac{2f}{\sqrt{(1+w)(1+w_5)} + h^2 + \sqrt{(1+w)(1+w_5)}} \sqrt{\frac{1+w}{1+w_5}} \ln b, \end{aligned} \quad (\text{C.29})$$

where w , w_5 , h , f are defined in Eq. (5.73). In order to obtain Eq. (C.29), we carry out the integral over θ by using the following formula (with a being a real constant):

$$\int_0^\pi d\theta \frac{\sin^2 \theta}{a^2 + \cos^2 \theta} = \frac{\pi}{a(\sqrt{a^2 + 1} + a)}. \quad (\text{C.30})$$

To the leading order of ϵ , we can ignore the term proportional to r on the right-hand side of (C.28). Then, by comparing Eqs. (C.27) and (C.28), we can rewrite Eq. (C.28) as

$$\begin{aligned} & i \left. \frac{\partial \Sigma_{\alpha\alpha}(\mathbf{0}, \omega)}{\partial \omega} \right|_{\omega \rightarrow 0} \\ &= - \frac{8vw}{\sqrt{(1+w)(1+w_5) + h^2} + \sqrt{(1+w)(1+w_5)}} \sqrt{\frac{1+w_5}{1+w}} \ln b, \end{aligned} \quad (\text{C.31})$$

where v is defined in Eq. (5.49). Using Eqs. (C.29) and (C.31), Eqs. (5.64) and (5.65) become

$$\Gamma_{l+1} = \Gamma_l (1 + f_l X_l \ln b) b^{d+z-\tilde{a}-a-2}, \quad (\text{C.32})$$

$$1 = (1 + 4v_l w_l X'_l \ln b) b^{d-\tilde{a}-a}, \quad (\text{C.33})$$

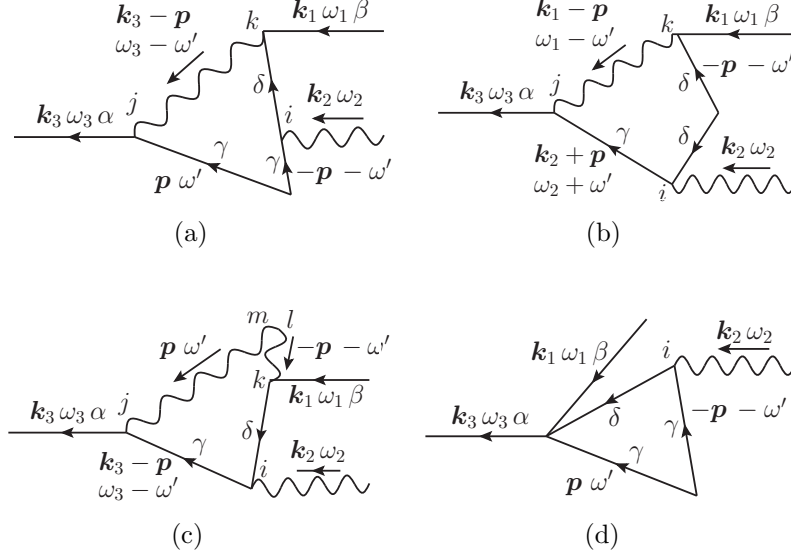
respectively, where X and X' are defined in Eq. (5.74). By substituting Eq. (C.33) into Eq. (C.32), we finally arrive at Eq. (5.75).

C.3 Vertex function \mathcal{V}

The lowest-order diagrams for $\mathcal{V}_{\alpha;\beta i}$ are depicted in Fig. C.3. We find that these diagrams with $\alpha \neq \beta$ and $i = 2$ satisfy the following identity in the limit $\mathbf{k}_1, \mathbf{k}_2 \rightarrow \mathbf{0}$ and $\omega_1, \omega_2 \rightarrow 0$:

$$\mathcal{V}_{\alpha;\beta 2}(\mathbf{0}, \mathbf{0}, 0, 0) = -i \frac{g\varepsilon_{\alpha\beta}}{\chi_5} \left. \frac{\partial \Sigma_{\gamma\gamma}(\mathbf{0}, \omega)}{\partial \omega} \right|_{\omega \rightarrow 0}. \quad (\text{C.34})$$

Note that the contribution from Fig. C.3(d) vanishes as long as $\alpha \neq \beta$. By substituting Eqs. (C.34), (5.47), and (5.65) into Eq. (5.70), we obtain Eq. (5.79). In particular, the loop correction of the interaction vortex, Eq. (C.34), is canceled by the response-field scaling factor which includes the loop correction originating from Eq. (5.65).

Figure C.3: Diagrams for $V_{\alpha;\beta i}$ at one-loop level

Instead of showing Eq. (C.34) from the explicit calculation as we carried out in Secs. C.1 and C.2, we show Eq. (C.34) as a consequence of the symmetry algebra. Our derivation is similar to that of Ref. [79] (see its section III. A), where the Ward-Takahashi identity for $O(N)$ symmetric systems is derived. We shall begin with the generating functional,

$$Z[\tilde{j}, j, \tilde{\mu}_5, \mu_5] \equiv \left\langle \exp \int dt \int d\mathbf{r} \left(\tilde{j}_\alpha \tilde{\phi}_\alpha + j_\alpha \phi_\alpha + \tilde{\mu}_5 \tilde{n}_5 + \mu_5 n_5 \right) \right\rangle. \quad (\text{C.35})$$

Here, \tilde{j}_α , j_α , $\tilde{\mu}_5$, and μ_5 are the external fields of $\tilde{\phi}_\alpha$, ϕ_α , \tilde{n}_5 and n_5 , respectively. We define

$$\tilde{\Phi}_\alpha \equiv \frac{\delta \ln Z}{\delta \tilde{j}_\alpha}, \quad \Phi_\alpha \equiv \frac{\delta \ln Z}{\delta j_\alpha}, \quad \tilde{N}_5 \equiv \frac{\delta \ln Z}{\delta \tilde{\mu}_5}, \quad N_5 \equiv \frac{\delta \ln Z}{\delta \mu_5}, \quad (\text{C.36})$$

which reduce to the expectation values of $\tilde{\phi}_\alpha$, ϕ_α , \tilde{n}_5 and n_5 , respectively, when the external fields are set to zero. We also define the effective actions

by the Legendre transformations of Eq. (C.36):

$$W[\tilde{\Phi}, \Phi, \tilde{\mu}_5, \mu_5] \equiv -\ln Z[\tilde{j}, j, \tilde{\mu}_5, \mu_5] + \int dt \int d\mathbf{r} \left(\tilde{j}_\alpha \tilde{\Phi}_\alpha + j_\alpha \Phi_\alpha \right), \quad (\text{C.37})$$

$$\Gamma[\tilde{\Phi}, \Phi, \tilde{N}_5, N_5] \equiv W[\tilde{\Phi}, \Phi, \tilde{\mu}_5, \mu_5] + \int dt \int d\mathbf{r} \left(\tilde{\mu}_5 \tilde{N}_5 + \mu_5 N_5 \right). \quad (\text{C.38})$$

One can show the following identities which will be used later (see, e.g., Sec. 4.4 of Ref. [66] for the derivations):

$$\frac{\delta W}{\delta \Phi_\alpha} = \frac{\delta \Gamma}{\delta \Phi_\alpha} = j_\alpha, \quad \frac{\delta \Gamma}{\delta N_5} = \mu_5, \quad (\text{C.39})$$

$$\frac{\delta^2 \Gamma}{\delta \tilde{\Phi}_\alpha(\mathbf{k}, \omega) \delta \Phi_\beta(\mathbf{k}, \omega)} = G_{\alpha\beta}^{-1}(-\mathbf{k}, -\omega), \quad (\text{C.40})$$

$$\frac{\delta^2 \Gamma}{\delta \Phi_\alpha \delta \Phi_\beta} = \frac{\delta^2 \Gamma}{\delta \Phi_\alpha \delta N_5} = 0, \quad (\text{C.41})$$

$$\frac{\delta^3 \Gamma}{\delta N_5 \delta \tilde{\Phi}_\alpha \delta \Phi_\beta} = V_{\alpha;\beta 2}. \quad (\text{C.42})$$

Here, note that $V_{\alpha;\beta 2}$ in Eq. (C.42) satisfies Eq. (5.39).

We use the condition that $W[\tilde{\Phi}, \Phi, \tilde{\mu}_5, \mu_5]$ is invariant under the $U(1)_A^{\tau^3}$ transformation defined in Eq. (5.6). Note that $W[\tilde{\Phi}, \Phi, \tilde{\mu}_5, \mu_5]$ is a functional of μ_5 , and changing μ_5 corresponds to the $U(1)_A^{\tau^3}$ transformation, because n_5 is its generator. Let us consider the variation of μ_5 at $t = 0$, $\delta\mu_5 = \vartheta\mu_5$ with ϑ being a small parameter. Then, the free energy (5.15) has an additional contribution,

$$\delta F = \int d\mathbf{r} n_5 \delta\mu_5. \quad (\text{C.43})$$

By using the reversible term of Eq. (5.12), an infinitesimal $U(1)_A^{\tau^3}$ transformation can be written as

$$\delta\Phi_\alpha = g \int_0^t dt' \varepsilon_{\alpha\beta} \Phi_\beta \delta\mu_5 = \vartheta g \varepsilon_{\alpha\beta} \Phi_\beta \mu_5 t. \quad (\text{C.44})$$

By applying Eq. (C.44) to $W[\tilde{\Phi}, \Phi, \tilde{\mu}_5, \mu_5]$, we obtain its variation as

$$\delta W = \vartheta \int dt \int d\mathbf{r} \mu_5 \left[\frac{\delta W}{\delta \mu_5} + g \varepsilon_{\alpha\beta} t \frac{\delta W}{\delta \Phi_\alpha} \Phi_\beta \right] \quad (\text{C.45})$$

$$= \vartheta \int dt \int d\mathbf{r} \frac{\delta \Gamma}{\delta N_5} \left[N_5 + g \varepsilon_{\alpha\beta} t \frac{\delta \Gamma}{\delta \Phi_\alpha} \Phi_\beta \right], \quad (\text{C.46})$$

where we use Eq. (C.39). Therefore, invariance of $W[\tilde{\Phi}, \Phi, \tilde{\mu}_5, \mu_5]$ leads to

$$\frac{\delta\Gamma}{\delta N_5} \left[N_5 + g\varepsilon_{\alpha\beta}t \frac{\delta\Gamma}{\delta\Phi_\alpha} \Phi_\beta \right] = 0. \quad (\text{C.47})$$

By taking a variation of this equation with respect to $\tilde{\Phi}_\alpha$ and Φ_β , we obtain

$$\frac{\delta^3\Gamma}{\delta N_5 \delta \tilde{\Phi}_\alpha \delta \Phi_\beta} N_5 = -g\varepsilon_{\gamma\beta}t \left(\mu_5 \frac{\delta^2\Gamma}{\delta \tilde{\Phi}_\alpha \delta \Phi_\gamma} + j_\gamma \frac{\delta^2\Gamma}{\delta N_5 \delta \tilde{\Phi}_\alpha} \right), \quad (\text{C.48})$$

where we use Eqs. (C.39) and (C.41). We take the functional derivative of Eq. (C.48) with respect to μ_5 and set all the external fields to zero. In frequency space, we obtain,

$$\frac{\delta^3\Gamma}{\delta N_5 \delta \tilde{\Phi}_\alpha \delta \Phi_\beta} = -i \frac{g\varepsilon_{\gamma\beta}}{\chi_5} \frac{\partial}{\partial\omega} \frac{\delta^2\Gamma}{\delta \tilde{\Phi}_\alpha \delta \Phi_\gamma} \Big|_{\omega \rightarrow 0} = \frac{g\varepsilon_{\gamma\beta}}{\chi_5} \left(1 - i \frac{\partial \Sigma_{\alpha\gamma}(\mathbf{0}, \omega)}{\partial\omega} \Big|_{\omega \rightarrow 0} \right). \quad (\text{C.49})$$

Here, we use $\chi_5 = \delta N_5 / \delta \mu_5$ and Eqs. (C.40) and (5.37). By using Eqs. (C.42), (5.35) and (5.39), we finally arrive at Eq. (C.34) when $\alpha \neq \beta$. Note here that one can write $\varepsilon_{\gamma\beta} \Sigma_{\alpha\gamma} = \varepsilon_{\alpha\beta} \Sigma_{11}$ (for $\alpha \neq \beta$) by using $\Sigma_{11} = \Sigma_{22}$, which can be shown from Eq. (C.24).

Appendix D

Linear-stability analysis on the fixed points (iii) and (iv)

We here show that the parameter region that leads to the fixed point (iv) under RG is much larger than (iii) within the linear-stability analysis around the fixed point (i). Let us look at the full propagator of the conserved fields, $D_{ij} = \bar{D}_{ij}(w, h)$ as a function of two relevant parameters w and h , which is transformed under the rescaling as

$$\bar{D}_{ij}(w, h) \sim \bar{D}_{ij}(l^{y_w} w, l^{y_h} h). \quad (\text{D.1})$$

Here, we assume that w and h are scaled by the eigenvalues $y_w \equiv 7\epsilon/10$, $y_h \equiv 1 - \epsilon/4$ obtained in Eq. (5.97), and we omit the overall factor. When the RG flow approaches $l \sim h^{-1/y_h}$, \bar{D}_{ij} becomes a function of $wh^{-\varphi}$ with $\varphi \equiv y_w/y_h$ being the crossover exponent. Then, \bar{D}_{ij} behaves differently depending on whether $wh^{-\varphi} \gg 1$ or $wh^{-\varphi} \ll 1$: in the former region, we see the behavior of the fixed point (iii); in the latter region, we see the behavior of the fixed point (iv). Since $\varphi = O(\epsilon)$ and $w \ll 1$ near the fixed point (i), the latter parameter region is much larger than the former. Note also that these two regions should be continuously connected and the crossover between the fixed point (iii) and (iv) takes place. The right-hand side of the original RG equations (5.84)–(5.87) are smooth functions of all the parameters, unless w and h are simultaneously infinity.

Bibliography

- [1] K. Fukushima and T. Hatsuda, “The phase diagram of dense QCD,” Rept. Prog. Phys. **74**, 014001 (2011).
- [2] M. Asakawa and K. Yazaki, “Chiral Restoration at Finite Density and Temperature,” Nucl. Phys. A **504**, 668 (1989).
- [3] T. Hatsuda, M. Tachibana, N. Yamamoto and G. Baym, “New critical point induced by the axial anomaly in dense QCD,” Phys. Rev. Lett. **97**, 122001 (2006),
- [4] N. Yamamoto, M. Tachibana, T. Hatsuda and G. Baym, “Phase structure, collective modes, and the axial anomaly in dense QCD,” Phys. Rev. D **76**, 074001 (2007).
- [5] H. Abuki, G. Baym, T. Hatsuda and N. Yamamoto, “The NJL model of dense three-flavor matter with axial anomaly: the low temperature critical point and BEC-BCS diquark crossover,” Phys. Rev. D **81**, 125010 (2010).
- [6] P. C. Hohenberg and B. I. Halperin, “Theory of Dynamic Critical Phenomena,” Rev. Mod. Phys. **49**, 435 (1977).
- [7] H. Fujii, “Scalar density fluctuation at critical end point in NJL model,” Phys. Rev. D **67**, 094018 (2003).
- [8] H. Fujii and M. Ohtani, “Sigma and hydrodynamic modes along the critical line,” Phys. Rev. D **70**, 014016 (2004).
- [9] D. T. Son and M. A. Stephanov, “Dynamic universality class of the QCD critical point,” Phys. Rev. D **70**, 056001 (2004).

- [10] Y. Minami, “Dynamics near QCD critical point by dynamic renormalization group,” *Phys. Rev. D* **83**, 094019 (2011).
- [11] K. Rajagopal and F. Wilczek, “Static and dynamic critical phenomena at a second order QCD phase transition,” *Nucl. Phys. B* **399**, 395 (1993).
- [12] M. A. Stephanov, “QCD phase diagram and the critical point,” *Prog. Theor. Phys. Suppl.* **153**, 139 (2004) [*Int. J. Mod. Phys. A* **20**, 4387 (2005)]
- [13] Brookhaven National Laboratory, “Beam Energy Scan Theory (BEST) Collaboration,” Retrieved November 4, 2019, from <https://www.bnl.gov/physics/best/>
- [14] S. L. Adler, “Axial vector vertex in spinor electrodynamics,” *Phys. Rev.* **177**, 2426 (1969).
- [15] J. S. Bell and R. Jackiw, “A PCAC puzzle: $\pi^0 \rightarrow \gamma\gamma$ in the σ model,” *Nuovo Cim. A* **60**, 47 (1969).
- [16] D. E. Kharzeev, L. D. McLerran and H. J. Warringa, “The effects of topological charge change in heavy ion collisions: “Event by event P and CP violation”,,” *Nucl. Phys. A* **803**, 227 (2008).
- [17] K. Fukushima, D. E. Kharzeev and H. J. Warringa, “The Chiral Magnetic Effect,” *Phys. Rev. D* **78**, 074033 (2008).
- [18] H. B. Nielsen and M. Ninomiya, “Adler-bell-jackiw Anomaly And Weyl Fermions In Crystal,” *Phys. Lett.* **130B**, 389 (1983).
- [19] A. Vilenkin, “Equilibrium Parity Violating Current In A Magnetic Field,” *Phys. Rev. D* **22**, 3080 (1980).
- [20] D. E. Kharzeev and H. U. Yee, “Chiral Magnetic Wave,” *Phys. Rev. D* **83**, 085007 (2011).
- [21] G. M. Newman, “Anomalous hydrodynamics,” *JHEP* **0601**, 158 (2006).
- [22] B. I. Abelev *et al.* [STAR Collaboration], “Azimuthal Charged-Particle Correlations and Possible Local Strong Parity Violation,” *Phys. Rev. Lett.* **103**, 251601 (2009).

- [23] B. I. Abelev *et al.* [STAR Collaboration], “Observation of charge-dependent azimuthal correlations and possible local strong parity violation in heavy ion collisions,” *Phys. Rev. C* **81**, 054908 (2010).
- [24] B. Abelev *et al.* [ALICE Collaboration], “Charge separation relative to the reaction plane in Pb-Pb collisions at $\sqrt{s_{NN}} = 2.76$ TeV,” *Phys. Rev. Lett.* **110**, no. 1, 012301 (2013).
- [25] S. A. Voloshin, “Testing the Chiral Magnetic Effect with Central U+U collisions,” *Phys. Rev. Lett.* **105**, 172301 (2010).
- [26] W. T. Deng, X. G. Huang, G. L. Ma and G. Wang, “Test the chiral magnetic effect with isobaric collisions,” *Phys. Rev. C* **94**, 041901 (2016).
- [27] Q. Li *et al.*, “Observation of the chiral magnetic effect in ZrTe5,” *Nature Phys.* **12**, 550 (2016).
- [28] N. Sogabe and N. Yamamoto, “New dynamic critical phenomena in nuclear and quark superfluids,” *Phys. Rev. D* **95**, no. 3, 034028 (2017).
- [29] M. Hongo, N. Sogabe and N. Yamamoto, “Does the chiral magnetic effect change the dynamic universality class in QCD?,” *JHEP* **1811**, 108 (2018).
- [30] R. Jackiw, “Field theoretic investigations in current algebra,” in *Lectures on Current Algebra and Its Applications*, ed. S. B. Treiman, R. Jackiw and D. J. Gross (Princeton University Press, Princeton, 1972).
- [31] L. D. Faddeev, “Operator Anomaly for the Gauss Law,” *Phys. Lett. B* **145**, 81 (1984).
- [32] P. C. Martin, E. D. Siggia and H. A. Rose, “Statistical Dynamics of Classical Systems,” *Phys. Rev. A* **8**, 423 (1973).
- [33] H-K. Janssen, “On a Lagrangean for classical field dynamics and renormalization group calculations of dynamical critical properties,” *Z. Phys. B* **23**, 377 (1976).
- [34] C. De Dominicis, “Dynamics as a substitute for replicas in systems with quenched random impurities,” *Phys. Rev. B* **18**, 4913 (1978).

- [35] A. Onuki, “Dynamic equations and bulk viscosity near the gas-liquid critical point,” *Phys. Rev. E* **55**, 403 (1997).
- [36] H. D. Politzer, “Reliable Perturbative Results for Strong Interactions?,” *Phys. Rev. Lett.* **30**, 1346 (1973).
- [37] D. J. Gross and F. Wilczek, “Ultraviolet Behavior of Nonabelian Gauge Theories,” *Phys. Rev. Lett.* **30**, 1343 (1973).
- [38] M. Tanabashi *et al.* [Particle Data Group], “REVIEW OF PARTICLE PHYSICS,” *Phys. Rev. D* **98**, no. 3, 030001 (2018).
- [39] G. 't Hooft, “Symmetry Breaking Through Bell-Jackiw Anomalies,” *Phys. Rev. Lett.* **37**, 8 (1976).
- [40] M. Kobayashi and T. Maskawa, “Chiral symmetry and eta-x mixing,” *Prog. Theor. Phys.* **44**, 1422 (1970).
- [41] V. P. Nair, *Quantum field theory: A modern perspective* (Springer, New York, 2005).
- [42] M. G. Alford, K. Rajagopal and F. Wilczek, “Color-flavor locking and chiral symmetry breaking in high density QCD,” *Nucl. Phys. B* **537**, 443 (1999).
- [43] L. N. Cooper, “Bound electron pairs in a degenerate Fermi gas,” *Phys. Rev.* **104**, 1189 (1956).
- [44] J. Bardeen, L. N. Cooper and J. R. Schrieffer, “Microscopic theory of superconductivity,” *Phys. Rev.* **106**, 162 (1957).
- [45] D. Bailin and A. Love, “Superfluidity and Superconductivity in Relativistic Fermion Systems,” *Phys. Rept.* **107**, 325 (1984).
- [46] M. Iwasaki and T. Iwado, “Superconductivity in the quark matter,” *Phys. Lett. B* **350**, 163 (1995).
- [47] M. G. Alford, K. Rajagopal and F. Wilczek, “QCD at finite baryon density: Nucleon droplets and color superconductivity,” *Phys. Lett. B* **422**, 247 (1998).

- [48] R. Rapp, T. Schäfer, E. V. Shuryak and M. Velkovsky, “Diquark Bose condensates in high density matter and instantons,” *Phys. Rev. Lett.* **81**, 53 (1998).
- [49] T. Schäfer and F. Wilczek, “Continuity of Quark and Hadron Matter,” *Phys. Rev. Lett.* **82**, 3956 (1999).
- [50] K. Landsteiner, “Notes on Anomaly Induced Transport,” *Acta Phys. Polon. B* **47**, 2617 (2016).
- [51] Y. Hidaka, “Field theory of equilibrium and nonequilibrium systems,” (unpublished).
- [52] S. L. Adler and W. A. Bardeen, “Absence of higher order corrections in the anomalous axial vector divergence equation,” *Phys. Rev.* **182**, 1517 (1969).
- [53] K. Fujikawa, “Path Integral Measure for Gauge Invariant Fermion Theories,” *Phys. Rev. Lett.* **42**, 1195 (1979).
- [54] D. T. Son and A. R. Zhitnitsky, “Quantum anomalies in dense matter,” *Phys. Rev. D* **70**, 074018 (2004).
- [55] M. A. Metlitski and A. R. Zhitnitsky, “Anomalous axion interactions and topological currents in dense matter,” *Phys. Rev. D* **72**, 045011 (2005).
- [56] K. Kawasaki, “Kinetic equations and time correlation functions of critical fluctuations,” *Ann. Phys. (N.Y.)* **61**, 1 (1970).
- [57] B. I. Halperin, P. C. Hohenberg and E. D. Siggia, “Renormalization-Group Calculations of Divergent Transport Coefficients at Critical Points,” *Phys. Rev. Lett.* **32**, 1289 (1974).
- [58] E. D. Siggia, B. I. Halperin and P. C. Hohenberg, “Renormalization-group treatment of the critical dynamics of the binary-fluid and gas-liquid transitions,” *Phys. Rev. B* **13**, 2110 (1976).
- [59] H. L. Swinney and D. L. Henry, “Dynamics of Fluids near the Critical Point: Decay Rate of Order-Parameter Fluctuations,” *Phys. Rev. A* **8**, 2586 (1973).

- [60] J. Polchinski, “Effective field theory and the Fermi surface,” In *Boulder 1992, Proceedings, Recent directions in particle theory* 235-274, and Calif. Univ. Santa Barbara - NSF-ITP-92-132 (92,rec.Nov.) 39 p. (220633) Texas Univ. Austin - UTTG-92-20 (92,rec.Nov.) 39 p [hep-th/9210046].
- [61] D. B. Kaplan, “Effective field theories,” arXiv:nucl-th/9506035.
- [62] D. B. Kaplan, “Five lectures on effective field theory,” arXiv:nucl-th/0510023.
- [63] P. M. Chaikin and T. C. Lubensky, *Principles of Condensed Matter Physics* (Cambridge University Press, Cambridge, 1995).
- [64] D. Forster, *Hydrodynamic fluctuations, broken symmetry, and correlation functions* (Perseus Books, New York, 1975).
- [65] G. F. Mazenko, *Nonequilibrium Statistical Mechanics* (WILEY-VCH, Weinheim, 2006).
- [66] U. C. Täuber, *Critical dynamics: a field theory approach to equilibrium and non-equilibrium scaling behavior* (Cambridge University Press, Cambridge, 2014).
- [67] B. I. Halperin, P. C. Hohenberg and Shang-keng Ma, “Renormalization-group methods for critical dynamics: I. Recursion relations and effects of energy conservation,” Phys. Rev. B **10**, 139 (1974).
- [68] B. I. Halperin, P. C. Hohenberg and Shang-keng Ma, “Renormalization-group methods for critical dynamics: II. Detailed analysis of the relaxational models,” Phys. Rev. B **13**, 4119 (1976).
- [69] S. Weinberg, *The quantum theory of fields. Vol. 2: Modern applications* (Cambridge University Press, Cambridge, 1996).
- [70] D. T. Son, “Low-energy quantum effective action for relativistic superfluids,” arXiv:hep-ph/0204199.
- [71] L. D. Landau and E. M. Lifshitz, *Statistical Physics, Part 1* (Pergamon Press, Oxford, 1980).

- [72] I. A. Shushpanov and A. V. Smilga, “Quark condensate in a magnetic field,” *Phys. Lett. B* **402**, 351 (1997).
- [73] R. D. Pisarski and F. Wilczek, “Remarks on the Chiral Phase Transition in Chromodynamics,” *Phys. Rev. D* **29**, 338 (1984).
- [74] M. E. Peskin and D. V. Schroeder, *An Introduction to quantum field theory* (Addison-Wesley, Reading, 1995).
- [75] A. Onuki, *Phase Transition Dynamics* (Cambridge University Press, Cambridge, 2007).
- [76] N. Goldenfeld, *Lectures on phase transitions and the renormalization group* (Addison-Wesley, Boston, 1992).
- [77] N. Sogabe and N. Yamamoto, “Triangle Anomalies and Nonrelativistic Nambu-Goldstone Modes of Generalized Global Symmetries,” *Phys. Rev. D* **99**, no. 12, 125003 (2019).
- [78] I. E. Dzyaloshinskii and G. E. Volovick, “Poisson brackets in condensed matter physics,” *Ann. Phys. (N.Y.)* **125**, 67 (1980).
- [79] U. C. Täuber and Z. Rácz, “Critical behavior of $O(n)$ -symmetric systems with reversible mode-coupling terms: Stability against detailed-balance violation,” *Phys. Rev. E* **55**, 4120 (1997).